

# Iowa Research Online

---

## **Noncanonical Wnt signaling in breast cancer initiation and progression**

Borcherding, Nicholas

[https://iro.uiowa.edu/discovery/delivery/01IOWA\\_INST:ResearchRepository/12730635930002771?l#13730826500002771](https://iro.uiowa.edu/discovery/delivery/01IOWA_INST:ResearchRepository/12730635930002771?l#13730826500002771)

---

Borcherding. (2014). Noncanonical Wnt signaling in breast cancer initiation and progression [University of Iowa]. <https://doi.org/10.17077/etd.qgs23k2g>

---

<https://iro.uiowa.edu>

Free to read and download

Copyright 2014 Nicholas Borcherding

Downloaded on 2023/01/03 14:59:39 -0600

NONCANONICAL WNT SIGNALING IN BREAST CANCER INITIATION AND PROGRESSION

by

Nicholas Borcherding

A thesis submitted in partial fulfillment  
of the requirements for the  
Master of Science degree in Pathology  
in the Graduate College of  
The University of Iowa

August 2014

Thesis Supervisor: Assistant Professor Weizhou Zhang

Copyright by

NICHOLAS BORCHERDING

2014

All Rights Reserved

Graduate College  
The University of Iowa  
Iowa City, Iowa

CERTIFICATE OF APPROVAL

---

MASTER'S THESIS

---

This is to certify that the Master's thesis of

Nicholas Borcherding

has been approved by the Examining Committee  
for the thesis requirement for the Master of Science degree  
in Pathology at the August 2014 graduation.

Thesis Committee: \_\_\_\_\_  
Weizhou Zhang, Thesis Supervisor

---

Dawn Quelle

---

Hasem Habelhah

**To my wife and best friend**, the only person I would ever take on a time travel mission.

**To Weizhou**, the singular individual that is more indefatigable about science than me.

**To my parents**, if I have seen further it is because I have stood on the shoulders of giants. I mean this figuratively, as you are both slightly above average in height.

There is a time in every man's education when he arrives at the conviction that envy is ignorance; that imitation is suicide; that he must take himself for better for worse as his portion; that though the wide universe is full of good, no kernel of nourishing corn can come to him but through his toil bestowed on that plot of ground which is given to him to till.

Ralph Waldo Emerson, Self-Reliance

## ACKNOWLEDGEMENTS

My entire goal in science is to one day be the smartest person in a room of researchers. Between Dr. Weizhou Zhang and Dr. Ryan Kolb, I have not had that opportunity over the last two years. Although their ever-present nature has hindered my grander aspirations, their guidance, insights, and compassion have not only allowed me to carry out my studies, but their passions for research were infectious. I would also like to thank my thesis committee, Dr. Dawn Quelle and Dr. Hasem Habelhah for their perspectives, specifically in cell signaling; many of these experiments and resulting figures are the product of their sage advice. In addition, I would like to thank Dr. Thomas Waldschmidt, for the opportunity to research within the Department of Pathology and for great movie suggestions through the years. Dr. Matthew Rowling and my undergraduate experience in his lab was the catalyst for my passion for research and science as a whole, I owe him a metric tonne for showing me what I want to do and who I want to be. Lastly, I want to thank Wei Li, Qing Xie, Lorraine Tygrett, Farah Itani, David Kusner, Corey Parlet, and Adam Koch. I was able to put together this thesis despite the constant distractions and/or fun times we shared.

## TABLE OF CONTENTS

LIST OF TABLES .....	vii
LIST OF FIGURES .....	viii
CHAPTER I. INTRODUCTION .....	1
Breast Cancer Incidence and Characterization .....	1
Molecular Subtypes of IDC .....	3
Cell-of-Origin and Cancer Stem Cells .....	4
Wnt Signaling in Development and Cancer.....	9
Structure of Noncanonical Wnt Receptor, ROR1.....	12
ROR1/2 Functions within Development.....	14
ROR1 in Cancer .....	16
ROR1 in Blood Malignancies.....	17
ROR1 in Solid Malignancies .....	19
ROR1, a Target of Immunotherapies.....	21
Purpose of Study .....	23
Specific Aims .....	24
CHAPTER II. CHARACTERIZATION OF ERBB2 MASC AND LP TUMORS.....	29
Rationale.....	29
Materials and Methods .....	30
RNA Isolation and Microarray.....	30
Microarray Data Processing and Analyses.....	31
Human Patient Sample Corroboration .....	32
Other Genomic Techniques Used in Analysis .....	32
Immunohistochemistry.....	33
Mammospheres .....	33
Cell Lines and Culture .....	34
Wnt5a ErbB2 Transgenic Mice.....	35
Statistical Analysis.....	35
Results .....	36
Delineation of LP- and MaSC-Derived Tumors .....	36
Loss of Wnt5a in MaSC and Human Breast Tumors .....	37
Tumor Suppressive Effects of Wnt5a.....	39
Discussion .....	41
CHAPTER III. THE BLBC-SPECIFIC ROLE OF ROR1 IN EMT AND CSCS .....	53
Rationale.....	53
Materials and Methods .....	55
Biostatistical Analyses of ROR1 Expression .....	55
Cell Lines and Cell Culture.....	55
Production of anti-ROR1 Immunotoxin .....	56

Flow Cytometry for Breast Cancer Cells .....	56
Immunoblot and Immunoprecipitation.....	57
RNA Isolation and RT-PCR.....	58
Immunofluorescence Staining .....	58
Results .....	58
ROR1 is a Basal/Mesenchymal Marker in Breast Cancer .....	58
Functional Advantage of ROR1 Expression in BLBC.....	60
Targeting ROR1 for Breast Cancer Therapy .....	62
Discussion.....	64
 CHAPTER IV. CONCLUSIONS AND FUTURE DIRECTIONS.....	77
Conclusions.....	77
Future Directions.....	79
 REFERENCES.....	82

## LIST OF TABLES

Table 1: Identified DEGs from MaSC versus LP Tumors .....	45
Table 2: RT Primers for Microarray Confirmation .....	46
Table 3: ROR1 Expression Correlations.....	68
Table 4: EMT-Related RT PCR Primers .....	73

## LIST OF FIGURES

1.	Model for Breast IDC and Molecular Subtyping .....	25
2.	Cell-of-Origin for HER2+ Breast Cancer.....	26
3.	Cancer Stem Cells (CSCs), EMT, and Breast Cancer Progression .....	27
4.	ROR1 Structure and Signaling in Cancer .....	28
5.	Computational Analyses of ErbB2-Derived Tumors .....	44
6.	Confirmation and Filtering Microarray Results .....	47
7.	Wnt5a is Reduced Through the Progression of ErbB2 Spontaneous Tumors and Correlates with Better Patient Survival .....	48
8.	Human Clinical Specimens Exhibit a Reduction of Wnt5a Expression from Normal Mammary Glands to Cancer Cells .....	49
9.	Heterozygous/Homozygous Loss of Wnt5a is Common in Breast and Other Cancers .....	50
10.	Wnt5a Inhibits Self-Renewal and Activates SMAD Pathway.....	51
11.	Heterozygous Loss of Wnt5a Increases Metastasis in ErbB2 Murine Model for Breast Cancer.....	52
12.	ROR1 Expression is Dependent on Molecular Subtypes and Correlates with Mesenchymal Phenotype .....	67
13.	ROR1 Protein Expression in Human Tumor Tissue Samples.....	69
14.	ROR1 Expression in Breast Cancer Cell Lines Correlates with CD24 <sup>-</sup> CD44 <sup>+</sup> CSC Markers .....	70
15.	ROR1 Modulates the Basal mRNA Level of EMT/CSC Genes.....	71
16.	Wnt5a-ROR1 Signaling in MDA-MB-231 Cells .....	72
17.	ROR1 Potentiates EGFR-Mediated AKT and SMAD Activation .....	74

18. <i>In Vitro</i> Analysis of ROR1-Immunotoxin .....	75
19. Initial <i>In Vivo</i> Assessment of ROR1-Immunotoxin .....	76
20. Noncanonical Wnt Pathway in Breast Cancer Initiation and Progression.....	81

## CHAPTER I

### INTRODUCTION

#### **Breast Cancer Incidence and Characterization**

Breast cancer is the leading cause of cancer-related morbidity and the second leading cause of cancer-related mortality for women in the United States, with greater than 232,000 new cases and nearly 40,000 deaths annually [1, 2]. With the current incidence rate, 12.4% of women or 1 in 8 women born in the U.S. today will be diagnosed with breast cancer in their lifetimes [2]. In 2008, worldwide breast cancer incidence was estimated at 1,383,500, with 458,400 deaths, a mortality to incidence ratio of 1 in 3 [3]. Per capita incidence of breast cancer is three-fold greater in developed nations when compared with developing nations. This increased burden may be due to greater screening effort, access to healthcare, differences in lifestyles, and greater awareness of the disease within developed nations [4, 5]. However, the disparity between incidences of breast cancer is expected to equilibrate as nations increase access to healthcare and adopt lifestyle changes associated with globalization [6]. A number of risk factors have been associated with breast cancer including age, geographical and ethnic variation, age at menarche and menopause, hormone-replacement therapy, and obesity [7-9]. The diversity of the risk factors for breast cancer underscores the variation within breast cancer as a whole. Collectively, breast cancer is a spectrum of diseases that are delineated clinically largely based on histological morphology and immunohistochemical staining.

The mammary duct, the most common site of breast malignancy, is comprised of two distinct layers. These layers are referred to as the luminal layer, adjacent to the lumen of the duct, and the basal layer, which has an interface with the basement membrane of the mammary duct. The second most common site of malignancy is at the lobules, the aggregation of milk-producing acini within the mammary glands. Carcinoma *in situ* (CIS) is a broad classification of pre-malignant and malignant cells residing within the defined structures of the mammary gland and have not compromised the basement membrane (**Figure 1A**). CIS consists of two subtypes, ductal carcinoma *in situ* (DCIS) and lobular carcinoma *in situ* (LCIS). CIS accounts for close to 30,000 diagnoses of breast cancer per year, with DCIS accounting for 85% of the diagnoses. DCIS is a widely divergent class of lesions based on histopathological and molecular observations, often presents at annual screenings, and is thought to be a precursor of invasive cancer [2,5].

The most common invasive breast cancer is infiltrating or invasive ductal carcinoma (IDC), representing 70-80% of total breast cancer diagnoses. Infiltrating or invasive lobular carcinoma (ILC) accounts for 10%. Rare invasive diseases of the mammary duct comprise smaller percentages of total diagnoses, including medullary (2-5%), mucinous (1-6%), tubular (1-4%), inflammatory (1-2%), and papillary (.5%) [10-15]. Clinically, IDC is further differentiated using immunohistochemistry and/or fluorescence *in situ* hybridization (FISH) for the estrogen receptor (ER), progesterone receptor (PR) and human epidermal growth factor receptor 2 (HER2 or EGFR2/ErbB2/Neu). The presence or absence of these receptors informs treatment options and is generally predictive of clinical outcomes. The presence of HER2 (HER2+) or the lack of all three

receptors, known as triple-negative breast cancer (TNBC) is considered prognostically worse, with an increased risk of recurrence, metastasis, and death relative to diseases with ER and/or PR expression [16-19].

### **Molecular Subtypes of IDC**

Molecular portraits utilizing microarray and RNAseq transcriptome analyses of invasive breast carcinomas have revealed distinct and intrinsic subtypes based on differential gene expression patterns (**Figure 1B**). These molecular or intrinsic subtypes of luminal A, luminal B, HER2, basal-like, and claudin-low are predictive for response to treatments and disease-free/overall survival [20-23]. Luminal A accounts for 40% of IDCs and is generally ER+/PR+ with common aberrations in the PI3K signal transduction pathway and mutations in Gata3. Additionally, Luminal A subtype is associated intact p53 and RB1 tumor suppressors. Luminal B diverges from Luminal A with varying expression of ER and HER2 and account for 20% of IDCs. As a quasi-intermediate molecular subtype, Luminal B has high levels of p53 mutations and aberrations of the PI3K pathway. HER2 is characterized by not only the overexpression/amplification of HER2, but lack of ER/PR expression, aneuploidy, and increased expression of cyclin D1 that is indicated in enhanced cell cycle progression for a variety of cancers. Basal-like breast cancer (BLBC) has low or no expression of ER/PR/HER2. BLBC is also associated with loss of RB1, p53 mutations, or gain of MDM2 that is part of the ubiquitin-mediated degradation machinery of p53. Additionally, BLBC is associated with sporadic and germline loss-of-function mutations or deletions of BRCA1/2 DNA repair genes [24].

BLBC and TNBC appear to be an overlapping classification, with an estimate of 70% of TNBC expressing a genetic profile designated as BLBC [25, 26]. Interestingly, the TNBCs that do not possess the BLBC phenotype have a better prognosis. These differences in prognosis, coupled with the characteristic genomic instability of BLBC, have led some researchers to conclude the necessity for the individual classification of TNBC/BLBC [27, 28].

### **Cell-of-Origin and Cancer Stem Cells**

The different molecular subtypes are associated with common expression patterns and mutations. These commonalities may be a result of differences from their cell-of-origins. As described previously, the mammary duct is comprised of two distinct layers, *e.g.* the luminal and basal compartments. Immunohistologically, these layers can be differentiated in humans and mice utilizing cytokeratin staining. Luminal cells are positive for cytokeratins 8 and 18; whereas basal cells are stained for cytokeratins 5 and 6 [29]. Cytokeratin 14 is present in both luminal and basal cells, however luminal expression of cytokeratin 14 is seen exclusively in large ducts [30]. The unique cell populations within these compartments have been well characterized within mice (**Figure 2A**). The luminal compartment contains mature luminal cells (LC), which are CD45<sup>-</sup>Ter119<sup>-</sup>CD31<sup>-</sup>(Lin<sup>-</sup>)CD24<sup>high</sup>CD49f<sup>low</sup>CD61<sup>-</sup>, and luminal progenitor cells (LP) identified as a Lin<sup>-</sup>CD24<sup>high</sup>CD49f<sup>low</sup>CD61<sup>+</sup> population. The basal compartment is composed of Lin<sup>-</sup>CD24<sup>low</sup>CD49f<sup>med</sup> myoepithelial cells (Myo) and Lin<sup>-</sup>CD24<sup>low</sup>CD49f<sup>high</sup> mammary stem cells (MaSC). An enriched MaSC population has traditionally been

isolated through Lin<sup>-</sup>CD24<sup>med</sup> CD29<sup>high</sup> or Lin<sup>-</sup>CD24<sup>med</sup> CD49f<sup>high</sup> [31-33]. However, recent evidence suggests CD10<sup>+</sup> can be used to isolate multipotent basal cells independent of CD24/CD29 [34]. These distinguishable cell populations in turn imply a hierachal structure of the mammary gland, in which the multipotent MaSC gives rise to cells of both luminal and basal cells in development. In addition, MaSCs are responsible for tissue homeostasis of the adult mammary gland and lactational hyperplasia during pregnancy and lactation [35, 36]. Indeed, LP and MaSCs produce colonies in *ex vivo* 3-dimensional growth assays, but only MaSCs can give rise to *de novo* mammary glands when allogenically transplanted into cleared mammary fat pads [31].

As the name implies, luminal IDC resembles luminal cells, in respect to expression of estrogen receptor  $\alpha$  (ER $\alpha$ ) and luminal cytokeratins. However, the cell-of-origin, the cell population responsible for luminal tumor initiation, is not straightforward. CD61<sup>+</sup> LP have a proliferative capacity, but lack ER $\alpha$  expression, a hallmark of luminal IDC [37]. In contrast, mature CD61<sup>-</sup> LCs have high levels of ER $\alpha$  expression, but rarely divide in the physiologic context due to p27-mediated cell cycle regulation [38]. Recently, researchers observed a distinct population ER $\alpha$ + cells that asymmetrically divide, which implies a further hierarchical step. These ER $\alpha$ + cells could represent committed progenitors in luminal maturation, but also the cell-of-origin for luminal A IDC [39]. Gata3, responsible for luminal cell differentiation and commonly mutated in Luminal A IDC, could be part of a signaling mechanism by which the ER $\alpha$ + committed progenitors escape maturation [24, 37].

Within HER2 IDC, two types of cells have emerged as potential candidates for the cell-of-origin and have come from work with the MMTV-ErbB2 transgenic (TG) mouse model of breast cancer (**Figure 2B**). Isolation of enriched MaSC and LP from preneoplastic mammary glands of MMTV-ErbB2 TG mice and subsequent transplants into the mammary fat pads of *Rag1<sup>-/-</sup>* mice, deficient of mature T and B cells, have shown that MaSC forms larger tumors at a greater incidence than LP [40]. However, mammary glands and spontaneous ErbB2 tumors are enriched for CD61<sup>+</sup> cells. These CD61<sup>+</sup> cells are major components of mammospheres, clonogenic assay for self-renewal capacity, derived from unsorted preneoplastic mammary glands of MMTV-ErbB2 TG mice [41, 42]. The enrichment of CD61<sup>+</sup> LP within ErbB2-driven tumors is similar to the proliferative burden of the LPs seen in mammary ducts during development, but does not preclude a model of MaSC as the cell-of-origin [35]. Within the MMTV-Neu TG mouse model utilizing the rat HER2/Neu transgene, a pronounced expansion exclusively in the MaSC in the mammary gland has been observed [42].

The strongest evidence for cell-of-origin in breast cancer has been for LP cells in BLBC. Mutations in BRCA1, a DNA repair protein implicated in familial breast cancers, are associated with BLBC in human patients. In human BRCA1 mutant carriers (BRCA1<sup>+-</sup>), the expansion of luminal progenitor cell population has been observed. When isolated, the gene expression profile of BRCA1<sup>+-</sup> LP cells most closely resembles BLBC, while the gene expression of BRCA1<sup>+-</sup> MaSCs most closely resembles claudin-low tumors [43]. Two mouse models have been generated to look at cell-of origin-in BLBC, the basal cell-targeted *K14-Cre Brca1<sup>flox/flox</sup> p53<sup>+-</sup>* and the LP-targeted *Btg-Cre*

*Brca1*<sup>flox/flox</sup> *p53*<sup>+/−</sup>. Using the basal cytokeratin 14 promoter, *K14-Cre Brca1*<sup>flox/flox</sup> *p53*<sup>+/−</sup> mice give rise to tumors with strong expression of basal genes; however, these aggressive tumors histologically resemble adenomyoepitheliomas. Conversely, using the β-lactoglobulin (*Blg*) promoter to target LPs, the *Blg-Cre Brca1*<sup>flox/flox</sup> *p53*<sup>+/−</sup> mice give rise to tumors that resemble BLBC histopathologically and genetically [44]. *In vitro* studies have provided a possible mechanistic link, as BRCA1 knockdown via small interfering (si) RNA within luminal cell lines increases the expression of basal markers, such as cytokeratins 5, 14, and P-cadherin. Conversely, stable expression of exogenous wild-type BRCA1 in BLBC cell lines leads to a repression of basal markers [45]. In a similar study, the restoration of wild-type BRCA1 in BRCA1-mutant cells leads to an increase in ERα expression [46]. BRCA1 appears to regulate transcription at the promoter region of ERα, while its interaction with c-Myc represses basal marker genes [45, 46]. Therefore, loss of BRCA1 may be a mechanism by which LP revert into a basal phenotype. Cell-of-origins for cancer can inform researchers on the earliest stage of initiation and how initial aberrancy manifests into malignancy. Through selective pressures within the tumor, the cell-of-origin(s) and their progeny are thought to give rise to cancer stem cells (CSC), representing another fundamentally important cell to characterize.

CSCs are cells within hematological or solid malignancies responsible for sustained growth through their self-renewal capacity and the generation of a complex heterogeneity of cells within tumors (**Figure 3**). Discovered in acute myelogenous leukemia (AML), the CSC field has grown rapidly, especially in solid malignancies, after the discovery of CSC in metastatic breast cancer [47-50]. CSCs have since been described

in glioblastoma, colorectal cancer, pancreatic cancer, melanoma, squamous cell cancer (SCC) and hepatocellular carcinoma [51-56]. Within these cancers, CSCs have been isolated utilizing a number of markers. The standard CSC markers within breast cancer are Lin<sup>-</sup>ALDH1<sup>+</sup>CD44<sup>+</sup>CD24<sup>-/low</sup>. The enriched ALDH1<sup>+</sup>CD44<sup>+</sup>CD24<sup>-/low</sup> CSCs consistently give rise to breast tumors in xenografts with as few as 200 cells [50, 57].

Serial xenograft passages of primary breast tumor and metastatic samples produce a sustained CSC population [50, 56, 58]. These findings suggest that CSC may be a common cell population in breast cancer tumors and metastases. Therapies that cycle through remission and relapse fail to adequately target CSCs, the cell responsible for repopulation within the tumor. The ability of CSCs to escape therapy has been documented through several mechanisms including overexpression of ABC drug transporters, resistance to radiation through enhanced DNA repair, and an increased capacity to mitigate reactive oxygen species [59-61]. More so, conventional therapies that target proliferating cells can fail to affect CSCs. A subset of CSCs, through complex interactions with the microenvironment, can enter quiescence and escape therapies. This escape into quiescence resembles the control of proliferation exerted by the niche in the context of normal stem cells [62-64]. Another example of anti-proliferating drugs failing to target CSCs occurs with case of chronic myelogenous leukemia (CML). The CML-CSCs generate a tumor hierarchy in which multipotent progenitor cells possess the proliferative burden and require the BCR-ABL fusion protein. Imatinib therapy directed against BCR-ABL fails to eliminate the CML-CSCs, and patients remain positive for the fusion-gene transcript even after prolonged imatinib therapy [65, 66]. A second aspect

of the importance of characterization of CSCs is that the self-renewal capacity of CSCs must be vital in the seeding and settlement of metastatic sites. Supporting the role of CSCs in breast cancer metastasis, CD44<sup>+</sup>CD24<sup>-</sup> cells have been often isolated from pleural effusion and bone marrow of breast cancer patients [50, 67]. In the bone marrow of breast cancer patients, greater than 70% of disseminated tumor cells are CD44<sup>+</sup>CD24<sup>-</sup> CSCs [67]. Targeting CSCs represents a delicate balance between selective destruction of CSCs and keeping normal adult stem cells intact for tissue homeostasis. However, as targeted therapy research progresses, targeting CSCs could abolish relapse potential and specifically abrogate metastatic potential. Thus, targeting CSC represents a fundamental paradigm shift for cancer therapies [68-70].

### **Wnt Signaling in Development and Cancer**

The Wnt pathway is integral in regulating self-renewal of normal stem cells; however, growing evidence has shown the involvement of Wnt pathway in the transition from cell-of-origin to CSC. Wnt is a family of 19 secreted glycoprotein ligands that are divided into two classes, canonical and noncanonical. Briefly, canonical Wnt signaling involves the binding of Wnt ligand to the Frizzled family receptors and lipoprotein receptor-related protein 5 (LRP5) or LRP6 co-receptors. In the absence of Wnt, glycogen synthase kinase 3 (GSK3), Axin, adenomatosis polyposis coli (APC), protein phosphatase 2A (PP2A), and casein kinase 1 $\epsilon$  (CK1 $\epsilon$ ) promote the ubiquitin-mediated destruction of  $\beta$ -catenin. When Wnt complexes with the Frizzled receptors and LRP5/6, the interaction leads to the reduced activity of the destruction complex and

subsequent stabilization of  $\beta$ -catenin. The increased level of  $\beta$ -catenin, in turn, allows its interaction with Tcf/Lef transcriptional factors within the nucleus [68, 71]. Canonical Wnt signaling has been implicated in organogenesis, but also self-renewal of stem cells in adult tissues. Within the breast, temporal canonical Wnt signaling regulates mammary gland morphogenesis. Disruption of the discrete Wnt signaling through inducible expression of Axin, leads to increased apoptosis in mammary epithelia and failure of lobular-alveoli differentiation during pregnancy [72-74]. Canonical Wnt potentiates the self-renewal capacity of MaSCs, as MMTV-Wnt1 TG mice have increased MaSC and LP populations [31, 75]. Similarly, LRP5-deficient mice have limited stem cell activity, which conversely implies the requirement of this co-receptor for maintaining self-renewal of MaSCs [76].

Canonical Wnt signaling has been implicated in breast tumorigenesis. Wnt1 hyperactivity has been shown to drive breast tumor initiation through the expansion of both LPs and MaSCs [31, 77-79]. More broadly, deregulation of canonical Wnt signaling has been implicated in CSCs in colorectal cancer, breast cancer, SCC, and leukemia [80]. The loss of  $\beta$ -catenin within the CSC of CML and SCC abolishes the intrinsic self-renewal capacity [81, 82]. Another aspect of canonical Wnt signaling in tumor progression is Wnt-mediated epithelial-mesenchymal transition (EMT), a process by which epithelial cells convert/revert into a mesenchymal phenotype. EMT is thought to be a step predisposing cancer cells to metastasis, generating cancer cells that have properties of cancer stem cells, invade tissues and survive outside of the primary tumor. In murine mammary epithelial cells, TGF $\beta$  and  $\beta$ -catenin participate in the generation of the

mesenchymal phenotype through the regulation of EMT-related genes [83]. Thus, through the subversion of Wnt-mediated self-renewal and induction of EMT, the dysregulation of canonical Wnt signaling could drive breast tumorigenesis and progression [84].

Noncanonical Wnt signaling is characterized by a lack of requirement for  $\beta$ -catenin transcriptional activity. The functions of non-canonical Wnt signaling are tissue-specific and dependent on several receptors. In the absence of the LRP5/6 coreceptor, Wnt interaction with Frizzled receptor regulates planar cell polarity (PCP). Through DVL, RHOA, RAC and CDC42, Wnt can modulate the cytoskeleton, which is necessary in gastrulation and organogenesis [85, 86]. Additionally, non-canonical Wnt signaling has been shown to induce calcium flux and leading to the activation of PKC, CAMKII, and JNK. Wnt-CAMKII signaling has been shown to affect dorsal positioning and vertebral axis formation in embryos [87-90]. This non-canonical Wnt/calcium signaling could be involved in a number of intracellular secondary messenger signaling or intercellular signaling networks, much like networks seen in the retina [91]. Another important aspect of non-canonical Wnt function is the antagonism of canonical signaling through an unelucidated mechanism that results in blocking the stabilization of  $\beta$ -catenin [92].

Wnt5a, a non-canonical Wnt, has been shown to be a negative regulator in colonic crypt regeneration and mammary gland development. After colon injury and during regeneration, cells that express the highest Wnt5a have the lowest Ki-67 expression, a marker for proliferation [93]. Absence of Wnt5a prevents the mouse colon from reforming the crypts by inhibiting focal and temporal points of quiescence. Wnt5a-

mediated antagonism of  $\beta$ -catenin could be a potential mechanism abrogating proliferation in colon regeneration [93]. In the context of mammary gland, transplant of *Wnt5a*<sup>-/-</sup> mammary epithelia into cleared mammary fat pads produces a highly branched mammary gland with pronounced elongation when compared with transplanted WT cells. *Wnt5a* expression is restricted to the terminal end buds, where loss of TGF $\beta$  signaling correlates with a decrease in *Wnt5a* expression [94]. Loss of *Wnt5a* or TGF $\beta$ -signaling in MMTV-PymT or MMTV-ErbB2 TG mice increases tumorigenicity, but further study is required to evaluate the noncanonical mechanism that *Wnt5a* serves in the suppression of breast tumorigenesis [95].

#### **Structure of Noncanonical Wnt Receptor, ROR1**

Receptor Tyrosine Kinase-Like Orphan Receptor (ROR) family of transmembrane proteins are within the receptor tyrosine kinase family and through the binding of *Wnt5a* participate in noncanonical Wnt signaling. ROR1/2 were initially discovered in a neuroblastoma cell line in a PCR screen for receptor tyrosine kinases and were formerly named neurotrophic tyrosine kinase receptor-related (NTRKR1/2). Human ROR1/2 share 58% amino acid identity and are closely related to MUSK and Trk family receptors [96, 97]. Both genes encode proteins with a predicted molecular weight of 104 kDa, but ROR1 has multiple N-glycosylation sites that generate a post-translationally modified ROR1 at 130 kDa. These N-glycosylation sites are necessary for the trafficking of ROR1 to the membrane and in turn the function of ROR1 [98]. The structure of human ROR1/2 (**Figure 4A**) consists of an extracellular immunoglobulin-like (IG) domain at the amino-

terminus, followed by a cysteine-rich domain known as a Frizzled domain (FZD), and then a Kringle domain (KRD) into a transmembrane domain. The FZD domain is seen in the Smoothened and Frizzled family receptors, as well as carboxypeptidase Z, collagen  $\alpha$ 1 XVIII, and LRPs and consists of ten conserved cysteine residues and five corresponding disulfide bonds. The FZD is thought to mediate receptor-ligand interaction [99-101]. Both ROR1 and to a greater extent in the literature, ROR2, have been shown to bind Wnt5a, a non-canonical Wnt via the FZD [101-104]. The KRD is a highly-folded, cysteine-rich domain that mediates in protein-protein and protein-ligand interaction in coagulation proteins, apolipoproteins, and hepatocyte growth factor [105-107].

The cytoplasmic portion of human ROR1/2 has a tyrosine kinase domain (TKD), followed by a Serine/Threonine-rich domain (Ser/Thr), a proline-rich domain (PRD), and a second Ser/Thr domain at the carboxy-terminus. The functionality of the tyrosine kinase domain (TKD) of ROR1 has been a subject of debate in literature. Early studies show strong autocatalytic kinase activity for ROR2, while ROR1 possesses weak to moderate kinase activity [96, 108]. More recently, ROR1 TKD was sufficient to phosphorylate c-SRC in NIH3T3 cells [109]. Conversely, another study concludes that ROR1 is a pseudokinase since ROR1 did not show any kinase activity in COS-7 cells [110]. The ROR family is one of the most divergent within the receptor tyrosine kinase family, containing only 21 of the 40 consensus residues in other TKDs described by Hanks and Quinn [111]. Notably, ROR1 possesses substitutions at C482G, K614R and L634F, that should modulate ATP binding and kinase function [96, 111]. The ROR family of proteins

are evolutionarily conserved and share a high level of homology between orthologs in: *Mus musculus*, *Caenorhabditis elegans*, *Xenopus laevevis*, *Drosophila melanogaster*, *Aplysia californica*, and *Gallus gallus* [97, 108, 112-115]. CAM-1 is the singular ROR1/2 ortholog in *C.elegans* and shares a greater amino acid identity to ROR1, but lacks the PRD and the second Ser/Thr domain. DROR and a structural intermediate of the ROR and TRK receptor family, DRNK are the *Drosophila* orthologs and lack the extracellular Ig domain and the intracellular PRD and Ser/Thr domains [113, 116]. The conservation of RORs across species underlies the importance of the ROR family through a number of processes during development.

#### **ROR1/2 Functions within Development:**

A series of studies that utilized *in situ* hybridization and mutant knockout characterizations in mice have implicated RORs in the context of skeletal, cardiorespiratory, and neurological development. The expression patterns of mROR1 and mROR2 in embryos partially overlap, namely in facial development, pharyngeal arches, nasal processes and much of the other derivatives of neural crest cells. In general, mROR1 is restricted to the cephalic mesenchyme and neural crest cells, while mROR2 is expressed more broadly in both neural and non-neural cells throughout development. Within the limb, a low level of mROR1 is detected at the proximal portion of the limb bud, while mROR2 expression extends throughout the mesenchyme of the limb. Later in development, strong expression of mROR2 is seen within the perichondrium of the developing digits, while mROR1 expression is seen in the necrotic

and interdigital zones [117, 118]. The expression of mROR2 within the subset of chondrocytes at the growth plate and perichondrium suggests a functional role within the development of bones with cartilaginous anlage [119]. The potential role of mROR2 in limb/skeletal formation is underscored by the identification of mutations in hROR2. Mutations of hROR2 in the intracellular Ser/Thr domains, PRD or nonsense mutations have been linked to the dominant Brachydactyly Type B, characterized hypoplasia and/or aplasia of the hands and feet [120]. hROR2 mutations in the CRD, KRD, TKD, and residues immediately following TKD have also been associated with Robinow syndrome, a recessive short-limbed dwarfism [121, 122]. In late stages of mouse development, the expression of mROR1 and mROR2 is seen within the heart and alveoli of the lungs. Mice with homozygous knockout of *mROR2* exhibit shortened limbs, cyanosis, septal defects of the heart and die within six hours of birth due to respiratory defect [123]. Likewise, *mROR1*<sup>-/-</sup> mice have perinatally lethal defects due to respiratory dysfunction; however, these mice do not exhibit the pronounced heart or skeletal abnormalities. When researchers generated a *mROR1/mROR2*-deficient mouse, they found a more severe phenotype than *mROR2*<sup>-/-</sup> alone, leading the authors to conclude that mROR1/2 have a redundant, yet none overlapping function in development [124]. In late stages of embryonic development, the expression of mROR2 is sustained in the hippocampus and caudate putamen, but mROR1 is no longer detectable [117]. The temporal and localized expression of both mRORs within the developing nervous system underscores their function in neurogenesis.

CAM-1, the only ROR homolog in *C. elegans*, has been extensively studied in

neuronal cell migration, asymmetric division and axonal outgrowth. Mutations within the cysteine-rich FZD and truncating mutations before the kinase domain result in the inhibition of axonal outgrowth, suggesting a ligand-mediated function, but kinase activity may be dispensable. However, kinase activity is necessary for asymmetric neuronal division [97]. Additionally mutations in CAM-1 lead to defects specifically in canal-associated neurons. CAM-1 is considered a negative regulator of canonical Wnt signaling; excess EGL-20, a canonical Wnt ligand, mirrors the neuronal phenotype of CAM-1 mutants. The extracellular FZD is necessary and sufficient to mediate the antagonistic role for canonical Wnt during neuronal migration [100, 125]. The role of RORs in neuronal migration is seen in other species. The *Xenopus* homolog xROR2 inhibits convergent extension of the neuroectoderm via non-canonical Wnt signaling [112]. RORs have also been indicated in synapse formation. The *Aplysia* ROR homolog clusters on bag neuron cells suggesting organization of functional sites or synapses in *Aplysia californica* [114]. Downregulation of ROR1 or ROR2 via siRNA decreases synaptogenesis in primary mouse embryonic neuronal cultures. mROR1 and mROR2 can form heterodimers within human embryonic kidney (HEK) 293 cells that bind to the putative ligand Wnt5a. Treating the primary embryonic cells with Wnt5a increases synapse number in a dose dependent manner, suggesting a functional role of Wnt5a-ROR1/2 in synapse formation [104].

### ROR1 in Cancer

While ROR1 expression is present during normal embryonic and fetal

development, it is absent within most mature tissues. A low level of ROR1 expression is seen in adipose tissue and to a lesser degree in the pancreas, lung and a subset of intermediate B cells [126-128]. However, the expression of ROR1 has been seen in numerous blood and solid malignancies. This differential expression pattern, low ROR1 expression in adult tissue and high expression in cancer, has led investigators to examine the functional advantage conferred to cancer by ROR1 expression and to explore the use of immune-based therapies against ROR1 for targeting cancer cells. [126, 129-132]

### **ROR1 in Blood Malignancies**

Strong expression of ROR1 was initially identified in B-cell chronic lymphocytic leukemia (CLL). Primary CLL cells express high levels of ROR1, but not ROR2, expression and the expression of ROR1 was not modulated by CD40 or IL-4 stimulation [126]. A second research group independently identified ROR1 in CLL after *ex vivo* transduction of CD40 ligand (CD154) and autologous infusions of the transduced cells into advanced stage CLL patients. This transduction reversed the characteristic immunosuppression of CLL and resulted in the generation of antibodies against ROR1. Furthermore, the anti-ROR1 immunoglobulins were shown to bind specifically with CLL cells, while being unreactive towards peripheral blood mononuclear cells (PBMCs) from CLL patients and healthy donors [102]. The expression of ROR1 increases through the progression of CLL. Thus, ROR1 is not only a biomarker for CLL, but it may serve as a potential prognostic indicator for CLL [131]. Constitutive phosphorylation of STAT3 is a hallmark of CLL and

STAT3 has been shown to bind multiple sites in the ROR1 promoter. In addition, the expression of ROR1 could be induced by IL-6 in a STAT3-dependent and dose-dependent manner [133, 134]. As Wnt5a was shown to bind ROR1 in HEK293 cells, resulting in NF- $\kappa$ B activation (**Figure 4B**) in a reporter construct, ROR1 may be responsible for controlling self-expression [102].

Since the discovery of the elevated expression of ROR1 in CLL, increased levels of ROR1 have been described in a variety of hematological malignancies including acute lymphocytic leukemia (ALL), non-Hodgkin lymphomas (NHL), and myeloid malignancies [126, 131, 132, 135]. Specifically for NHLs, when compared to PBMCs, ROR1 mRNA and/or protein are elevated in all or a subset of primary samples of mantle cell lymphoma (MCL), marginal zone lymphoma (MZL), diffuse large B-cell lymphoma (DLBCL), and follicular lymphoma [131, 132]. A high level of ROR1 expression is seen in ALL patients, specifically those with the t(1;19)(q23;p13) translocation. ROR1 is identified to be important for the survival of ALL cells with t(1;19)(q23;p13) translocation when using an siRNA library for the tyrosine kinase screen critical tyrosine kinases for ALL pathogenesis [128]. Examination of the expression levels in normal and B cells at early developmental stages shows a lack ROR1 expression; however, normal B cells in an intermediate stage of development (large/small pre-BII and immature B cells) show relatively high levels of ROR1 expression, which is absent within mature B cells [127, 128]. Interestingly, t(1;19) ALL cells are generally characterized as residing in late stages of B cell differentiation, such as large/small pre-BII. Therefore, the presence of ROR1 in t(1;19) ALL cells may represent an arrested

intermediate stage during B cell maturation. ROR1 expression is upregulated at the pre-BII large stage may allow for the maintenance of pro-survival signaling through MEK/ERK activation, which would be otherwise absent during pre-BCR internalization [128].

### ROR1 in Solid Malignancies

High expression of ROR1 is also observed in a wide variety of solid malignancies. Tissue microarray analysis shows strong staining of ROR1 in 30% or greater of primary samples in colon, lung, and pancreatic cancers. However, moderate staining is detected in the majority of ovarian, lymphoma, skin, testicular, uterine, prostate and adrenal cancers [130]. An RNAi-based screening in HeLa cells identified an important role of ROR1 in regulating apoptosis [136]. In lung adenocarcinoma, NKX2-1 (TITF1) has been shown to drive ROR1 expression and the subsequent increase in ROR1 has two distinct proposed functions (**Figure 4B**). ROR1 allosterically potentiates EGF ligand-induced EGFR signaling and phosphorylates c-Src, regardless of ligand induction [109]. As previously mentioned, researchers have seen mild to moderate autophosphorylation of ROR1 [96, 108]. However, the autophosphorylation was not seen in immunoprecipitated ectopic ROR1 in COS-7 cells, leading to the conclusion that ROR1 is a pseudokinase. In the same study, phosphorylated ROR1 was identified in a number of cell lines. This phosphorylation was found to be mediated by MET (HGFR), but not EGFR or ErbB2 (**Figure 4B**). Within non-small cell lung cancer cells (NCI-H1993), silencing of ROR1 disrupts the ability to escape anoikis, anchorage-dependent programmed cell death, and decreased primary tumor growth when the cells are transplanted into nude mice.

[110]. In another study, Wnt5a, but not Wnt3a, binds to ROR1 which in turn recruits Frizzled 4 (FZD4) through FZD4's cysteine-rich domain. The transient localization allows FZD4-associated glycogen synthase kinase 3 $\beta$  (GSK3 $\beta$ ) to phosphorylate ROR1 on Ser/Thr residues [137]. Therefore, ROR1 may serve as a common node for kinase phosphorylation and allow for subsequent pathway activation through adaptor/effectector protein recruitment.

Segueing into breast cancer, ROR1 has been shown to be expressed in human neoplastic breast cancer cells, while remaining absent within stromal cells [129]. Furthermore, high expression of ROR1 is associated with higher grade and more aggressive disease. ROR1, when stimulated by recombinant Wnt5a, interacts with CK1 $\epsilon$ , whose subsequent interaction with phosphoinositide 3-kinase (PI3K) results in the phosphorylation of AKT and CREB [129]. High levels of ROR1 expression in patients and cell lines are associated with genes involved in EMT such as ZEB1 and vimentin, and inversely associate with adherent junction proteins. Silencing of ROR1 in triple-negative-derived cell lines reduces EMT genes, SNAI1, SNAI2, ZEB1, and vimentin (**Figure 4B**). In MDA-MB-231 cells, a triple negative breast cancer cell line, knockdown of ROR1 by small hairpin (sh) RNA reduces *in vitro* cell migration and bone and lung foci size in xenografts [138].

Although protein levels of ROR1 are low or undetectable within the kidney of healthy individuals, *ROR1* mRNA can be detected in 81.3% of tissue samples and 94% of PBMCs samples from renal cancer patients as determined by RT-PCR [139]. Furthermore, PBMCs from renal cancer patients showed significantly higher ROR1

expression, compared to healthy controls. While these findings suggest that ROR1 expression is a hallmark of renal cancer, it is important to note that the protein levels of ROR1 are not measured in this study. The expression of ROR1 is detected in multiple melanoma cell lines, as assessed by RT-PCR, western blot, and flow cytometry. Silencing ROR1 in melanoma cell lines tested induces apoptosis [140]. An interesting paradigm has been suggested in melanoma cell lines where transcriptomic analysis of a melanoma cell lines reveal expression of ROR1 correlates with proliferative signatures, but also correlates with a non-invasive phenotype. Treatment of poorly invasive cell lines with Wnt5a leads to a significant decrease in ROR1 expression and overall protein level. Interestingly, silencing ROR1 leads to an increase in Wnt5a and ROR2 expression, and a more invasive phenotype. The ROR1 and ROR2 expressions are differentially regulated under hypoxic conditions that leads to decreased ROR1 expression and increased expression of ROR2 [141].

### **ROR1, a Target of Immunotherapies**

The discovery of ROR1 expression in CLL and other cancers has informed a diverse array of research on immuno-based strategies to target ROR1 [102, 126]. In CLL, there are an estimated  $1-7 \times 10^4$  ROR1 molecules on the surface, which is 10-100-fold lower than conventional targets of monoclonal antibody (mAb) therapies. Thus, the results from *ex vivo* analyses of mAbs against ROR1 in CLL have been mixed. A number of studies have reported anti-ROR1 induces ROR1 internalization [126, 131, 142, 143]. Low levels of antibody-dependent cellular cytotoxicity (ADCC) and even lower

complement-dependent cytotoxicity (CDC) have been reported in primary CLL samples and MCL cell lines treated with anti-ROR1 mAbs [142, 143]. In contrast, several mAbs directed against the FZD and KRD of the extracellular region possess high levels of cytotoxicity in primary CLL samples. These FZD/KRD-specific mAbs exhibit a significantly greater cytotoxicity than primary CLL samples treated with rituximab, an FDA-approved mAb against CD20 [131]. In breast cancer, inhibiting ROR1 by a mAb reduces metastatic foci in lungs assessed by bioluminescence and histology with xenografts of MDA-MB-231 cells [138]. Within melanoma cell lines, treatment with anti-ROR1 mAb results in varying degrees of apoptosis, between 4% and 54%, which is dependent upon the specific anti-ROR1 mAb and melanoma cell lines. This can be attributed partially to the antibody-mediated CDC and/or ADCC. Importantly, treatment of anti-ROR1 mAb, either directly or through CDC or ADCC, has no effect on apoptosis in the ROR1-negative cell line T47D [140]. Research into immunotoxin therapies has been moving forward as well. A ROR1-immunotoxin has been generated with the Fc region of an anti-ROR1 monoclonal antibody has been fused to PE38, a modified exotoxin from *Pseudomonas*. The immunotoxin exhibits similar specificity for ROR1 in MCL cell lines, but has a higher rate of dissociation from the receptor after internalization, which may be a limiting factor for translation into clinical studies [143]. Another approach also has been developed by the transduction of T cells with a ROR1-chimeric antigen receptor (ROR1-CAR) from healthy individuals to CLL patients. These ROR1-CAR T cells can recognize tumors cells and lyse primary CLL and MCL cells. The limitation to this approach is observed in the same study. While there is no ROR1 expression in hematopoietic progenitors, ROR1 is

expressed in the median stages of B-cell maturation, in thymus-derived CD8+ and CD4+ T cells, adipose tissue and adult lungs. This warrants further study of its toxic effect for clinical usage [127, 128].

### **Purpose of Study**

The identification and characterization of tumor-initiating cells (TICs), an inclusive term referring to both cell-of-origin and CSCs, is a focus in cancer research. A greater understanding of TICs represents potential improvements at every stage of clinical management for cancer care. Within this vein of cancer research, it provides the potential to identify women at greater risk for breast cancer beyond familial mutations, to increase specificity and sensitivity of screening techniques, and to target disease-promoting cells in order to limit the growth/relapse/metastatic potential of cancer [144].

The cell-of-origin(s) for HER2+ tumors have not been clearly defined. From work with MMTV-ErbB2 TG mouse, both MaSC and LP have been theorized and tested to be the cell populations responsible for ErbB2-driven tumorigenesis. Despite the enrichment of CD61<sup>+</sup> cells in spontaneous tumors from MMTV-ErbB2 TG mice, when cell populations were isolated and transplanted into fatpads, MaSC-derived tumors had larger volumes and greater incidence than LP-derived tumors [40-42]. To date, researchers have looked at the self-renewal capacity and tumorigenic potential of these two cell populations, but have not looked at the differences in genetic expression in tumors derived from ErbB2-driven MaSCs and LPs. Understanding the genetic differences between MaSC-derived

and LP-derived tumors has the potential to better frame the conclusions for the cell-of-origin in ErbB2/HER2+ tumors. More so, understanding the differential gene expression profiles of these tumors could help further to elucidate the incipient stages of breast cancer development, transition into CSCs, and to improve screening techniques.

CSCs have an established role in establishing breast cancer when transplanted into immunodeficient mice and promoting cancer progression [50, 57, 67]. However, targeting CSCs has failed due to both the innate resistance of CSC to therapy and increased ability of CSCs to escape therapy [59-66]. Recently, the Cancer Genome Atlas (TCGA) initiative by the National Cancer Institute (NCI) has released multiplatform data from 1063 breast cancer samples and normal samples (BRCA) [24]. Intriguingly, the TCGA dataset can be assayed to identify genes within the Wnt signaling pathway vital for self-renewal and aberrant in breast cancer that may play a central role in tumor progression, but also may serve as a target for therapy.

### **Specific Aims**

1. Characterize ErbB2 tumors derived from MaSC and LP TICs and determine if Wnt5a is acting as a tumor suppressor in the ErbB2 model.
2. Determine the role of ROR in driving epithelial-mesenchymal transition and develop novel immunotoxin to target ROR1 for cancer therapy.

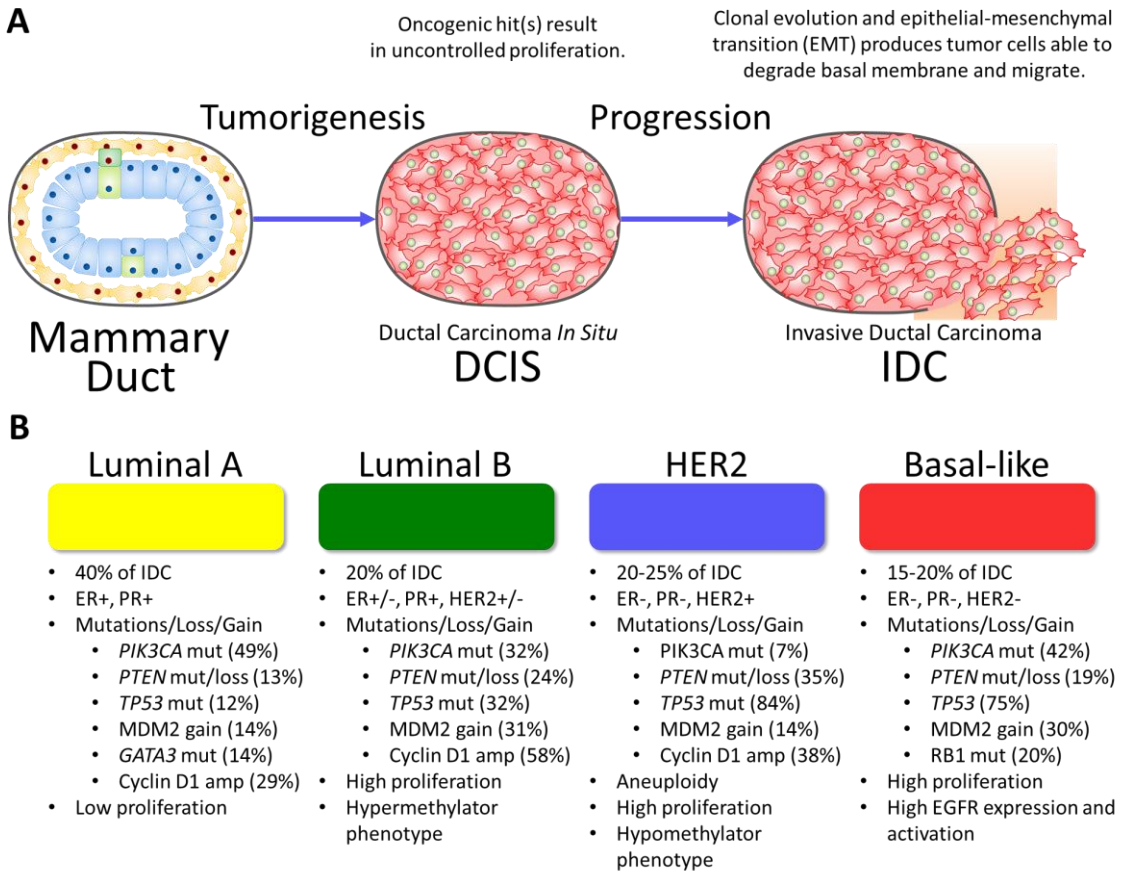


**Figure 1: Model for Breast IDC and Molecular Subtyping. A.** A schematic for the initiation and progression of breast tumorigenesis. Oncogenic hit(s) in cell of the normal mammary duct results in dysplasia and DCIS. A subset of DCIS progress via clonal evolution and EMT to produce invasive disease. **B.** Summary of the comprehensive molecular portraits of IDC based on molecular subtypes [24].

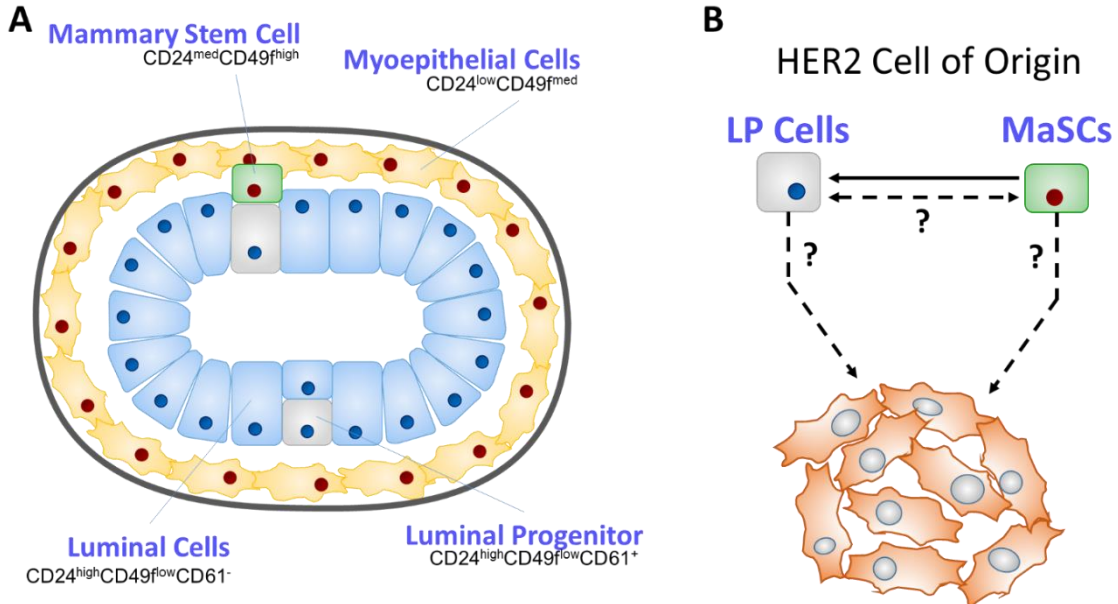


**Figure 2: Cell-of-Origin for HER2+ Breast Cancer.** **A.** The virgin mouse mammary gland is comprised of 4 distinct populations that can be identified with surface markers: Lin<sup>-</sup> CD24<sup>high</sup>CD49<sup>flow</sup>CD61<sup>-</sup> mature luminal cells (LC), Lin<sup>-</sup>CD24<sup>high</sup>CD49<sup>flow</sup>CD61<sup>+</sup> luminal progenitor (LP) cells, Lin<sup>-</sup>CD24<sup>low</sup>CD49<sup>fmed</sup> myoepithelial cells (Myo), and Lin<sup>-</sup> CD24<sup>med</sup>CD49<sup>fhigh</sup> mammary stem cells (MaSC). **B.** Both MaSCs and LP cells have been theorized to be the cell-of-origin for HER2+ breast cancer.

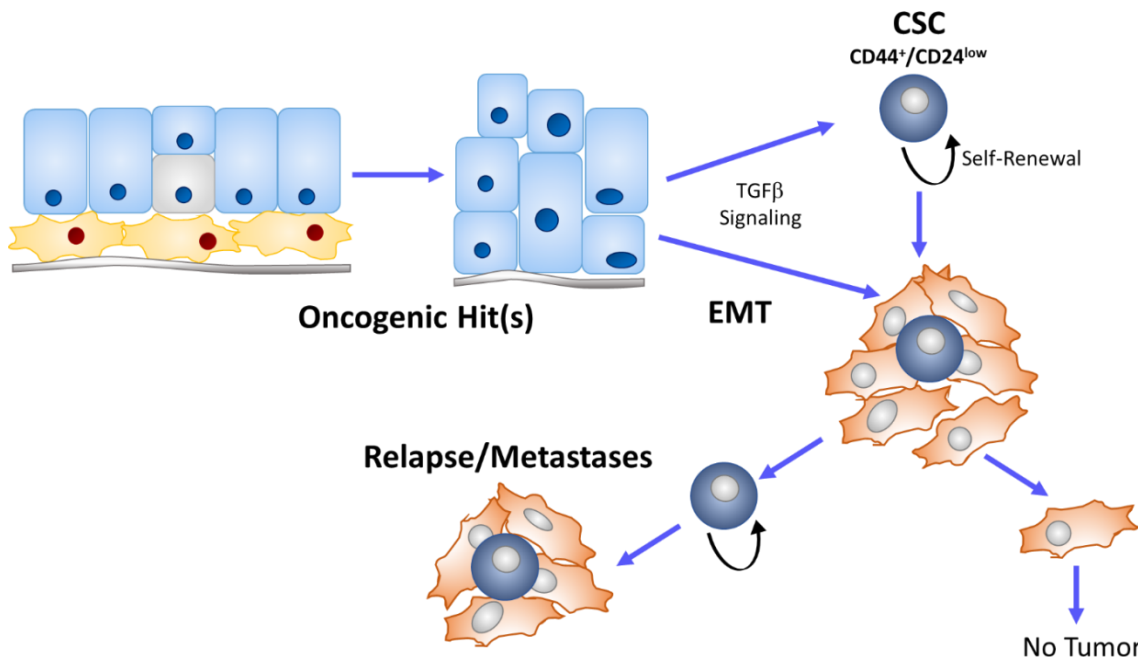


**Figure 3: Cancer Stem Cells (CSCs), EMT, and Breast Cancer Progression.** Normal human mammary epithelial cells undergo a series of oncogenic hits that result in uncontrolled proliferation, dysplasia and *in situ* tumors. Cells from *in situ* tumors lack the ability to degrade/invoke through the basement membrane, and survive outside the resident tissue of the mammary duct. Epithelial-mesenchymal transition (EMT) is a multifaceted signaling and genetic program by which cancer cells acquire phenotypic changes to produce invasive cells. Cancer cells that have undergone EMT share features of cancer stem cells, including gaining cancer stem cell markers, having self-renewal ability, and forming tumors in mice. Both post-EMT cancer cells and cancer stem cells are proposed to be important for recurrence and metastasis of cancer.

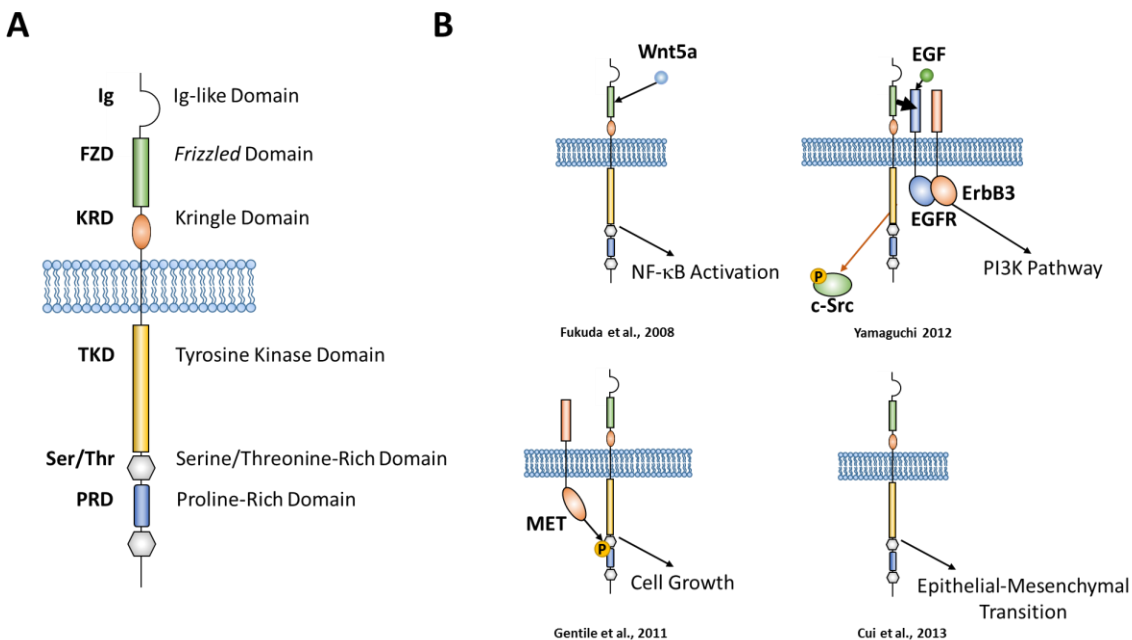


**Figure 4: ROR1 Structure and Signaling in Cancer.** **A.** Human ROR1 consists of an immunoglobulin-like domain (IG), two cysteine-rich domain, *frizzled* (FZD) and kringle domain (KRD). On the intracellular side, ROR1 possesses a tyrosine kinase domain (TKD), two serine/threonine-rich domains (Ser/Thr) and a proline-rich domain (PRD). **B.** ROR1-mediated signaling has been reported in a number of cell lines. Wnt5a, the ligand of ROR1, increased NF-κB activation in HEK293T cells expressing ROR1. In lung adenocarcinoma cell lines, ROR1 is able to phosphorylate c-SRC and through allosteric interaction of the FZD with EGFR magnify the EGF-induced signaling. Alternatively, in lung carcinoma and gastric carcinoma cell lines, ROR1 is phosphorylated by MET; the silencing of ROR1 impairs cell growth. In MDA-MB-231 breast cancer cells, ROR1 expression is highly associated with EMT genes and the silencing of ROR1 reduces the ability of MDA-MB-231 cells to form metastatic foci.

## CHAPTER II

### CHARACTERIZATION OF ERBB2 MASC AND LP TUMORS

#### Rationale

The cell-of-origin is a cell or cells that undergo a series of oncogenic hits: the physical or functional loss of tumor suppressors, genomic amplification through abortive replication attempts, epigenetic changes, or gain-of-function mutations in proto-oncogenes [145]. The array of mechanisms that drive or bolster the initiation of a tumor can be simplified through understanding the population of cells responsible for initial steps of tumorigenesis. Furthermore, understanding the cells responsible for tumor initiation can improve clinical strategies for risk reduction, early detection, and primary prevention, especially as genomic medicine establishes a greater presence in clinical care [144].

High-throughput transcriptomics have been used to characterize individual genetic patterns of breast cancer patient samples, predict clinical outcomes, and delineate genes involved in metastasis [21-24]. The same techniques can be used to describe genetic differences of breast tumors that have been initiated from different cell populations of the mammary gland. Previous studies have reported conflicting conclusions on the cell-of-origin for ErbB2/HER2 tumors in mice. Whereas ErbB2-TG MaSC-derived tumors give rise to larger tumors after syngeneic transplant, spontaneous ErbB2 tumors and clonogenic assays are enriched for LP cells [40-42]. To date, no research group has examined genetic profiles of ErbB2-driven breast tumors derived

from MaSCs and LPs. With the release of TCGA multiplatform data for breast cancer (BRCA) dataset, computational characterization of MaSC- and LP-derived tumors can be used to evaluate the similarity of LP and/or MaSC tumor models with HER2+ breast cancer samples [24].

This chapter will address differences in transcriptomes of ErbB2-TG MaSC- and LP-derived tumors using computational biology. The differences in expression will be used for pathway analysis associated with proliferation and prognosis. In addition, these genetic expression patterns will be correlated with HER2+ human samples in order to assess the proximity of MaSC- and LP-derived ErbB2-driven tumors to HER2+ human patients. Using the *in silico* assessment for the HER2+ cell-of-origin, we will further focus on Wnt5a, one of differentially expressed genes to study its potential suppressive role in mammary tumorigenesis *in vitro* and *in vivo*. We will also attempt to examine the involvement of Wnt5a-mediated signaling pathways in its tumor-suppressive function.

## **Materials and Methods**

### **RNA Isolation and Microarray**

Tumors were generated from a previous study [40] where individual cell populations of ErbB2-TG cells from the preneoplastic mammary gland were injected into a mammary fat pad of FVB/N female mice. Tumors (20 mg) were homogenized with a glass mortar and pestle on ice directly into RLT buffer (QIAGEN, Venlo, Limburg, Netherlands). RNA was isolated using the RNeasy Plus mini kit (QIAGEN), according to the manufacturer's instruction. RNA quality was assessed by Agilent 2100 Bioanalyzer.

Briefly, 100 ng of RNA was submitted to the Genomics Division for cDNA synthesis and *in vitro* transcription, converting RNA to Biotin-aRNA using the Epicentre Target AMP-Nano labeling Kit (Illumina San Diego, CA). Converted Biotin-aRNA was purified with RNeasy MinElute cleanup column (QIAGEN) according to the instruction by Epicentre. In Illumina hybridization buffer, 750 ng of Biotin-aRNA and were placed onto Illumina Mouse WG-6 v2.0 Beadchip (Illumina) at 58° C for 17 h with oscillation. Succeeding hybridization, the arrays were washed, blocked with Illumina Direct Hybridization Kit, and stained with streptavidin-Cy3 (Amersham/GE Healthcare, Piscataway, NJ) according to Illumina Direct Hybridization Assay protocols. Beadchips were assayed with the Illumina iScan System and data was collected using GenomeStudio software v2011.1.

### **Microarray Data Processing and Analyses**

Microarray data was quantile normalized and transformed into log2 expression by the Genomics Division. Transcriptome heatmap and the heatmap for differentially-expressed genes (DEG) were generated in R using the gplots package. The volcano plot was made in R using the ggplot2 package. Fold change was found by the average log2 expression difference in paired MaSC-derived and LP-derived tumors. Significance was evaluated using a paired T-test and plotted as –log10 (P-value). Genes highlighted in the volcano plot have a P-value <0.05 and an average log2 fold change of > 1.58 or 3-fold in linear fold change. Gene Set Enrichment Analysis (GSEA) (<http://www.broadinstitute.org/gsea/index.jsp>) was conducted comparing MaSC-derived and LP-derived expression data as previously described [146]. RNA isolated from

tumors (above) was reversed transcribed into cDNA with iScript cDNA Synthesis Kit (Bio-Rad, Hercules, CA), as per manufacturer's instruction. PCR was performed with iTaq Universal SYBR Green Supermix (Bio-Rad) in a 15 µl reaction volume with primers for genes identified differentially expressed in the microarray (**Table 1**).

### **Human Patient Sample Corroboration**

Altered expression of Log2 1-fold DEGs in MaSC- and LP-derived tumors were examined in HER2 human patient samples (n=58) in the TCGA [24]. The cBio Cancer Genomics Portal (<http://www.cbiportal.org/public-portal/>) was used for the visualization of human patient samples [147]. The DEGs were then ranked by percentage of HER2+ patient samples with mRNA upregulation ( $Z > 1.96$ ) or genomic amplification (GISTIC2 = 2). The expression of the top 20 genes represented in HER2+ patient samples were collated into MaSC and LP signatures using the TCGA level 3 AgilentG4502A microarray expression. Samples were combined with level 3 Biotab clinical information downloaded from the Cancer Genome Atlas DCC (available at <https://tcga-data.nci.nih.gov/tcga/>). For survival curves, samples were divided into tertiles (n=177) based on expression of the gene and overall survival information from the Biotab clinical information, comparing the highest signature expression tertile to the lowest tertile.

### **Other Genomic Techniques Used in Analysis**

Survival curves for individual genes were generated with level 3 AgilentG4502A

microarray gene expression and with level 3 Biotab clinical information. Copy number aberration and expression analysis were done using centralized level 3 Illumina HiSeq 2000 RNAseq for 962 completed primary tumor samples and GISTIC2 threshold method for copy number estimates. Data was downloaded at <https://genome-cancer.ucsc.edu>.

### **Immunohistochemistry**

Mouse tissues were collected in previous experiments [40]. Human breast carcinoma tissues embedded in paraffin were obtained from the University of Iowa Tissue Procurement Core. Both human and mouse tissues were deparaffinized in xylene. For the mouse tissues, antigens were retrieved with Antigen Unmasking Solution (Vector Laboratories, Burlingame, CA) at 95° C for 1 hour, followed by 30 minutes of temperature equilibration in room temperature water. Human tissues antigens were retrieved with S1700 (Dako, Glostrup, Denmark) at 95° C for 1 hour, followed by 20 minutes in 1:2 dilution of room temperature water and the S1700 antigen solution. Slides were stained overnight at 4° C with Wnt5a antibody (Genetex, Zeeland, MI) at a 1:200 dilution. Human tissue samples stained for Wnt5a were rinsed and incubated with Rabbit on Rodent HRP-Polymer (Biocare Medical, Concord, CA), while mouse tissue utilized anti-Rabbit-HRPO. Both tissues were counterstained with hematoxylin.

### **Mammospheres**

Mammary glands were harvested and cut into 2mm<sup>3</sup> pieces. The fragments were digested with 300 µg/ml collagenase and 100 µg/ml hyaluronidase (Stemcell,

Vancouver, BC, Canada) for 16 hr. in 2% FBS-containing HBSS at 4° C, followed by 1 hr. incubation at 37° C with oscillation at 250 RPM. After digestion tissues were resuspended in 0.25% trypsin-EDTA (Mediatech, Corning, NY) for 3 min. In 2% FBS-containing HBSS, 5 µg/ml dispase I (Stemcell) and 0.1 µg/ml DNase I (Worthington, Lakewood, NJ) was diluted and cells were exposed to solution for 1 min. Cells were filtered through 40 µm mesh and resuspended in 2% FBS-containing PBS. Filtered mammary epithelial cells were stained with antibodies and magnetically purified using a Mammary Epithelial Cell Enrichment Kit (Stemcell) to remove lineage-positive (CD45-, CD31-, and Ter119-positive) cells. From the single-cell suspension, 1000 cells were placed in each well of a Poly-HEMA-coated 24-well plate. Cells were maintained in 1 mL/well of F12 medium with 20 ng/mL EGF, 20 ng/mL bFGF, and 4 µg/mL heparin. Recombinant Human/Mouse Wnt5a (R&D Systems, Minneapolis, MN), diluted in PBS, was added to half of the wells, at a concentration of 100 ng/mL. Mammospheres were counted and imaged after 7 days of incubation.

### **Cell Lines and Culture**

HMLE cells were maintained in RPMI supplemented with 10% FBS and 1% Penicillin and Streptomycin (Life Technologies, Carlsbad, CA). Wnt5a (R&D) time course was conducted at 100 ng/ml. Treated HMLE cells were lysed in cell lysis Buffer (50 mM Tris-HCL pH7.5, 1 mM EDTA, 1 mM EGTA, 1% Triton X-100, 100 mM KCl, 50 mM NaF, 10 mM Na 2-glycerophosphate, and 1 mM Na<sub>3</sub>VO<sub>4</sub>). The lysates were diluted to 1 µg/µL in SDS and separated via SDS-PAGE. SMAD 1/2/3 (Santa Cruz Biotechnologies, Dallas, TX)

and p-SMAD2/3 (Cell Signaling Technology, Beverly, MA) antibodies were used to probe the lysates. RNA from treated HMLE cells was isolated using RNeasy Mini Plus kit (QIAGEN) and reverse-transcribed with iScript cDNA Synthesis Kit (Bio-Rad) per manufacturer's instructions. PCR was performed with iTaq Universal SYBR Green Supermix (Bio-Rad) in a 15 µl reaction volume with cyclin D1 forward primer: 5'-GCTGCGAAGTGGAAACCATC-3' and reverse primer: 5'-CCTCCTTCTGCACACATTGAA-3'. CTNNB1 forward primer: 5'-CCTCAGATGGTGTCTGCTATTG-3' and reverse primer: 5'-CCTCCATCCCTCCTGTTAG-3'.

### **Wnt5a ErbB2 Transgenic Mice**

Mice were maintained under according to University of Iowa IACUC guidelines. *MMTV-ErbB2* TG mice [148] were intercrossed with B6;129S7-Wnt5a<sup>tm1Amc</sup> mice [149]. Homozygous deletion of Wnt5a is perinatally lethal, thus the resulting ErbB2 TG heterozygotes and WT Wnt5a mice were maintained to evaluate tumorigenesis. Tumors were monitored weekly after two weeks of initial palpable presentation.

### **Statistical Analysis**

Data are presented as mean values ± SD for bench results and mean values ± 95% CI for genomics data, unless indicated otherwise in the figure. Welch's T-test was used for genomic results, while student's T-test was used for the remaining experiments. Mantel-Cox log-rank test was used for survival curve analysis. Analyses were performed on R (<http://www.r-project.org/>) and Prism (GraphPad, San Diego, CA).

## Results

### **Delineation of LP- and MaSC-Derived Tumors**

Both LPs and MaSCs from ErbB2 TG mice have the capacity to give rise to tumors [40-42]. Despite the enrichment of CD61<sup>+</sup> cells in tumors and clonogenic assay, in paired syngeneic transplants of ErbB2-TG MaSC and LP cells, MaSC gave rise to larger tumors and at a greater incidence [40]. RNA from these paired LP-, MaSC-, and Myo-derived tumors were isolated and underwent transcriptomic analysis (**Figure 5A**). LP- and MaSC-derived tumors had distinct RNA expression patterns. Interestingly, two Myo-derived tumors clustered with LP-derived, while a third clustered with MaSC-derived tumors (unsupervised clustering not shown). When Gene Set Enrichment Analysis (GSEA) was conducted using the microarray data for MaSC and LP tumors, MaSC-derived tumors were enriched for 7 mesenchymal/fibroblastic genesets (**Figure 5B, C**). In addition, MaSC-derived tumors had higher enrichment scores in proliferation (3) and poor prognosis (4) gene sets (**Figure 5C**). To identify principle genes that could drive the differences in GSEA results, we plotted average difference in log2 expression (log2 Fold Change) and –log10(P-value). A total of 54 differentially-expressed genes (DEGs, **Table 1**) were found to have a 1.58 log2 fold change (3-fold linear change) and P-value < 0.05 (**Figure 5D,E**).

To confirm the expression results from the microarray, we used the previously isolated RNA from LP- and MaSC-derived tumors for RT-PCR and used select primers (**Table 2**) from our DEG list. Despite relative mRNA expression variation in MaSC tumors, RT-PCR results showed consistant differential-expression in LP and MaSC tumors (**Figure**

**6A).** In order to further characterize LP and MaSC tumors, we compared one-fold (log2) DEGs to TCGA data for HER2+ breast cancer samples (n=58). Genes that were upregulated in MaSC tumors showed greater percentage of mRNA upregulation or genomic amplification in HER2 patient samples than genes upregulated in LP tumors (**Figure 6B**). The DEGs with the highest upregulation in HER2+ patients were used to generate LP and MaSC signatures. The survival across all molecular subtypes was worse for samples with the highest expression of the MaSC signature relative to the lowest MaSC signature expression, 18.6% versus 48.6% overall survival, respectively (**Figure 6C**). In contrast, samples that varied in expression of the LP signature did not have significant difference in overall survival (**Figure 6C**). Taken together, MaSC-derived tumors have a greater incidence, larger volume, more aggressive pathway enrichment, and greater genetic resemblance to HER2+ patient samples. In addition, using a rank-based signature in human breast cancer patients, the MaSC signature had a worse prognosis than the LP signature.

### **Loss of Wnt5a in MaSC and Human Breast Tumors**

To further elucidate the variance seen in tumorigenicity [40] and GSEA results in MaSC- and LP-derived tumors, we focused further on studying the Wnt pathway. Wnt5a expression was observed to be 5.78-fold lower in MaSC tumors compared to LP tumors (**Figure 7A**). Furthermore, Wnt5a expression decreased through spontaneous ErbB2 tumor progression (**Figure 7B**). The normal mammary gland and early tumors (5-6 months) have strong immunohistochemical (IHC) staining for Wnt5a. In contrast, late

tumors (7-8 months) and lung metastasis have low to negligible level of Wnt5a expression. In order to further show that decreased Wnt5a is not an artifact of our murine model, we examined Wnt5a mRNA expression via TCGA microarray results for HER2+ tumors. When compared with normal tissue samples, HER2+ primary tumor samples had reduced levels of Wnt5a mRNA expression in Stage II-IV tumors, mirroring our ErbB2 spontaneous tumor IHC results (**Figure 7C**). Survival data from TCGA BRCA dataset without regard to molecular subtype revealed that breast cancer patients with the lowest mRNA levels of Wnt5a had significantly lower 10-year overall survival percent than compared with the highest Wnt5a expression tertile (**Figure 7D**).

Histopathologic analysis of human breast tissue samples shows a similar decrease in Wnt5a protein when comparing normal mammary ducts to adjacent malignant cells (**Figure 8A**). Interestingly, unlike the murine mammary gland where Wnt5a stains strongly in the basal and luminal compartments (**Figure 7B**), Wnt5a expression in human patient samples is at the luminal interface of the mammary duct (**Figure 8A, B**). Low levels of Wnt5a expression, 60% and 75% of samples, were seen in TNBC and HER2+ tumor samples, respectively (**Figure 8B, C**). In all of the TNBC and HER2+ tumor samples assayed, there was lower expression of Wnt5a than adjacent normal mammary ducts. In contrast, ER+ tumor samples were more variable for Wnt5a expression, where 50% of ER+ tumor samples had maintained expression of Wnt5a (**Figure 8B, C**). The diversity of expression for Wnt5a in ER+ histological samples conformed with our findings in the TCGA BRCA dataset, with a subset of luminal A and B breast tumor samples expressing high levels of Wnt5a mRNA (**Figure 8D**).

We were interested in the mechanism that leads to reduced Wnt5a expression in both ErbB2-TG model and patient samples from the TCGA and IHC. We assayed both methylation (data not shown) and copy number aberration (CNA) data from the BRCA TCGA dataset. We found that CNA of Wnt5a is common in breast cancer, accounting for 31.1% of 962 tumor samples (**Figure 9A**). The heterozygous or homozygous deletion of Wnt5a results in median 1.64- and 1.71-fold reductions in mRNA expression, respectively, when compared with the mRNA of Wnts5a with intact copy number (**Figure 9B**). The loss of Wnt5a is common in various malignancies, accounting for greater than 20% of cases in 19 different malignancies in the TCGA (**Figure 9C**). Prominently, the heterozygous or homozygous loss is seen in: Kidney Renal Clear Cell Carcinoma (88.3%), Head and Neck Squamous Cell Carcinoma(77.8%), Uterine Carcinosarcoma (Provisional, 67.3%), Lung Squamous Cell Carcinoma (61.2%), Cervical Squamous Cell Carcinoma and Endocervical Adenocarcinoma (Provisional, 58.3%), Bladder Urothelial Carcinoma (32.3%), Ovarian Serous Cystadenocarcinoma (32.3%), Stomach Adenocarcinoma (28.3%), and Breast Invasive Carcinoma (25.5%) published or soon-to-be published TCGA datasets (**Figure 9C**).

### Tumor Suppressive Effects of Wnt5a

To identify the mechanism for Wnt5a-mediated tumor suppression and the potential selection pressure for CNA in breast cancer, mammary epithelial cells were isolated from preneoplastic ErbB2 TG mice. Individual cell suspensions were used to perform mammosphere assays (**Figure 10A**). After 7 days of incubation, untreated

epithelial cells had an average of 42.3 spheres per well, while Wnt5a-treated (100 ng/mL) wells had an average of 11.7 spheres (**Figure 10B**). Wnt5a not only reduced the mean number of spheres per 1000 cells by 30.7, but also reduced the size of mammospheres in the Wnt5a-treated wells (**Figure 10A**). Mechanistically, treatment of Wnt5a (100 ng/mL) in HMLE cells, immortalized human mammary epithelial cells, induced the phosphorylation of SMAD prominently at 30 minutes and 1 hour post-treatment (**Figure 10C**), a known TGF $\beta$ -downstream signaling molecule. TGF $\beta$  signaling has established functions in inhibiting tumor initiation and early development stages. To further examine the tumor-suppressive role of Wnt5a, HMLE cells were treated for 4 or 8 hours with Wnt5a (100 ng/mL). Among many genes we screened by real-time PCR, Cyclin D1 and  $\beta$ -catenin were significantly downregulated by Wnt5a treatment. Cyclin D1, important for G1-S phase progression, reached a nadir (> 3-fold reduction) at 8 hours of exposure to Wnt5a (**Figure 10D**). In addition,  $\beta$ -catenin, with known function in classical Wnt signaling and maintaining stem cell self-renewal, had a nearly 3-fold reduction in mRNA levels after the 4-hour treatment with Wnt5a, rebounding at the 8-hour time point (**Figure 10D**). We thus reason that Wnt5a inhibits tumorigenesis via promoting tumor-suppressive TGF $\beta$ /SMAD signaling and inhibiting tumor-promoting Wnt/ $\beta$ -catenin and cyclin D1.

With nearly a third of breast cancer patients with mono- or bi-allelic loss of Wnt5a, we wanted to examine the effect of Wnt5a heterozygous loss in the ErbB2-tumorigenesis (**Figure 11A**). Over the course of 12 months, tumors developed in 5 of the ErbB2/Wnt5a $^{+/-}$  mice, but only in 1 ErbB2/Wnt5a $^{+/+}$  mouse. Unfortunately, direct

comparison of tumor volume and growth cannot be conducted due to lack of spontaneous tumors in the negative control Wnt5a<sup>+/+</sup> mice. Despite this limitation, the heterozygous loss of Wnt5a produced a pronounced pervasive disease, with secondary and tertiary palpable tumors at the time of sacrifice (**Figure 11B**). Our previous cohorts of ErbB2 TG females normally don't give rise to histological nodules until the primary tumors reach 2.5 cm. With our current protocol that only allows 2 cm tumors, we have never detected lung metastasis before. Here we found all four ErbB2/Wnt5A<sup>+-</sup> having histologically detectable metastasis in the lung (**Figure 11C**). This study will continue to evaluate overall tumor incidence, growth, and metastasis in ErbB2/Wnt5a<sup>+/+</sup> and ErbB2/Wnt5a<sup>+-</sup> ErbB2 TG mice.

### **Discussion**

The spectrum of diseases that comprise breast cancer can be categorized using genetic patterning. The four extensively-characterized molecular subtypes including luminal A, luminal B, HER2, and basal-like breast cancer suggest a commonality in not only the steps leading to invasive diseases, but potentially a common cell-of-origin for individual subtypes [20-23]. HER2+ IDC is thought to be an aggressive subtype of breast cancer, accounting for 20-25% of all diagnoses. High level of mutations, as a result of TP53 mutation (75%) or gain of MDM2 (30%) with characteristic genomic instability/aneuploidy, contribute to the aggressive phenotype of HER2+ IDC [24]. However, this genomic instability also contributes to obscuring the nascent stages of HER2+ tumorigenesis. Early work has shown mammary glands and spontaneous HER2

tumors are enriched for CD61<sup>+</sup> cells, the cell population used to define LP in the mammary gland. When unsorted mammary epithelial cells from MMTV-ErbB2 TG mice were used in mammosphere assay, there was an enrichment of CD61<sup>+</sup> LP cells [41, 42]. These observations have led to the conclusion by some researchers that LP cells are the cell-of-origin for HER2+ tumors. Another laboratory identified parity-identified mammary epithelial cells (PI-MEC), a bi-potent progenitor cells in the luminal compartment of the mammary glands, as the cell-or-origin for HER2+ tumors [150]. However, the early foundation of PI-MEC is the high CD49f staining, the cell surface marker used to define basal epithelial cells and MaSC. The CD49f<sup>high</sup> PI-MEC were also identified as the cell-of-origin for HER2+ tumors from the same research group that lay the ground for identification of PI-MEC [151]. Recently, our lab has shown for the first time that both MaSC and LP from ErbB2-TG mice are able to give rise to tumors with MaSC as the major cell-of-origin for HER2+ tumors [40]. Interestingly, the PI-MECs and MaSC are located in the terminal duct lobular unit, the primary secretory structure of the human mammary gland [36, 150]. Intriguingly, the self-renewal capacity of PI-MECs is sensitive to TGFβ, analogous to the inhibition of TGFβ exerted on the terminal end buds within mice [94, 152]. As Wnt5a is downstream of TGFβ signaling in the mammary gland, tumor outgrowth from the PI-MEC or MaSC may be enhanced or a product of the heterozygous deletion of Wnt5a.

Decreased Wnt5a expression has been previously associated with increased risk of breast cancer relapse and accelerated tumor growth, with implications in the antagonism of β-catenin stabilization [94]. In TNBC and HER2 clinical samples and ErbB2

tumor samples, Wnt5a expression was substantially decreased. Owing to the complexity of noncanonical Wnt signaling, the mechanism for the repression of tumorigenesis by Wnt5a has not been fully explored. Wnt5a abrogates self-renewal capacity of primary ErbB2-TG cells, potentially through the activation of the SMAD pathway and decrease in cyclin D1 and  $\beta$ -catenin mRNA. As the HER2+ subtype is characterized by high levels of aneuploidy and genomic amplification of cyclin D1, heterozygous loss of Wnt5a may be another mechanism to increase cyclin D1 expression and subsequent cell cycle proliferation [24]. Despite the implications that TGF $\beta$  signaling induces Wnt5a, we have shown a putative positive feedback loop as Wnt5a leads to SMAD activation, a hallmark of TGF $\beta$  signaling and negative regulator for self-renewal of tumor-initiating cells.

Interestingly, within the ErbB2 background, the heterozygous loss of Wnt5a produced a trend towards greater tumor incidence/accelerated presentation and enhanced metastasis. This is counterintuitive for two reasons: primarily, noncanonical Wnt signaling should enhance cell migration through the regulation of the cytoskeleton of a cancer cell [153]. Secondly, we have shown in this chapter, Wnt5a can activate the SMAD pathway, which plays a major role in driving metastasis in intermediate and late stage breast cancer [154-157]. In summary, the function of Wnt5a as a breast cancer tumor suppressor is more complex than the antagonism of  $\beta$ -catenin stabilization. With the heterozygous and homozygous loss of Wnt5a seen in greater than 20% of samples in 19 TCGA datasets, the tumor suppressive role of Wnt5a is likely to vary based on receptor expression, but requires further study.

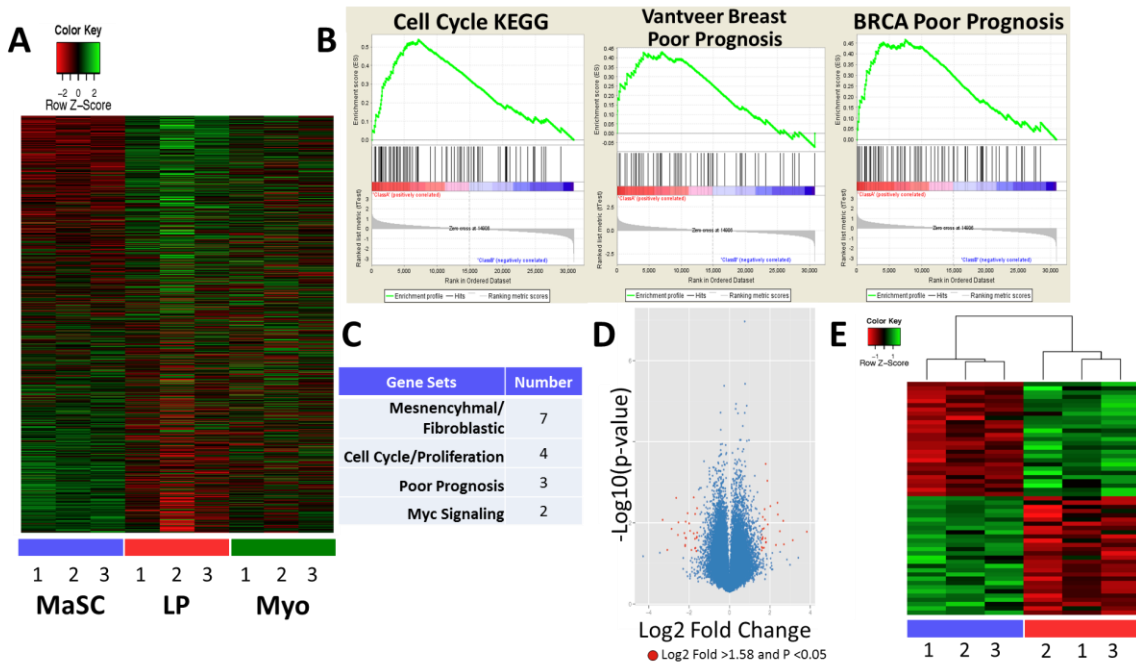


**Figure 5: Computational Analyses of ErbB2-Derived Tumors.** **A.** Normalized Illumina W6 microarray data from ErbB2 tumors derived from MaSCs (blue), LPs (red), and Myo (green). **B.** Representative enrichment plots for MaSC-derived tumors versus LP-derived tumors. **C.** A summary of GSEA result in MaSC-derived tumors versus LP-derived tumors. Gene sets in summary have  $P$ -value  $< 0.05$  and FDR  $\leq 0.25$ . **D.** Volcano plot of genes with differentially expressed genes in MaSC- vs. LP-derived tumors, genes with  $P$ -value  $< 0.05$  and log<sub>2</sub> fold-change  $> 1.58$  are highlighted in red. **E.** 54 genes were identified to fit the criteria, with exclusive expression in tumors with different cell-of-origins.

**Table 1: Identified DEGs from MaSC versus LP Tumors.**

Gene ID	Average Fold Change	P-value	Gene ID	Average Fold Change	P-value
GCNT1	1.5854	0.0112	GPRASP2	-3.3101	0.0008
BICC1	1.5925	0.0127	CD177	-3.0796	0.0339
RELL1	1.5937	0.0321	BC026585	-2.8687	0.0020
LOC626152	1.6009	0.0222	OLFML3	-2.6384	0.0043
PTPRA	1.63	0.0223	CSN2	-2.5575	0.0096
ST3GAL4	1.6327	0.017	WNT5A	-2.5340	0.0038
SCL0003799.1_2	1.64	0.0038	CPSF4L	-2.2381	0.0025
PNPLA3	1.6446	0.0025	LY6D	-2.1986	0.0207
RNASE1	1.651	0.0418	HOXB2	-2.1962	0.0186
PIK3R3	1.7015	0.0076	CP	-2.1722	0.0057
H1FO	1.7049	0.0184	LOC380706	-2.1718	0.0009
AKAP12	1.7397	0.0008	LOC381957	-2.1453	0.0166
ANKRD37	1.757	0.0058	SMOC1	-2.0719	0.0031
GLRX1	1.7807	0.006	MFGE8	-1.9999	0.0005
CHIT1	1.7979	0.0064	FBLN2	-1.9531	0.0018
ESM1	1.8107	0.0041	GM1673	-1.8875	0.0154
DNMT3B	1.8743	0.0013	GPR77	-1.7720	0.0046
OTX1	1.8975	0.0018	SCNN1G	-1.7709	0.0020
LRP11	2.0244	0.0133	SERPINA3H	-1.7123	0.0133
ANGPT2	2.2965	0.0062	DPYD	-1.7062	0.0085
ATP10B	2.3731	0.001	SCNN1B	-1.6994	0.0006
PSP	2.3931	0.0088	AABP3	-1.6878	0.0116
4930533K18RIK	2.494	0.0069	CASP4	-1.6404	0.0081
PDLIM4	2.6606	0.0022	CD200	-1.6261	0.0145
RAB6B	2.6914	0.0094	SLC38A3	-1.6165	0.0270
EG545886	3.1337	0.0342	ANK	-1.6056	0.0162
DMRT3	3.8298	0.0011	4933427D14RIK	-1.6003	0.0030

Note: Index of genes that are upregulated (log2 fold change) in MaSC tumors (blue) or upregulated in LP tumors (red), visually represented in **Figure 4D, E**. As these analyses are based on relative fold-change, the DEGs downregulated in MaSC tumors can also be thought of as upregulated in LP tumors.

**Table 2: RT Primers for Microarray Confirmation.**

Primers	Sequence
<b>mDMRT3-1</b>	GAGCTCCTCTGATCGGTGTC
<b>mDMRT3-2</b>	AGCGCAGCTTGCTAAACCAG
<b>mANGPT2-1</b>	TCTGGTTCTGCACCACATT
<b>mANGPT2-2</b>	ACAACACACAGTGGCTGATGA
<b>mIDH2-1</b>	CACCGTCCATCTCCACTACC
<b>mIDH2-2</b>	CAGCACTGACTGTCCCCAG
<b>mYWHAZ-1</b>	GAAGCATTGGGGATCAAGAA
<b>mYWHAZ-2</b>	CAGCAGATGGCTCGAGAATA
<b>mTNFRSF19-1</b>	CTGGAGACGGTGGAGGAGAT
<b>mTNFRSF19-2</b>	CAAGACATGGAGTGTGTGCC
<b>mDNMT3B-1</b>	CTGGCACCCCTTCTTCATT
<b>mDNMT3B-2</b>	ATCCATAGTGCCTGGGACC
<b>mPIK3R3-1</b>	GCTGGAGTCATTGGCTTAGG
<b>mPIK3R3-2</b>	TGATGATGCCCTATTGACA
<b>mPDK1-1</b>	TTACTCAGTGGAACACCGCC
<b>mPDK1-2</b>	GTTTATCCCCGATTAGGT

---

Note: Primers were used in the experiments and results displayed in **Figure 6**.

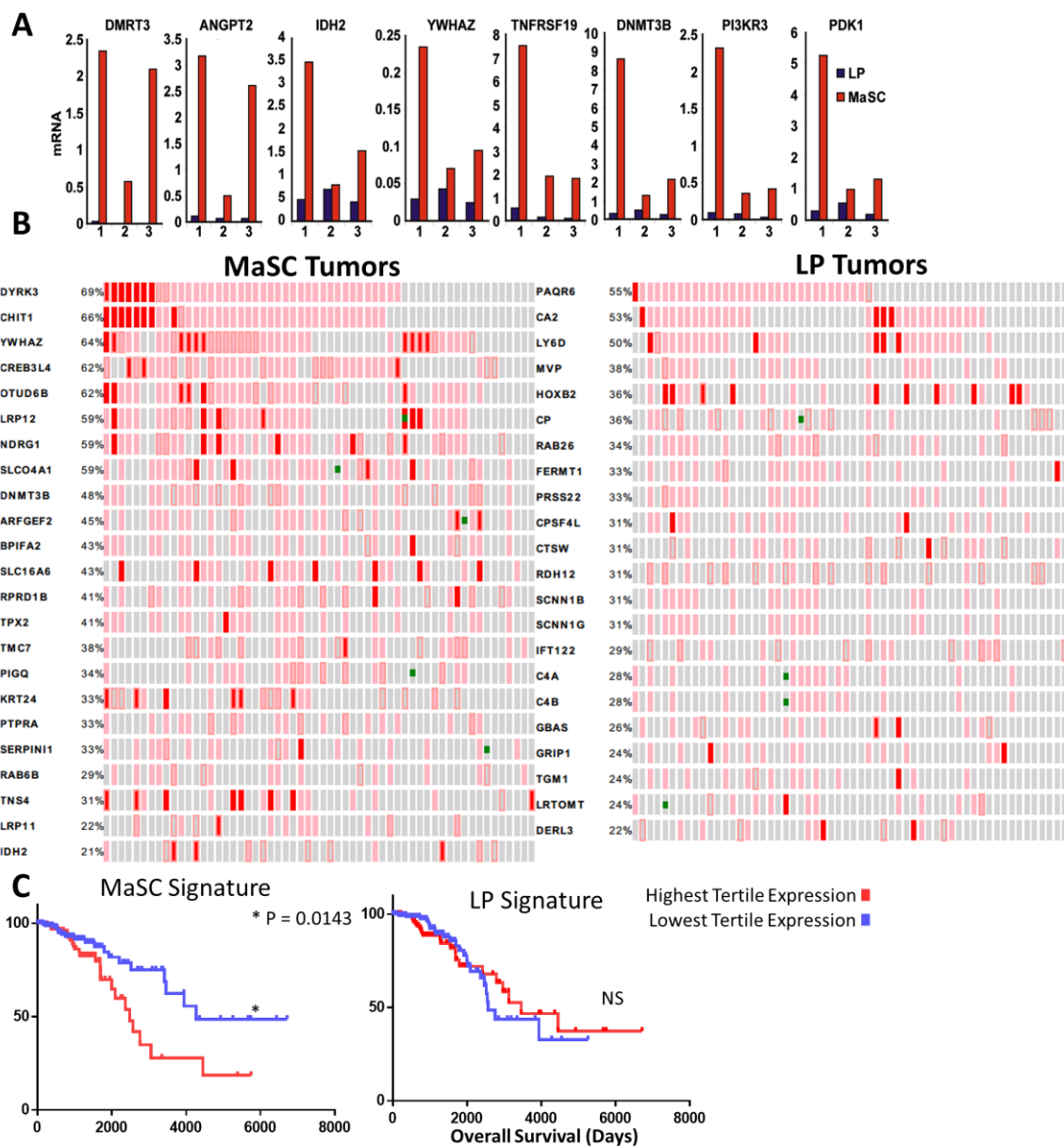


**Figure 6: Confirmation and Filtering Microarray Results.** **A.** RT-PCR results for upregulated genes in MaSC-derived tumors identified by microarray (**Figure 4D, E**). **B.** Heatmap of 22 genes overexpressed in MaSC and LP tumors with the highest percentile of mRNA upregulation and/or genomic amplification in the TCGA for HER2+ patients. **C.** Survival comparison of the DEGs from MaSC and LP tumors with the highest representation in HER+ patients in TCGA breast cancer dataset (each tertile has n=177).

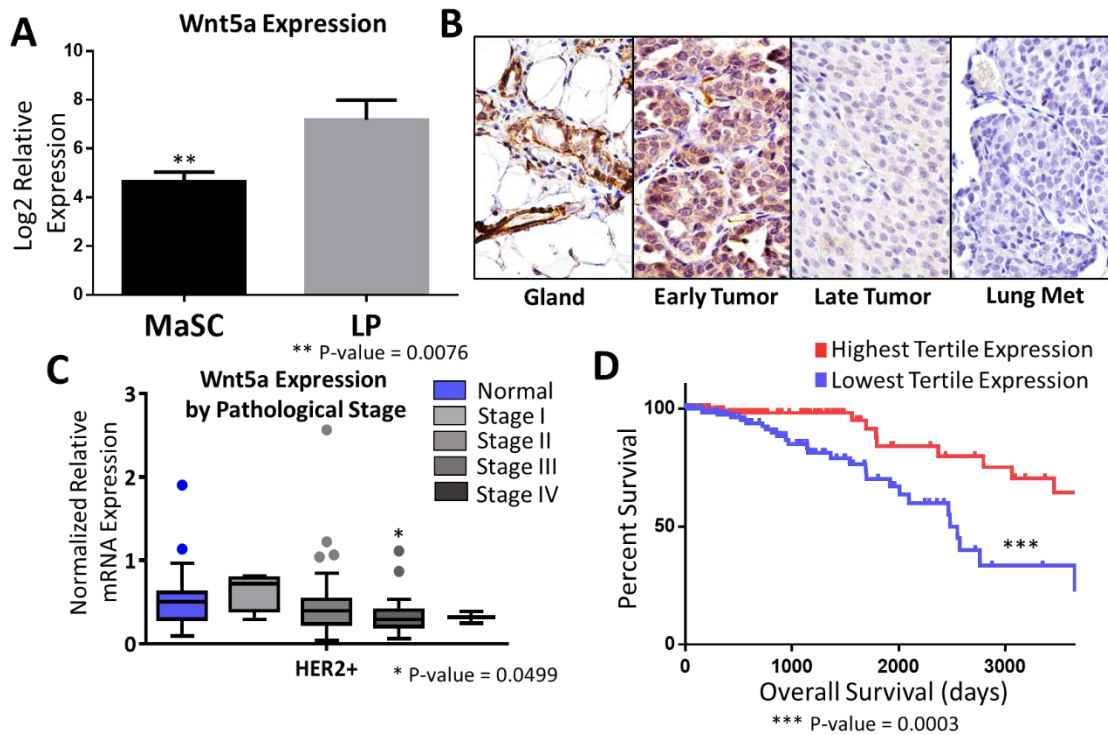


**Figure 7: Wnt5a is Reduced During the Progression of ErbB2 Spontaneous Tumors and Correlates with Better Patient Survival. A.** Mean Wnt5a mRNA expression MaSC- and LP-derived tumors from Illumina microarray data (mean  $\pm$  SD). **B.** Representative Wnt5a IHC staining from ErbB2-TG tumors. Early tumors were collected at 5-6 months of age when tumors were within 0.5 cm; while late tumors (2.5 cm) and paired lung metastases were collected at 7-8 months of age. The same tissue samples were also stained with control IgG to ensure specificity anti-Wnt5a (data not shown). **C.** Average TCGA AgilentG4502A level 3 microarray expression of Wnt5a in HER2+ patients by pathological stage (mean  $\pm$  95% CI). **D.** Ten-year survival comparison for the highest Wnt5a-expressing samples (n=177) was compared with the lowest Wnt5a-expressing samples (n=177) in the AgilentG4502A level 3 microarray TCGA BRCA dataset.

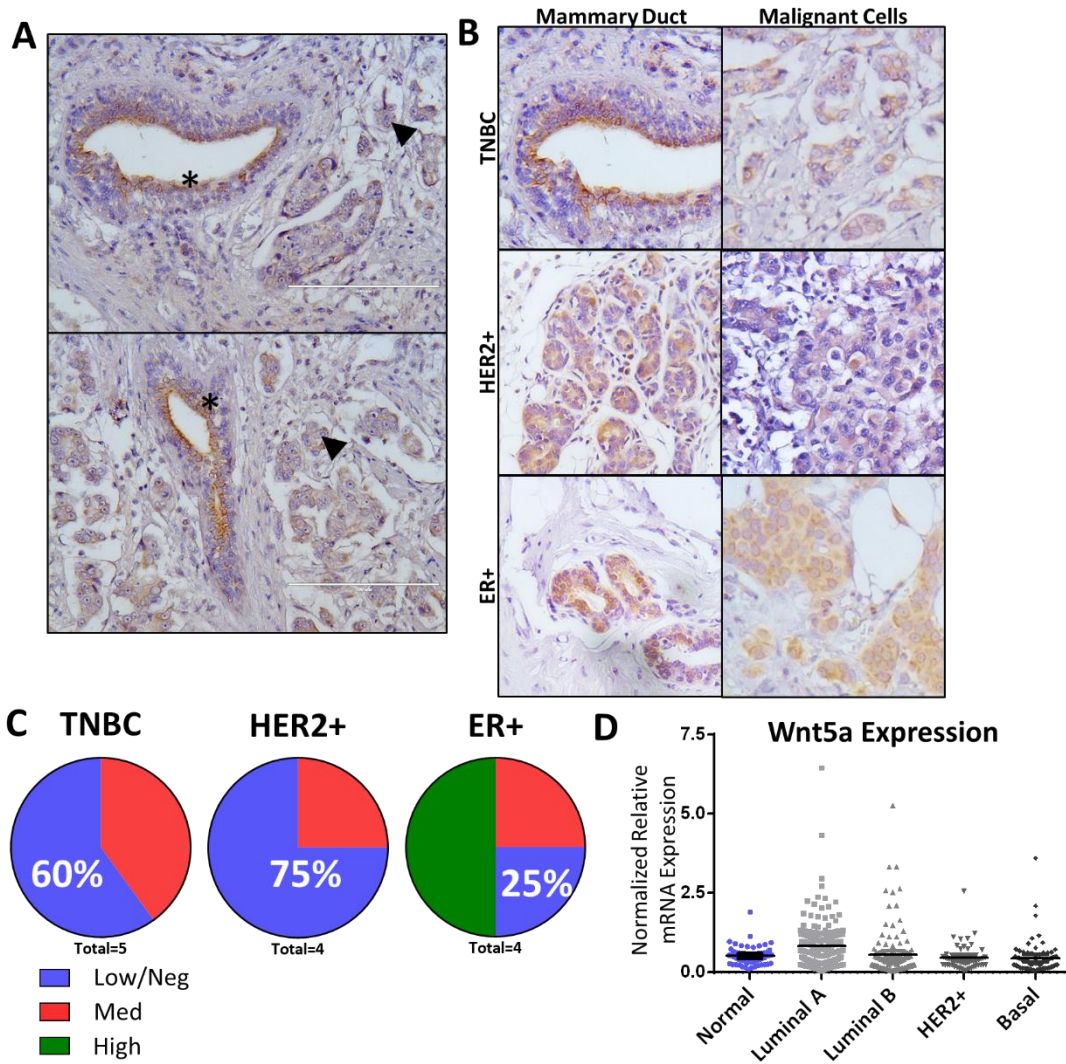


**Figure 8: Human Clinical Specimens Exhibit a Reduction of Wnt5a Expression from Normal Mammary Glands to Cancer Cells.** **A.** TNBC patient samples stained for Wnt5a; normal mammary gland (asterisk) adjacent to malignant cells (arrowhead). **B.** Representative Wnt5a staining pattern for TNBC, HER2+, and ER+ patient samples. Normal mammary glands are from the same patients distal from tumor cells. **C.** Quantification of Wnt5a staining in TNBC, HER2+, and ER+ patient tissue samples. **D.** TCGA AgilentG4502A level 3 microarray Wnt5a mRNA expression for individual molecular subtypes (Horizontal Bar = mean value, 95% CI).

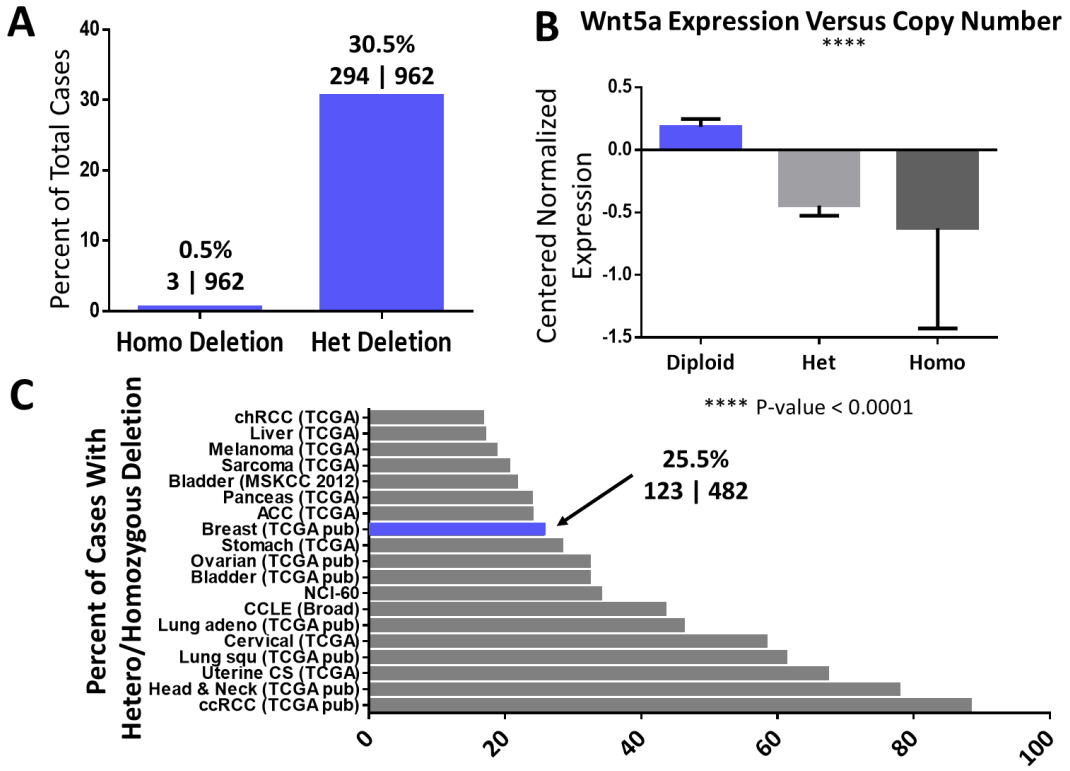


**Figure 9: Heterozygous/Homozygous Loss of Wnt5a is a Common in Breast and Other**

**Cancers.** **A.** Percent of completed tumor samples in the TCGA BRCA dataset exhibiting copy number aberration (CNA) evaluated by the TCGA Firhose pipeline and GISTIC2 method. **B.** Level 3 Illumina HiSeq 2000, RSEM normalized and mean-centralized expression data sorted by GISTIC2 CNA for Wnt5a. **C.** GISTIC2 -1 and -2 values for indicated TCGA dataset. Provisional datasets or datasets in revision for publications are indicated by (TCGA).

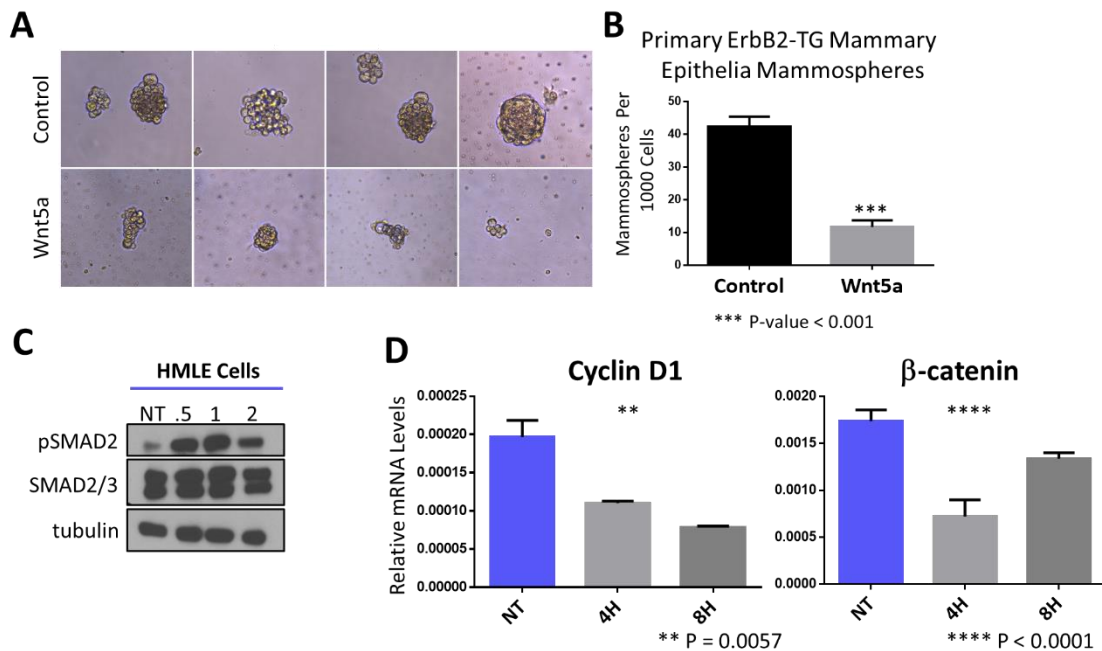


**Figure 10: Wnt5a Inhibits Self-Renewal and Activates SMAD pathway.** **A.**

Representative mammospheres from preneoplastic ErbB2 mammary epithelial cells treated with or without Wnt5a (100 ng/mL). **B.** Quantification of the number of mammospheres per 1000 cells. **C.** HMLE cells treated with Wnt5a (100 ng/mL) for 30 min, 1, or 2 hrs., cell lysates were immunoblotted with the indicated antibodies. **D.** RT-PCR results from RNA derived from HMLE cells treated with Wnt5a (100 ng/mL) for 4 or 8 hrs.

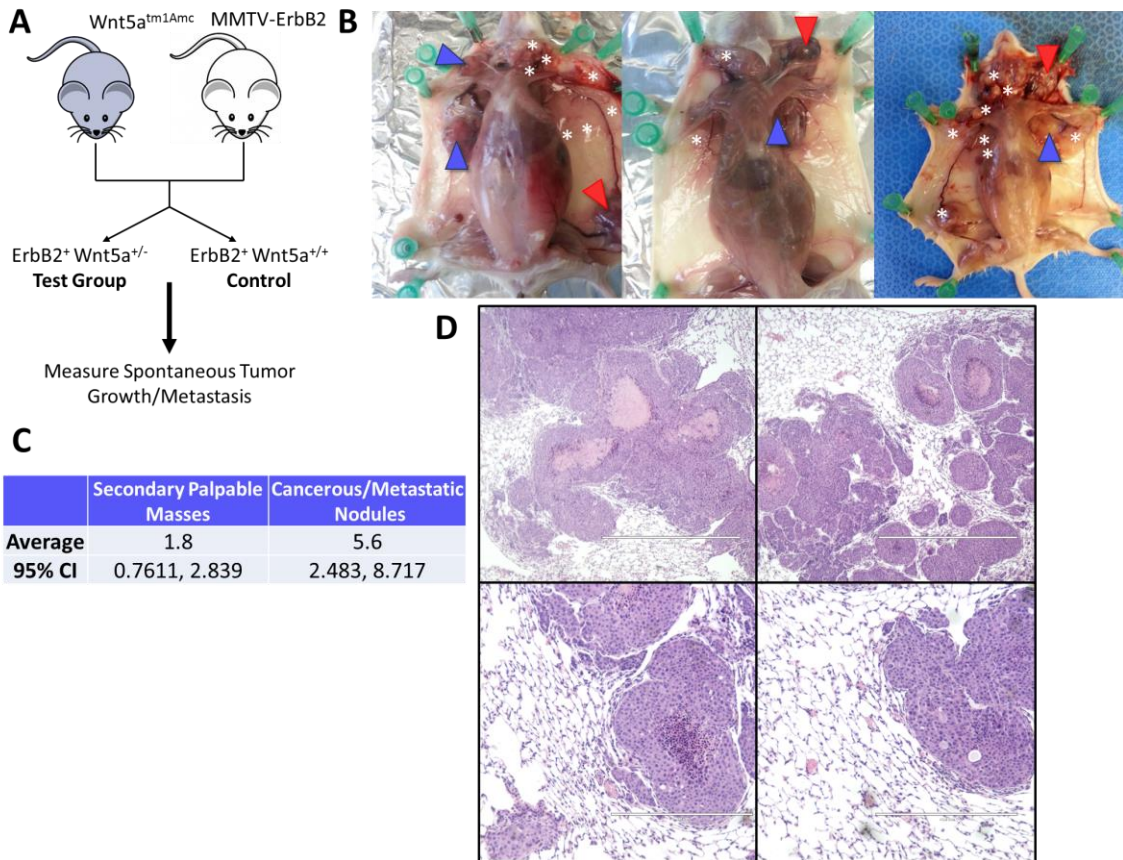


**Figure 11: Heterozygous Loss of Wnt5a Increases Metastasis in ErbB2 Murine Model for Breast Cancer.** **A.** Long-term design to examine the effect of heterozygous loss of Wnt5a on the generation of spontaneous tumors. **B.** Wnt5a<sup>+/−</sup> ErbB2 TG mice at necropsy. Initial palpable mass (red arrow), secondary palpable masses (blue arrow), and cancerous nodules (asterisks) were indicated. **C.** Summary of the mean secondary palpable masses and cancerous/metastatic foci present at necropsy in ErbB2/Wnt5a<sup>+/−</sup> mice. **D.** Lung sections of a Wnt5a<sup>+/−</sup> ErbB2 TG stained with H&E (Upper Row 40x, Lower Row 100x). Note that all four ErbB2/Wnt5a<sup>+/−</sup> mice developed lung metastases.

## CHAPTER III

### THE BLBC-SPECIFIC ROLE OF ROR1 IN EMT AND CSCS

#### Rationale

ROR1 is a noncanonical receptor for Wnt5a which has been extensively reported to have elevated expression in a variety of malignancies [102, 110, 126, 128, 130-132, 135, 137, 139-141]. In breast cancer, ROR1 expression is limited to basal type and has been associated with higher grade and more aggressive disease [129]. Whereas ROR1 is upregulated in mesenchymal breast cancer cells, a potential mechanism for the observed enhanced aggressiveness is ROR1-driven EMT [138, 158]. EMT plays a central role in tumor progression and is characterized by the loss of E-cadherin, lack of integrity of the basement membrane, and the deregulation of Wnt signaling [159]. Generating the mesenchymal phenotype involves a complex signaling network of extracellular ligands, intracellular signaling pathways, and transcription factors, SNAI1/2, Twist, and ZEB1/2.

In Chapter 2 we have described TGF $\beta$ /SMAD signaling having a tumor-suppressive role in initiation and early development of cancer; however, in late stage, TGF $\beta$ /SMAD signaling has been shown to be a major pathway for EMT, cancer progression and metastasis [154-157]. Briefly, TGF $\beta$  ligand binds TGF-Beta Receptor Type I and II (TGF $\beta$ R1/2), which leads to the phosphorylation of SMAD2/3. TGF $\beta$  appears to increase the expression of Snai1/2 through a SMAD-dependent transcriptional program; in addition, SMAD3 has been shown to increase the activity of SNAI1/2 [160,

161]. Interestingly, in both colon and breast, Wnt5a has been reported to be downstream of TGF $\beta$  signaling and is upregulated during EMT [68, 94, 162]. Recently, Twist and BRD4, a bromodomain-containing histone acetylase, were shown to be necessary for Wnt5a expression [163]. In BLBC cell line xenografts, loss of Wnt5a abrogated tumorigenesis; while pharmacologic inhibition of BRD4 partially abolished tumor growth presumably via inhibition of Wnt5a expression [163].

EMT is thought to propel cells into the cancer stem cell phenotype.

Overexpression of TGF $\beta$ , Twist, or SNAI1 in untransformed breast epithelial cell line, HMLE, results in decreased CD24 expression and increased CD44 expression [164]. The overexpression of these EMT-drivers leads to the generation of a distinct CD24 $^-$ CD44 $^+$  CSC population. The CSCs isolated from the TGF $\beta$ /TWIST/SNAI1 HMLE populations have greater clonogenicity and self-renewal capacity [164]. In a separate experiment, treatment of HMLE and MCF10A, another immortalized mammary epithelial cell line, with TGF $\beta$  produces a similar CD24 $^-$ CD44 $^+$  CSC population [165]. Together, these results suggest TGF $\beta$ -mediated EMT could generate CSCs in breast cancer.

The content of this chapter will address the expression of ROR1 in breast cancer and the role of ROR1 in signal transduction during BLBC progression. Previous work has reported increased expression of EMT-related genes in TNBC cell lines with elevated ROR1 [138]. However, our work suggests a novel mechanism of ROR1-mediated EMT related to EGFR signaling in breast cancer. In an effort to further investigate the role of ROR1 in BLBC, cell-based and pre-clinical therapeutic studies against ROR1 were evaluated. The lack of significant expression of ROR1 in adult tissue and lack of

observable side effects in our trials suggest a promising potential for therapy that may be centered on targeting mesenchymal/CSC population. Taken together, the data supports the role of ROR1 in BLBC progression and provides a rationale to target ROR1 for therapeutic intervention in highly-aggressive breast cancer.

### **Materials and Methods**

#### **Biostatistical Analyses of ROR1 Expression**

TCGA level 3 AgilentG4502A microarray expression and Biotab clinical information were downloaded from the Cancer Genome Atlas DCC. Gene expression was reported by combining clinical and expression for individual samples and subdividing by the listed categorical information. ROR1 was correlated with other genes using the cBio Cancer Genomics Portal. Pearson product-moment correlation coefficient was generated using Z-scores for normalized RSEM values of the TCGA BRCA RNAseq data.

#### **Cell Lines and Cell Culture**

Cell lines were maintained in 10%-FBS containing RPMI supplemented with 1% Penicillin and Streptomycin (Life Technologies). Silencing of ROR1 in MDA-MB-231 cells was conducted as previously described using the sequences 5'-  
TCCGGATTGGAATTCCCATG-3' (shRNA1), and 5'- CTTTACTAGGAGACGCCAATA-3'  
(shRNA2) [129].

### **Production of anti-ROR1 Immunotoxin**

The anti-ROR1 immunotoxin was provided by Speed BioSystems via collaboration. Briefly the variable regions of heavy and light chains from anti-ROR1 monoclonal antibody (clone 2A2) were fused with a peptide linker and further stabilized by an introduced disulfide bond, followed by genetic conjugation with PE-LO10, an immunogenicity-reduced form of PE. The Fv part of control immunotoxin comes from mouse monoclonal antibody clone MOPC21, which does not recognize any known antigens. The proteins were expressed in *E. Coli* and purified.

For cytotoxicity assay, different cells were cultured and treated with different doses of immunotoxin or control immunotoxin for 72 hrs. The cells were trypsinized into single cell suspensions and labeled with 7-AAD, followed by flow cytometry. 7-AAD positive cells are defined as dead cells.

For xenograft study, 2 million of HS-578T cells were orthotopically injected into the 4<sup>th</sup> mammary glands of 8-week-old NOD/SCID/IL-2R $\gamma^{-/-}$  female mice. Tumor-bearing mice were treated with either anti-ROR1 immunotoxin or control immunotoxin via I.V. at 5mg/kg body weight, twice a week for five weeks. Tumor size was measured by a caliper and tumor volumes were calculated as length x width<sup>2</sup> x 0.52. Body weights were measured to determine the toxicity of immunotoxins to mice.

### **Flow Cytometry for Breast Cancer Cells**

HS-578T cells were incubated with 1000 ng/mL of anti-ROR1 (Cell Signaling, Danvers, MA) or control-IgG for 72 hours. The treated HS-578T cells were harvested

using 2 mL of 0.25% trypsin-EDTA (Mediatech, Corning, NY, USA), incubating at 37° C for 3 minutes. Cells were surface-labeled with ROR1, CD24, and CD44 in PBS supplemented with 2% fetal bovine serum before flow cytometric analysis.

### **Immunoblot and Immunoprecipitation**

Cell lysates were prepared in ice-cold cell lysis buffer (50 mM Tris-HCl pH7.5, 1 mM EDTA, 1 mM EGTA, 1% Triton X-100, 100 mM KCl, 50 mM NaF, 10 mM Na 2-glycerophosphate, and 1 mM Na<sub>3</sub>VO<sub>4</sub>). Cell lysates were centrifuged at 15,000 RPM, 4° C for 15 minutes. Protein concentration was measured via Bradford protein assay. Supernatants were diluted to 1000 ug/mL with lysis buffer and denatured with 1x Laemmli buffer; samples were then boiled at 95° C for 5 minutes. Cell lysates (20 µL) were separated by SDS-PAGE and immunoblotted with anti-p-AKT (Santa Cruz Biotechnology), anti-AKT (Santa Cruz Biotechnology), and anti-tubulin (Sigma-Aldrich) antibodies.

HEK293T cells were transiently transfected with ROR1-FLAG plasmid and GeneTrans III (Biomiga, San Diego, CA); 48 hours post-transfection, cells were treated with indicated ligand and lysed in RIPA buffer after 15 minutes. Lysates were incubated overnight at 4° C with anti-M2-FLAG plot and immunoprecipitated. Immunoprecipitates were separated by SDS-PAGE and probe with anti-HER2 (Cell Signaling Technologies), anti-TGFBR1 (Santa Cruz Biotechnology), and anti-ROR1 (Cell Signaling Technologies).

### **RNA Isolation and RT-PCR**

RNA for cell lines were isolated with RNeasy Plus mini kit (QIAGEN), according to the manufacturer's instruction. Samples (1000ng) were reverse-transcribed into cDNA with iScript cDNA Synthesis Kit (Bio-Rad) and diluted 1:12 with nuclease free water. PCR was performed with iTaq Universal SYBR Green Supermix (Bio-Rad) in a 15 µl reaction volume with primers in **Table 4**. Real-time PCR was performed using the ViiA™ 7 real-time PCR system (Life Sciences) and quantified against cyclophilin as housekeeping gene.

### **Immunofluorescence Staining**

The 8 µm frozen sections from human breast cancer specimens with paired normal tissues were air-dried for 30 minutes and fixed in ice-cold 35% methanol/65% acetone. The slides were then washed with ice-cold PBS, permeabilized by 0.3% Triton X-100 in PBS with 5% goat serum, and stained with anti-ROR1 antibody (Cell Signaling). Anti-Rabbit Alexa 546 (Life Sciences), phalloidin-TRITC (Life Sciences) and DAPI were mixed and stained after primary antibody staining. Slides were then mounted with anti-Fade mounting solution (Life Sciences) for fluorescent microscopy.

## **Results**

### **ROR1 is a Basal/Mesenchymal Marker in Breast Cancer**

We were interested in examining the expression of Wnt5a receptors in breast cancer for further elucidation of Wnt5a-mediated tumor suppression. As we expected

based on previous publications [129, 138], we found ROR1 mRNA expression was significantly reduced in luminal A, luminal B and HER2+ tumor samples (**Figure 12A, B**). Counterintuitively, we found that ROR1 expression is maintained and increased through the progression of BLBC. More so, within the primary tumor samples of the BRCA dataset, ROR1 expression was correlated with basal markers, CSC markers, EMT drivers, and genes implicated in lung and bone metastasis (**Figure 12C**, summarized in **Table 3**). Specifically, ROR1 mRNA expression was highly correlated with SNAI1 ( $r=0.45$ ), SNAI2 ( $r=0.47$ ) and ALDH1A3 ( $r=0.49$ ), an aldehyde dehydrogenase isoform found to be expressed on CD44<sup>+</sup>CD24<sup>-</sup> CSC populations (**Figure 12C**).

To corroborate our genomic analysis for ROR1 mRNA expression, we performed immunofluorescent staining on human patient samples. Consistently, we observed low to negative levels of ROR1 staining in human mammary ducts, while ROR1 expression was seen in 50% of breast tumors (**Figure 13A**). The 3 samples with the highest ROR1 expression were triple-negative breast cancer samples; while the moderate ROR1 protein expression was seen in samples that varied in expression of the ER (**Figure 13B**). In a similar vein, we assayed cell lines for ROR1 and CD24<sup>-</sup>CD44<sup>+</sup> expression (**Figure 14A, B**). We found high levels of ROR1 expression in 3 cell lines, HS-578T, MDA-MB-231, and MDA-MB-468, are all derived from TNBC. In addition, moderate ROR1 expression was seen in 6 cell lines. ROR1 expression occurs concomitantly with the presence of CD24<sup>-</sup>CD44<sup>+</sup> populations. All 3 cell lines with the highest expression of ROR1 had pronounced CD24<sup>-</sup>CD44<sup>+</sup> populations, while in moderate ROR1-expressing cell lines, 50% had defined CD24<sup>-</sup>CD44<sup>+</sup> populations (**Figure 14B, C**). When we incubated HS-578T cells (high ROR1-

expressing) with a mAb directed against ROR1, there was an increase in CD24 expression when compared to cells incubated with an isotype control (**Figure 14D**). This increase in CD24 expression with mAb corresponds to a more luminal phenotype and suggests that increased ROR1 expression may serve a functional role in cancer stem cells.

### **Functional Advantage of ROR1 Expression in BLBC**

To begin to address ROR1-mediated signaling in breast cancer progression, we transiently transfected HMLE cells with plasmid encoding FLAG-tagged ROR1 at the C-terminus. Transfection of ROR1 led to a 1.62-fold increase in ROR1 mRNA, corresponding to increases in TGF $\beta$ -targets EMT genes including SNAI2 (1.51-fold), IL-11 (1.50), CTGF (1.40), and CD44 (1.75) compared to the GFP-transfect control (**Figure 15A**). Similarly, in MDA-MB-231 cells with stable transfection of shCON and shROR1, we found a reduction in mRNA levels of SNAI2 (11-fold), IL-11 (2.5), and CTGF (1.4) when ROR1 was knocked down (**Figure 15B**). Next, we wanted to examine the role of Wnt5a, the ligand of ROR1, in signaling the mesenchymal phenotype we have established. In MDA-MB-231 with shCON and shROR1 expression (**Figure 16A**) we performed a time course with Wnt5a. Wnt5a treatment in the shCON cells led to the phosphorylation of AKT and SMAD2 (**Figure 16B**). However, when ROR1 expression was knocked down, Wnt5a treatment led to a greater level of phosphorylation in both AKT and SMAD2 (**Figure 16B**). A time course of Wnt5a in the same MDA-MB-231 shCON/ROR1 cells showed altered dynamics in the transcription of metastatic genes (CTGF, IL-11, and

CXCR4), but not a complete abrogation of Wnt5a-mediated induction in shROR1 cells (**Figure 16C**). We found that SNAI2, although not responsive to Wnt5a, was significantly reduced in the shROR1 cells when compared with shCON (**Figure 16C**). Other drivers of EMT, SNAI1 and TWIST1, were assayed, but mRNA levels were too low or undetectable, preventing us from being able to differentiate basal levels or Wnt5a-mediated induction dynamics (data not shown). Our data suggests that ROR1-mediated EMT gene expression is irrelevant of Wnt5a and ROR1 has other functions than mediating Wnt5a signaling in BLBC cells.

In another avenue for the role of ROR1 in BLBC, we found that ROR1 expression was highly correlated with the expression of EGFR (**Figure 17A**). ROR1 has been reported to interact with EGFR signaling in lung cancer cells and specifically potentiates signal transduction from EGFR/HER3 heterodimer [109]. When we treated MDA-MB-231 expressing control shRNA with EGF, we found a sustained phosphorylation of AKT and SMAD2; while silencing ROR1 appeared to decrease the duration of the phosphorylation of SMAD2 and AKT (**Figure 17B**). In order to assess the potential interaction between ROR1 and EGFR, we transiently transfected HEK293T cells with ROR1-FLAG. Consistent with the lung cancer cell result, EGF treatment induced a complex formation between ROR1 and EGFR, as well as TGF $\beta$ R1, a receptor for a major pathway of EMT in breast cancer (**Figure 17C**). More importantly, TGF $\beta$ , but not Wnt5a, led to an even more pronounced interaction between ROR1 and EGFR, as well as TGF $\beta$ R1 (**Figure 17C**). Our data suggests that ROR1 doesn't mediate Wnt5a signaling in breast cancer; rather it may bridge the signaling network between EGFR and TGF $\beta$  receptor, two important

pathways in EMT and basal breast cancer.

### **Targeting ROR1 for Breast Cancer Therapy:**

With the paradigm of low ROR1 expression in adult tissues and specific, high expression of ROR1 in TNBC/BLBC, we wanted to evaluate the therapeutic potential for targeting ROR1. In collaboration with Speed BioSystems LLC., we developed an ROR1-immunotoxin (ROR1-ITX), a variable heavy and light chain derivative of anti-ROR1 (clone 2A2) stabilized with a peptide linker and disulfide bond. The antibody derivative is conjugated with a low immunogenic *Pseudomonas* exotoxin (PE), which inhibits elongation factors and subsequent translation (**Figure 18A**) [166]. The ROR1-ITX shows similar binding affinity to MDA-MB-231 cells as anti-ROR1 2A2, while we see a similar lack of affinity to our negative control, MCF7 (**Figure 18B**). Next we screened the ability of ROR1-ITX to induce dose-dependent cell death in *in vitro* experimentation. Indeed, in cell lines with high-ROR1 expression (MDA-MB-231, MDA-MB-468, HS-578T), we saw that the ROR1-ITX potently induced cell death (**Figure 18C**). In quantitative analyses, high-ROR1 cell lines treated with ROR1-ITX showed dose-dependent decrease in percentage of cells surviving and increase in percentage of cells positive for 7-AAD, a fluorescent stain for DNA indicative of late-stage apoptosis or necrosis (**Figure 18D**). HS-578T cells seemed notably sensitive to ROR1-ITX; with 200 ng/mL of ROR1-ITX, 47.5% of HS-578T cells stained positive for 7-AAD, but only 22.8% of cells were present relative to non-treated controls (**Figure 18D**). Importantly, in ROR1-negative cell lines, only BT474 was consistently below 100 percent survival when treated with ROR1-ITX; whereas 1000

ng/mL and 5000 ng/mL had 81.7% and 82.3% survival, respectively. More so in HMLE and MDA-MB-436 cells treated, there was a 2-9% increase in overall survival (**Figure 18C**).

Next we moved into our *in vivo* model for preclinical safety and efficacy trials described in (**Figure 19A**). HS-578T cells were injected into the mammary fat pads (corresponding to the 4<sup>th</sup> mammary glands) of 4 NOD/SCID/IL2R $\gamma$  (NSG) mice. After tumors grew to palpable masses, 2 mice were treated twice a week, intravenously (IV) with either 5 mg/kg of non-specific V<sub>L</sub>-V<sub>H</sub>-PE conjugate (C) or ROR1-ITX (R). We found ROR1-ITX reduced tumor volume by an average of 85.6 mm<sup>3</sup> after 1 week of treatment, or nearly a 35% reduction in tumor volume (**Figure 19B**). At the end of the treatment cycle, the ROR1-ITX treated group retained an average of 18 mm<sup>3</sup> reduction from initial tumor volume. In contrast, the control group average tumor volume increased from 98 mm<sup>3</sup> to 373.9 mm<sup>3</sup>, an average increase of 276 mm<sup>3</sup> (**Figure 19C**). Notable was a lack in observable off-target effects of ROR1-ITX, whereas the treated mice had a 1.28% reduction in bodyweight over the 5-week period, while the control mice had an average reduction of 0.76% (**Figure 19D**). The obvious limitation of mice for a safety trial is the potential lack of ROR1-ITX binding to the mROR1 homolog. However, the lack of observable immunological complications with the conjugated *Pseudomonas* exotoxin is promising. In summary, ROR1-ITX shows promise initial reduction in tumor volume and appears safe. However the modification of dosages, immunotoxin delivery, and PE structure itself needs to be further evaluated to optimize preclinical trials.

## **Discussion**

ROR1 has an emerging role in both hematologic and solid malignancies [130, 167]. The number of cancer types with ROR1 expression has been increasing, so do the tumor-promoting signal pathways that have been linked to ROR1. The size of established literature on ROR1 in cancer support the notion that the increased expression of ROR1 is not just a bystander of oncogenesis, but rather a tumor-promoting factor. Our results are diverged into two highly related implications, therapeutic potential and ROR1 in the pathogenesis of BLBC.

Our results indicate increased mRNA and protein expression of ROR1 in BLBC. One promising avenue of the therapeutic potential of ROR1 targeting in breast cancer is the inhibition of metastasis. ROR1 expression has been linked to epithelial-mesenchymal transition in breast cancer, where antibody-targeting of ROR1 can reduce the metastatic potential of MDA-MB-231 cell xenografts [138]. Our results suggest the inhibition of metastatic foci by targeting ROR1-expressing BLBC cells, may be the result of preferentially targeting CSCs or invasive cells. ROR1-based therapies for primary tumor volume are more complicated. Previous monoclonal antibody therapies targeting ROR1 have been mixed in the ability to induce cell death through ADCC and CDC [126, 131, 142, 143]. In order to circumvent the mixed results of traditional monoclonal antibody therapy for ROR1, we established a ROR1-ITX with similar binding capacity of anti-ROR1 2A2. Preliminary *in vitro* assessment demonstrated that ROR1-ITX possesses a high-degree of specificity and efficacy. Despite the limitations of our initial safety trial, ROR1-immunotoxin led to a 34.2% initial reduction in tumor volume with the first week

of therapy (**Figure 19B**). The initial tumor reduction paired with the absence of observable side effects, suggests for the first time that ROR1-based therapy can reduce tumor volume in solid malignancies.

In support of previous work, we found the presence or absence of ROR1 alters the expression of EMT driver SNAI2 and downstream genes [138]. In agreement with our results in Chapter 1, we found that Wnt5a leads to the activation of the SMAD pathway, however the knockdown of ROR1 enhanced the phosphorylation of SMAD and AKT and led to only a partial abrogation of CTGF, CXCR4, and IL-11. The increased SMAD phosphorylation and modulation of metastatic gene induction suggests that Wnt5a is not signaling solely or primarily through ROR1 in basal breast cancer cells.

In lung adenocarcinoma and BLBC, ROR1 interacts with EGFR and potentiates EGF signaling [109]. The reduction in AKT phosphorylation we observed in with ROR1 knockdown suggests that ROR1 plays a role in sustaining signaling at the level of receptor/adaptor interaction or can somehow prevent negative feedback. The interaction of ROR1 with EGFR and TGF $\beta$ R1 through incubation with both EGF and TGF $\beta$  unites two major pathways where efforts for targeted therapy research are being directed [168, 169]. ROR1 may represent a central node or switch in TGF $\beta$ -mediated metastatic signaling and EGFR-mediated survival/proliferation signaling. Recent clinical trials TNBC/BLBC patients with cetuximab, a monoclonal antibody directed against EGFR, showed low efficacy in terms of response rates and inhibition of EGFR signaling [170]. Our data suggest that ROR1 expression maybe a potential mechanism of resistance to EGFR-based therapies. ROR1 expression increases through the progression

of BLBC, much like in CLL, ROR1 expression may act as a clinical biomarker or metric of progression in the clinic. More so, if clinical trials progress for antibody and small molecule inhibitors for EGFR in BLBC, ROR1 expression may prove to be an interesting therapy-response marker. In a similar vein, the compensatory upregulation of ROR2 and Wnt5a when ROR1 was silenced in melanoma may be a mechanism of ROR1 resistance. More so, the shifting of melanoma cell lines from proliferative to invasive phenotypes with the silencing of ROR1, suggests ROR2 should be examined as ROR1 therapy moves forward [141].

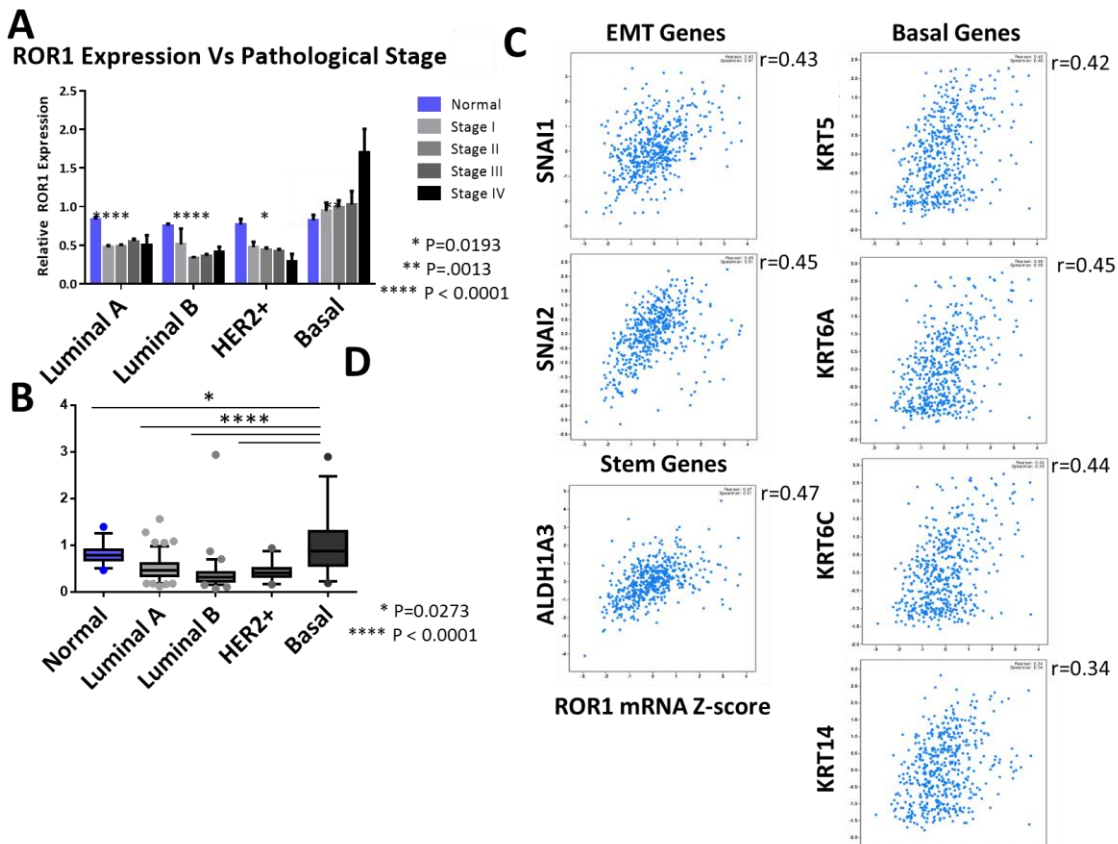


**Figure 12: ROR1 Expression is Dependent on Molecular Subtypes and Correlates with Mesenchymal Phenotype.** **A.** Mean TCGA AgilentG4502A level 3 microarray ROR1 mRNA expression by pathological stages and individual subtypes (mean  $\pm$  SEM). **B.** Mean TCGA AgilentG4502A ROR1 mRNA expression by individual molecular subtype (mean  $\pm$  95% CI). **C.** Plots and Pearson product-moment correlation coefficients of ROR1 TCGA Level 3 RNAseq expression (Z-score) with indicated genes (Z-scores) across the BRCA TCGA dataset and summarized in **Table 3**.

**Table 3: ROR1 Expression Correlations.**

		Pearson's r	P-Value	T-Score
EMT Genes	<b>SNAI1</b>	0.45	< 0.0001	15.564
	<b>SNAI2</b>	0.47	< 0.0001	16.44657
	<b>ZEB2</b>	0.35	< 0.0001	11.54034
	<b>TGFBR2</b>	0.39	< 0.0001	13.08177
CSC Markers	<b>ALDH1A3</b>	0.49	< 0.0001	17.36169
	<b>KRT5</b>	0.41	< 0.0001	13.88425
	<b>KRT6A</b>	0.44	< 0.0001	15.13393
	<b>KRT6C</b>	0.43	< 0.0001	14.71083
Basal Markers	<b>KRT6B</b>	0.33	< 0.0001	10.79754
	<b>KRT14</b>	0.34	< 0.0001	11.1668
	<b>FYN</b>	0.5	< 0.0001	17.83255
	<b>MCAM</b>	0.49	< 0.0001	17.36169
Bone and Lung Metastatic Genes	<b>MMP7</b>	0.44	< 0.0001	15.13393
	<b>LTBP1</b>	0.43	< 0.0001	14.71083
	<b>ADAMTS1</b>	0.41	< 0.0001	13.88425
	<b>CTGF</b>	0.38	< 0.0001	12.68885
	<b>CXCR4</b>	0.37	< 0.0001	12.30114
	<b>PTGS2</b>	0.37	< 0.0001	12.30114
	<b>CXCL1</b>	0.35	< 0.0001	11.54034
	<b>MMP2</b>	0.3	< 0.0001	9.713478

---

Note: Pearson's product-moment correlation coefficient using RNAseq mRNA expression Z-scores. P-values and T-score were calculated using n=952.

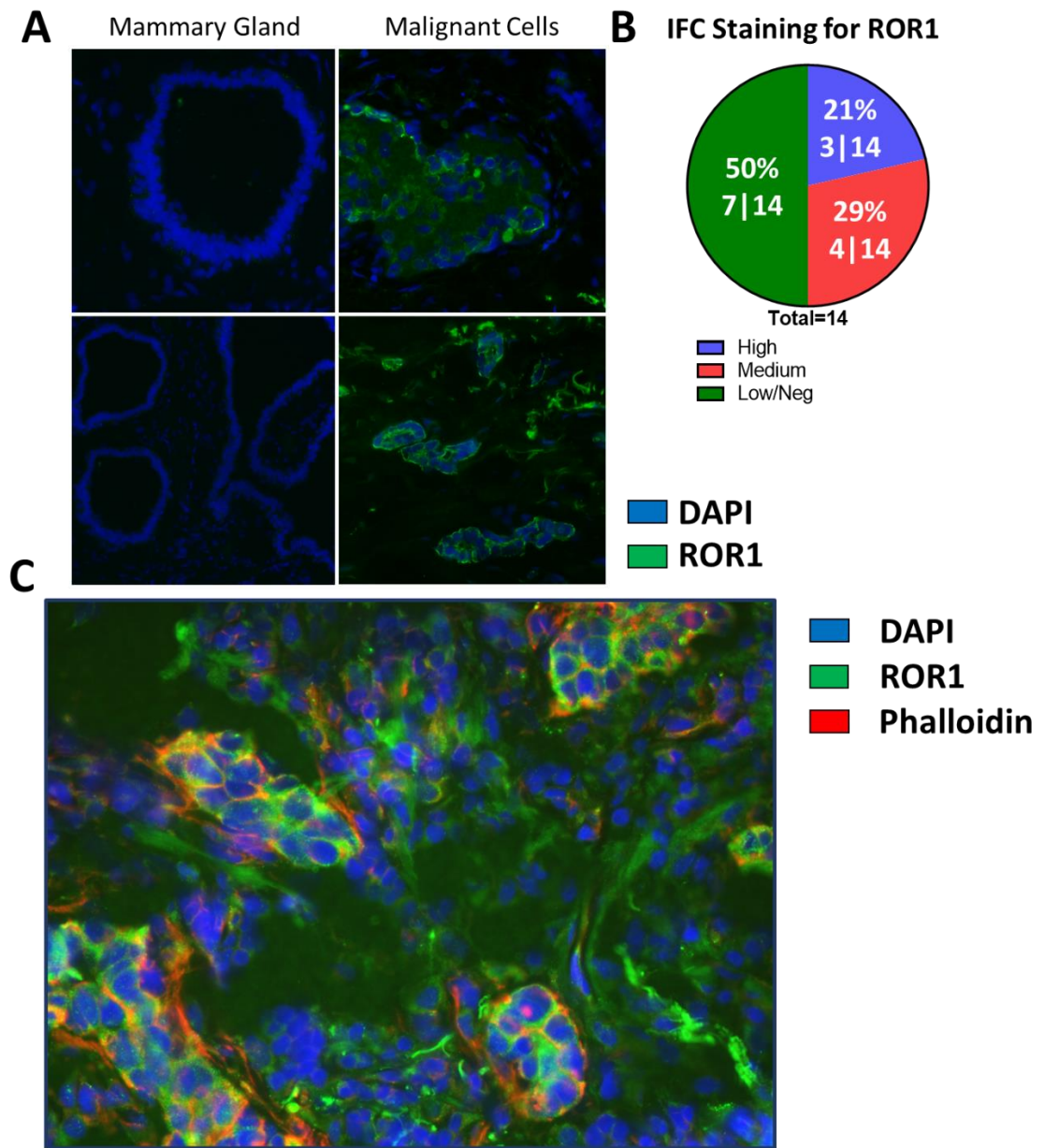


**Figure 13: ROR1 Protein Expression in Human Tumor Tissue Samples.** **A.** Comparison of ROR1 expression in normal mammary duct and tumor samples. **B.** Quantification of ROR1 IFC staining for 14 tumor samples. **C.** Triple-negative patient sample stained for DAPI (Blue), F-actin (Red), and ROR1 (Green).

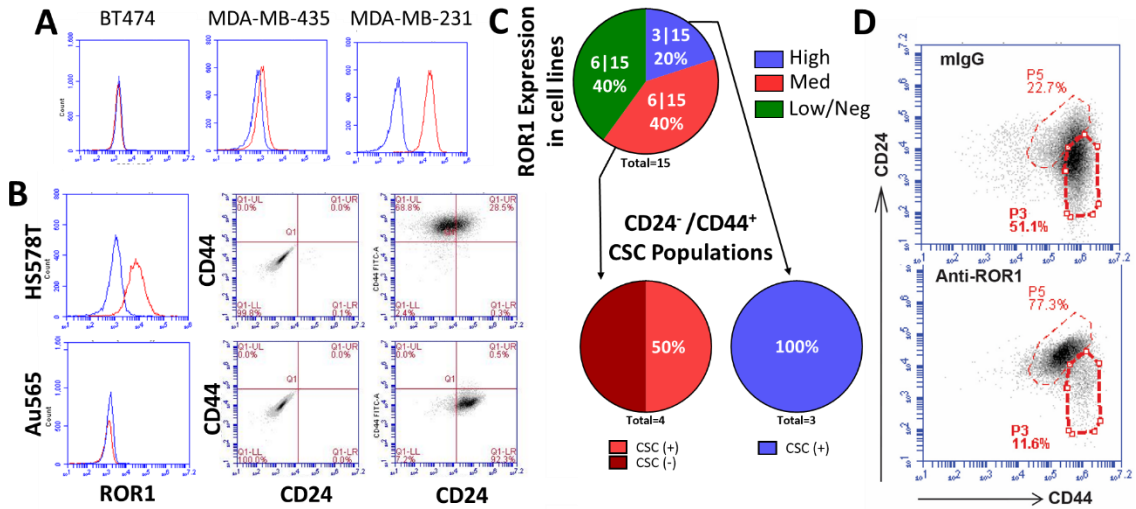


**Figure 14: ROR1 Expression in Breast Cancer Cell Lines Correlates with CD24<sup>-</sup>CD44<sup>+</sup> CSC**

**Markers.** **A.** Representative flow cytometry result for low/negative (BT474), medium (MDA-MB-435), and high (MDA-MB-231) ROR1-expressing cell lines. **B.** Representative plots for CD24/CD44 surface expression. **C.** Quantification of ROR1 expression in 15 breast cancer cell lines and corresponding CD24/CD44 staining for medium and high ROR1 expressing cells. **D.** HS-578T cells treated with control antibody or anti-ROR1 at 1000 ng/mL for 72 hrs. followed with flow cytometry of surface labeling with CD24-FITC and CD44-PE.

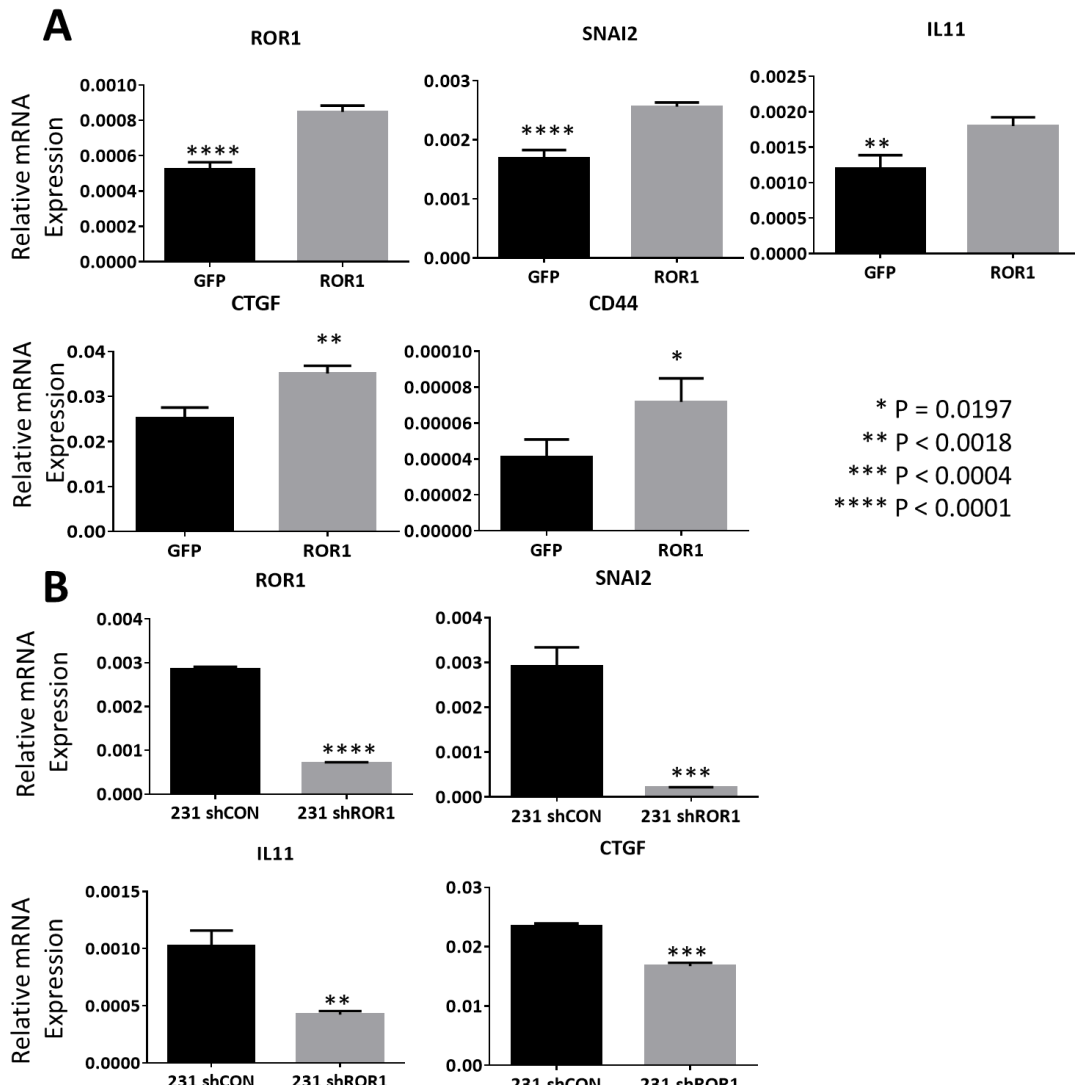


**Figure 15: ROR1 Modulates the Basal mRNA Level of EMT/CSC Genes.** A. RNA from HMLE cells 48 hours post-transfection with GFP or ROR1-FLAG plasmid was harvested. RT-PCR was done using primers from **Table 4**. B. RT-PCR results for basal level of indicated genes in MDA-MB-231 with stable expression of shCON or shROR1.

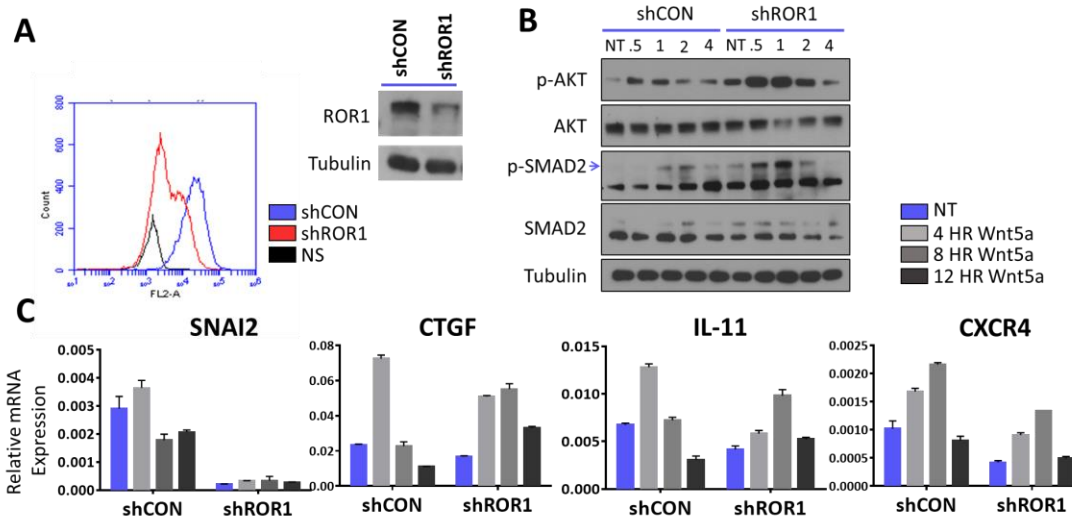


**Figure 16: Wnt5a-ROR1 Signaling in MDA-MB-231 Cells. A.** Flow cytometric plot and immunoblot of MDA-MB-231 cells with stable expression of plasmid containing shCON (blue) or shROR1 (red). Non-stained control cells are in black. **B.** MDA-MB-231 shCON and shROR1 cells were treated with 100 ng/mL Wnt5a for 0.5, 1, 2, or 4 hrs.; cell lysates were separated by SDS-PAGE and immunoblotted with the indicated antibodies. **C.** RT-PCR results for EMT-related gene in MDA-MB-231 shCON and shROR1 treated with 100 ng/mL of Wnt5a for indicated times (mean  $\pm$  SD); primers listed in **Table 4**.

**Table 4: EMT-Related RT PCR Primers.**

Primers	Sequence
<b>hSnai2-1</b>	CTCTCTCCTTTCCGGATACT
<b>hSnai2-2</b>	CAGTGCAGCTGCTTATGTTG
<b>hIL-11-1</b>	GAGAGGCTTGCTGGATATAG
<b>hIL-11-2</b>	CTTGACCTGGAGACAGTCATT
<b>hMMP1-1</b>	TCTCTTGGACTCTCCCATTCT
<b>hMMP1-2</b>	CCTGAACAGCCCAGTACTTATT
<b>hCTGF-1</b>	GCCCAGACCCAACATATGATTAG
<b>hCTGF-2</b>	TCTCCGTACATCTCCTGTAGT
<b>hCXCR4-1</b>	GAGAAGCATGACGGACAAGTA
<b>hCXCR4-2</b>	TGACAATACCAGGCAGGATAAG
<b>hROR1-1</b>	CAGCGCATCAGACCATAAGA
<b>hROR1-2</b>	CCTAGAGCCCATTGACCATAAG
<b>CD44-1</b>	GGTGGAAAGAAGAGACCCAAATC
<b>CD44-2</b>	CCAGCTCCCTGTAATGGTTATG

---

Note: RT-Primers were used in the results in  
**Figure 15** and **Figure 16**.

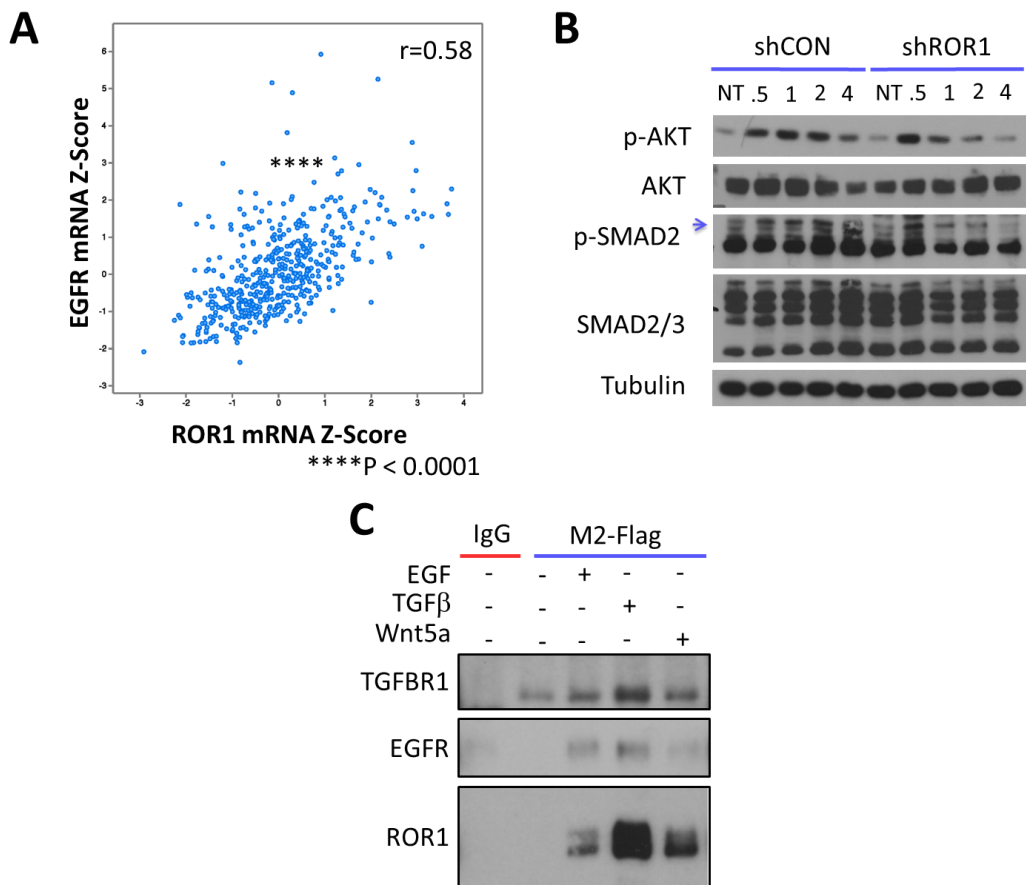


**Figure 17: ROR1 Potentiates EGFR-Mediated AKT and SMAD Activation.** **A.** ROR1 and EGFR TCGA Level 3 RNAseq expression (Z-scores) across the BRCA TCGA dataset. **B.** MDA-MB-231 shCON and shROR1 cells were treated with 10 ng/mL EGF for 0.5, 1, 2, or 4 hrs.; cell lysates were separated by SDS-PAGE and immunoblotted with the indicated antibodies. **C.** HEK 293T cells 48 hours post-transfection with ROR1-FLAG constructs were treated with indicated ligand for 15 minutes. Cells were lysed and immunoprecipitated with an isotype control (IgG) or anti-FLAG. Immunoprecipitates were separated with SDS-PAGE and probed with indicated antibodies,

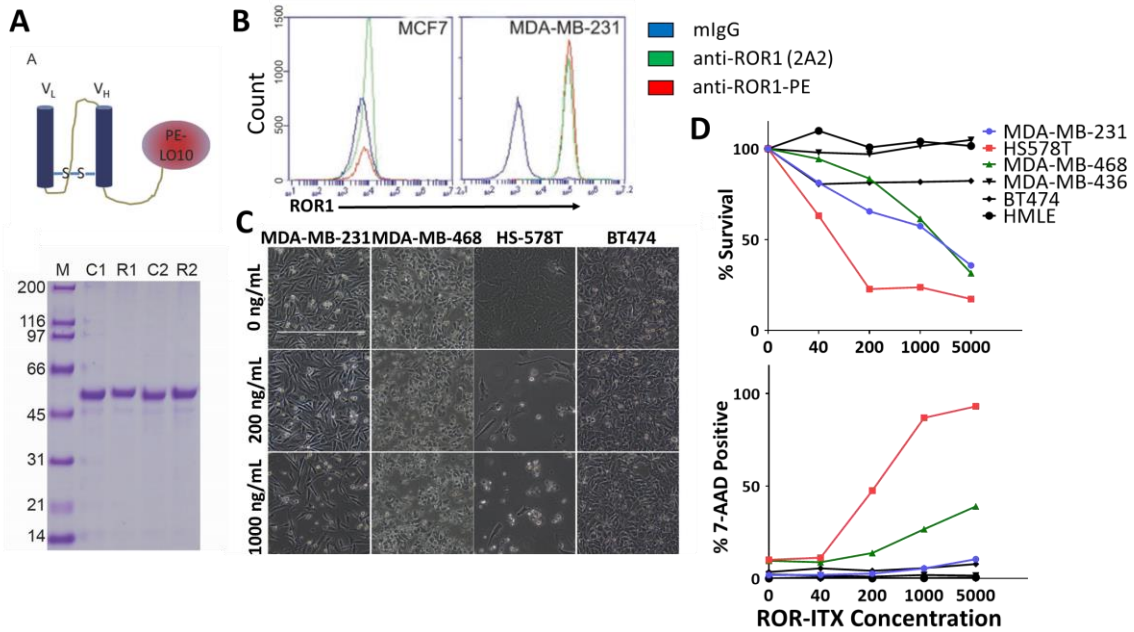


**Figure 18: *In Vitro* Analysis of ROR1-Immunotoxin. A.** Schematic of anti-ROR1 immunotoxin; variable regions of heavy and light chains from anti-ROR1 monoclonal antibody (clone 2A2) are fused with a peptide linker and disulfide bond, then genetically conjugated with PE-LO10. Purification and refolding of bacteria-expressed immunotoxin. C1, control Fv-PE. The Fv part of C1 is from mouse monoclonal antibody clone MOPC21, which does not recognize any known antigens. **B.** Representative affinity for cell lines incubated with 200 ng/uL of a control IgG, anti-ROR (2A2), and anti-ROR1-PE. **C.** High ROR1-expressing cell lines (MDA-MB-231, MDA-MB-468, and HS-578T) and low-expressing cell lines (BT474) were incubated with indicated ROR1-ITX concentrations for 120 hours. **D.** Percent survival and percent 7-AAD positive cells after treatment of ROR1-ITX at indicated concentrations. Colored lines indicate cells with high ROR1 expression, while black lines indicated cell lines negative for ROR1 expression.

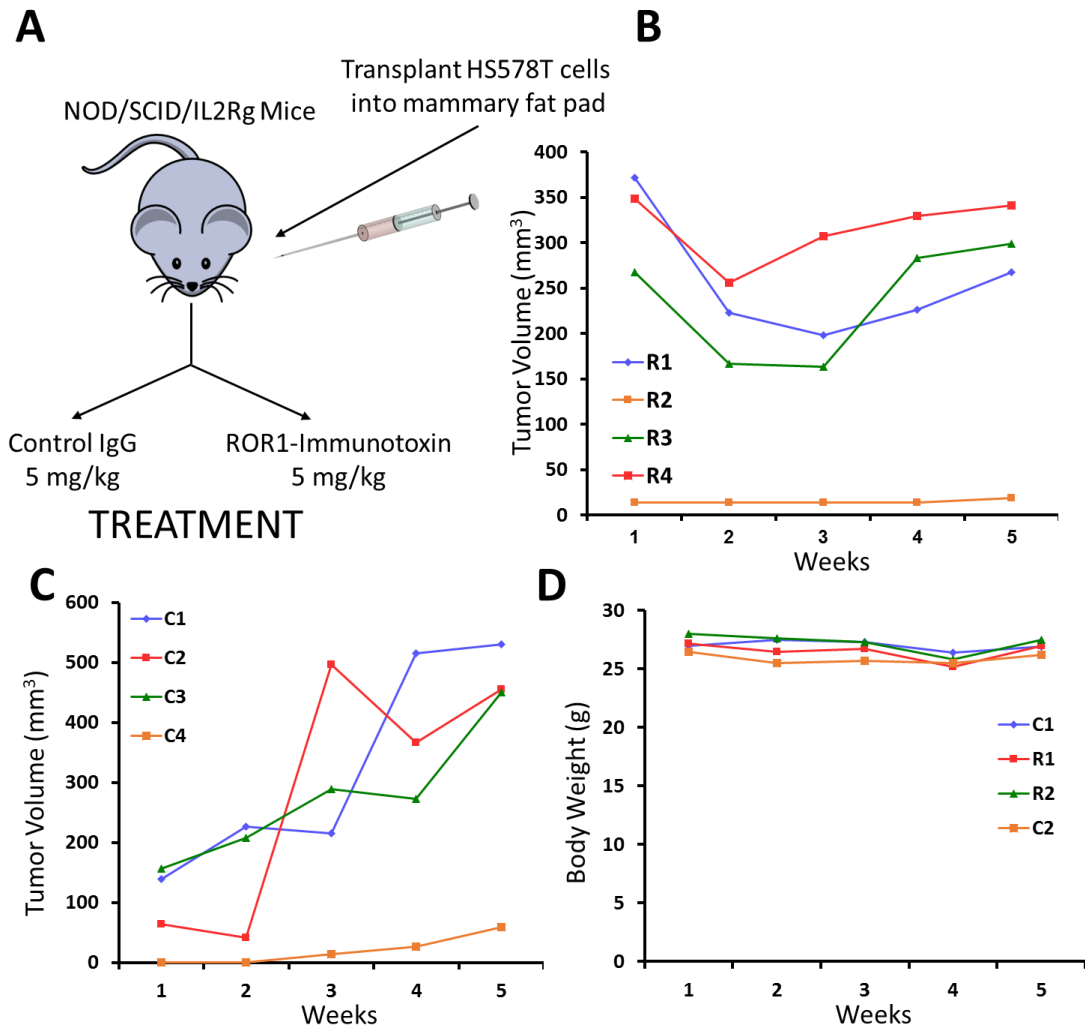


**Figure 19: Initial *In Vivo* Assessment of ROR1-Immunotoxin.** **A.** Schematic of HS-578T xenografts and treatment of NOD/SCID/ILR2y mice with control Ig or ROR1-immunotoxin. **B., C.** Tumor volume measurement at week intervals of tumors treated with the 5 mg/kg twice per week with ROR1-ITX (R1-4) or control IgG (C1-4). **D.** Body weight measurements at week intervals for mice receiving control IgG or ROR1-immunotoxin.

## CHAPTER IV

### CONCLUSIONS AND FUTURE DIRECTIONS

#### **Conclusions**

Breast cancer is initiated and sustained by tumor-initiating cells. In the United States, HER2+ IDC accounts for 20-25% of IDC diagnoses per year or approximately 40,000 cases [1, 2, 24]. To date, the cell-of-origin for HER2+ breast cancer represents a knowledge gap in the initiation of the aggressive HER2+ subtype of breast cancer. One aspect of the studies within this thesis was the genomic characterization of the cell of origin candidates using tumors derived from ErbB2 transgenic mammary stem cells and luminal progenitor cells. Despite earlier work that found sporadic MMTV-ErbB2 murine tumors to be enriched for CD61<sup>+</sup> LP, our previous work has shown that MaSC possess greater tumorigenicity [40-42]. In agreement, tumors derived from MaSC were found to have a greater genetic resemblance to HER2+ patients. This suggests that not only are MaSC the leading candidate for the cell-of-origin for HER2+ breast cancer; as LP enrichment is seen in both tumors and clonogenic assays, MaSC may shift the proliferative burden to LP. ErbB2 may have a role to commit MaSC to luminal differentiation, a process known to be driven by Notch activation [171]. This coerced tumor initiation hierarchy, where LP are the cell of proliferation, may contribute to both the high rates of initial resistance and developed resistance reported in nearly 66-89% of HER2+ patients treated with trastuzumab as a single-agent therapy [172, 173].

Comparing the genomic profiles from LP and MaSC tumors, we focused on Wnt5a, which previous research has suggested as a negative regulator in mammary gland development [94]. The mono-allelic loss of Wnt5a is seen in 55% of HER2+ breast cancer patients and nearly a third of all breast cancer samples in the TCGA. The importance of Wnt5a in tumor initiation/progression is underscored by the abstruse observations in the final portion of Chapter 2. We showed that Wnt5a, congruent with

the noncanonical Wnt family, inhibits self-renewal, likely through the activation of SMAD signaling and the antagonism of Wnt/β-catenin. Downstream of TGFβ signaling, the activation of SMAD has an established role in tumor suppression in early stages of tumorigenesis and an antithetical role in promoting metastasis in late-stage disease [154-157]. Previous work has shown TGFβ signaling induces Wnt5a expression; our work further extends the axis and suggests that Wnt5a activates SMAD (**Figure 20A**) [94, 95]. Through SMAD or an independent pathway, Wnt5a reduces the transcription of cyclin D1 and β-catenin. The regulation of β-catenin transcription does not fit the current model of noncanonical Wnt signaling. Most intriguingly, the heterozygote loss of Wnt5a *in vivo* resulted in a more pervasive tumor burden in the context of increased metastatic nodules and secondary/tertiary palpable masses. The increase in tumor and metastatic burden suggests the allelic loss of Wnt5a does not only function in increasing self-renewal capacity and cell cycle, but also in promoting metastasis.

ROR1 has shown to be upregulated in a number of cancers [130]. We found increased ROR1 expression in basal-like breast cancer and triple-negative breast cancer. ROR1 expression is highly correlated with the expression of genes associated with epithelial-mesenchymal transition. The introduction or knockdown of ROR1 expression modulated the expression of genes associated with EMT, metastasis, and CSCs. This suggests that increased ROR1 expression in BLBC is not a product of EMT, but drives EMT. Our investigation of Wnt5a signaling in BLBC shows a similar activation of the SMAD pathway and induction of metastatic genes; however, the knockdown of ROR1 results in a greater level of phosphorylation of SMAD2 and only a partial modification of IL-11, CTGF, and CXCR4 mRNA induction. Thus, ROR1 may serve in sequestering the Wnt5a ligand from a second receptor that activates SMAD. Recent work has suggested ROR1 interaction with the EGFR-ErbB3 heterodimer in lung adenocarcinoma [109]. We found that upon stimulation with EGF or TGFβ, ROR1 can interact with EGFR and TGFβR1. As ROR1 appears to modulate EGF-mediated p-AKT and p-SMAD, the

interaction of ROR1 with both TGFBR1 and EGFR is promising for the mechanism of ROR1 signaling in BLBC (**Figure 20B**).

ROR1-based immunotherapies have been studied in the context of blood malignancies and preventing metastatic foci in breast cancer. The efficacy of these therapies have been limited by the utilization of standard IgG structure and the lower presence of ROR1 on the cell surface compared to traditional monoclonal antibody targets. In lieu of previous work, we opted to use a ROR1-immunotoxin, which after binding the cogent antigen and internalization, blocks translation through the conjugated bacterial exotoxin. In initial assessment, we show ROR1-specific killing in cell line screening, but also an initial reduction in tumor volume in xenograft models. This suggests that ROR-based therapies have the potential to reduce tumor volumes in BLBC. Due to the short duration of the efficacy trial for the ROR1-immunotoxin, we were unable to assess ROR1 therapy on metastases, which our work has alluded to as one of the functional roles of ROR1 expression in BLBC.

### **Future Directions**

The goal of this thesis is to understand and characterize the tumor-initiating cell populations in breast cancer. It serves as a proof-of-concept of using big data and bioinformatics to frame hypotheses in real-time and leads us to pursue a unique, biphasic role of noncanonical Wnt signaling in breast cancer of two distinct molecular subtypes. Future experiments based on the distinct two phases on noncanonical Wnt signaling are outlined as follows:

1. To refine Wnt5a signaling in tumor and metastasis suppression. Wnt5a in both MDA-MB-231 and HMLE cells leads to the phosphorylation of SMAD. Preliminary evidence suggests ROR1 does not appear to be integral in Wnt5a-SMAD signaling (**Figure 15**). *In vitro* double-knockdown systems have been

generated for ROR1 and other Wnt5a receptors to pinpoint the receptor responsible for Wnt5a-mediated SMAD activation.

2. To investigate the mechanism by which heterozygous loss of Wnt5a results in pervasive metastatic burden. Counterintuitively, decreased Wnt5a, which would in turn decrease SMAD activation, results in increased secondary tumors and metastatic nodules (**Figure 10**). We have just received a conditional knockout Wnt5a mouse strain to delineate the role of decreased Wnt5a post-initiation. These mice will still require breeding into the ErbB2-TG background.
3. To elucidate the ROR1-TGF $\beta$ R1-EGFR interaction and signaling paradigm. Characterizing the domains of interaction between the receptors and regulatory effects are important in understanding the function of ROR1 in BLBC. In parallel, our lab has generated an inducible ROR1 murine model to evaluate spontaneous tumor growth and progression with or without ROR1 expression.
4. To optimize and evaluate the efficacy of ROR1-immunotoxin as a cancer/metastasis therapy. Preliminary data (**Figures 17 and 18**) have shown efficacy and safety of the immunotoxin, warranting larger *in vivo* trials. We propose to use human patient xenografts from TNBC to generate tumors in NSG mice. Through our collaborations with Speed BioSystems, we have several variants of ROR1 that show promise in *in vitro* screens that will be used. Our dosing protocol for our safety trial (5 mg/kg, twice a week) was based on monoclonal antibody dosing, which will need to be modified to compensate for decreased stabilization of the immunotoxin structure.

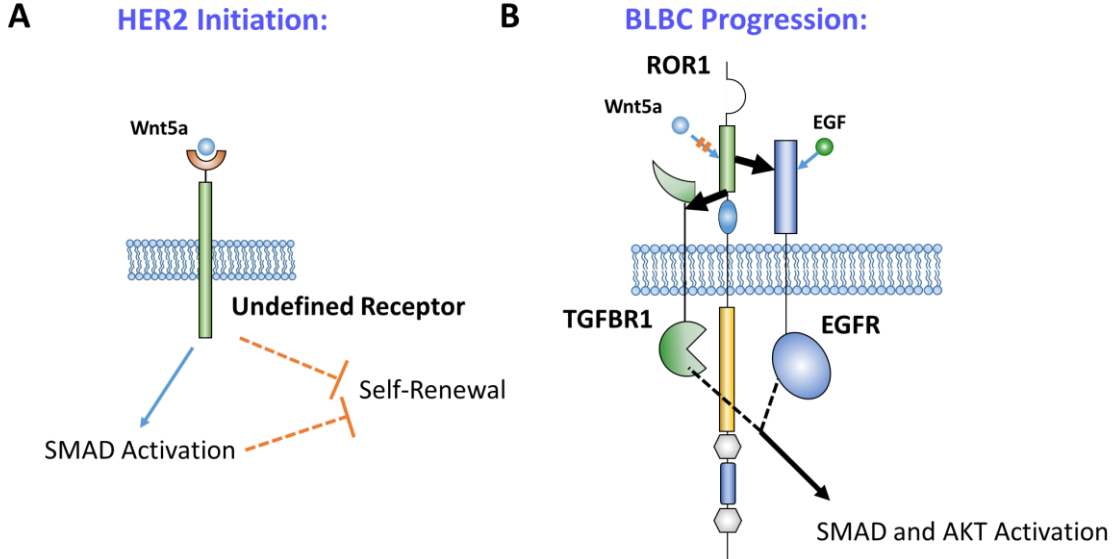


**Figure 20: Noncanonical Wnt Pathway in Breast Cancer Initiation and Progression.** **A.** Wnt5a inhibits the self-renewal capacity of ErbB2 TG mammary epithelium, measured via mammosphere assay. This may be a product of the ability of Wnt5a to induce SMAD activation or an independent pathway, but Wnt5a also appears to regulate cyclin D1 and  $\beta$ -catenin at the transcriptional level. **B.** ROR1 appears to promote progression of BLBC through EMT and generating more stem-like tumor cells. The likely mechanism is through the interaction of ROR1 with TGFBR1 and/or EGFR, and not signaling induced by Wnt5a-ROR1 interaction.

## REFERENCES

1. U.S. Cancer Statistics Working Group. *United States Cancer Statistics: 1999–2010 Incidence and Mortality Web-based Report*. 2013 [cited 2014 March 17]; Available from: <http://apps.ncccd.cdc.gov/uscs/>.
2. Howlader N, N.A., Krapcho M, Neyman N, Aminou R, Waldron W, Altekruse SF, Kosary CL, Ruhl J, Tatalovich Z, Cho H, Mariotto A, Eisner MP, Lewis DR, Chen HS, Feuer EJ, Cronin KA (eds). *SEER Cancer Statistics Review, 1975-2009*, N.C. Institute, Editor. 2012: Bethesda, MD.
3. Society, A.C. *Global Cancer Facts & Figures*. 2011 [cited 2014 March 17]; Second Edition:[Available from:  
<http://www.cancer.org/acs/groups/content/@epidemiologysurveillance/documents/document/acspc-027766.pdf>.
4. Kamangar, F., G.M. Dores, and W.F. Anderson, *Patterns of Cancer Incidence, Mortality, and Prevalence Across Five Continents: Defining Priorities to Reduce Cancer Disparities in Different Geographic Regions of the World*. Journal of Clinical Oncology, 2006. **24**(14): p. 2137-2150.
5. Parkin, D.M., *Global cancer statistics in the year 2000*. The Lancet Oncology, 2001. **2**(9): p. 533-543.
6. Benson, J.R. and I. Jatoi, *The global breast cancer burden*. Future Oncology, 2012. **8**(6): p. 697-702.
7. Helmrich, S.P., et al., *Risk Factors for Breast Cancer*. American Journal of Epidemiology, 1983. **117**(1): p. 35-45.
8. McPherson, K., C.M. Steel, and J.M. Dixon, *Breast cancer--epidemiology, risk factors, and genetics*. BMJ : British Medical Journal, 2000. **321**(7261): p. 624-628.
9. Yang, X.R., et al., *Differences in Risk Factors for Breast Cancer Molecular Subtypes in a Population-Based Study*. Cancer Epidemiology Biomarkers & Prevention, 2007. **16**(3): p. 439-443.
10. Anderson, W.F., et al., *Epidemiology of inflammatory breast cancer (IBC)*. Breast disease, 2005. **22**: p. 9-23.
11. Bae, S.Y., et al., *Mucinous Carcinoma of the Breast in Comparison with Invasive Ductal Carcinoma: Clinicopathologic Characteristics and Prognosis*. Journal of Breast Cancer, 2011. **14**(4): p. 308-313.

12. Pal, S.K., et al., *Papillary Carcinoma of the Breast: An Overview*. Breast cancer research and treatment, 2010. **122**(3): p. 637-645.
13. Rakha, E.A., et al., *Tubular Carcinoma of the Breast: Further Evidence to Support Its Excellent Prognosis*. Journal of Clinical Oncology, 2010. **28**(1): p. 99-104.
14. Vu-Nishino, H., et al., *Clinicopathologic features and long-term outcome of patients with medullary breast carcinoma managed with breast-conserving therapy (BCT)*. International journal of radiation oncology, biology, physics, 2005. **62**(4): p. 1040-1047.
15. Institute, N.C. *PDQ® Breast Cancer Treatment*. 2014 [cited 2014 March 17]; Available from: <http://www.cancer.gov/cancertopics/pdq/treatment/breast/healthprofessional>.
16. Slamon, D.J., et al., *Studies of the HER-2/neu proto-oncogene in human breast and ovarian cancer*. Science (New York, N.Y.), 1989. **244**(4905): p. 707-712.
17. Slamon, D.J., et al., *Human breast cancer: correlation of relapse and survival with amplification of the HER-2/neu oncogene*. Science, 1987. **235**(4785): p. 177-182.
18. Press, M.F., et al., *Her-2/neu expression in node-negative breast cancer: direct tissue quantitation by computerized image analysis and association of overexpression with increased risk of recurrent disease*. Cancer research, 1993. **53**(20): p. 4960-4970.
19. Dent, R., et al., *Triple-negative breast cancer: clinical features and patterns of recurrence*. Clin Cancer Res, 2007. **13**(15 Pt 1): p. 4429-34.
20. Prat, A., et al., *Phenotypic and molecular characterization of the claudin-low intrinsic subtype of breast cancer*. Breast Cancer Res, 2010. **12**(5): p. R68.
21. Perou, C.M., *Molecular Stratification of Triple-Negative Breast Cancers*. The Oncologist, 2011. **16**(Supplement 1): p. 61-70.
22. Perou, C.M., et al., *Molecular portraits of human breast tumours*. Nature, 2000. **406**(6797): p. 747-752.
23. van 't Veer, L.J., et al., *Gene expression profiling predicts clinical outcome of breast cancer*. Nature, 2002. **415**(6871): p. 530-536.
24. Network, T.C.G.A., *Comprehensive molecular portraits of human breast tumours*. Nature, 2012. **490**(7418): p. 61-70.

25. Tan, D.S.P., et al., *Triple negative breast cancer: molecular profiling and prognostic impact in adjuvant anthracycline-treated patients*. Breast cancer research and treatment, 2008. **111**(1): p. 27-44.
26. Rakha, E.A. and I.O. Ellis, *Triple-negative/basal-like breast cancer: review*. Pathology, 2009. **41**(1): p. 40-47.
27. Cheang, M.C.U., et al., *Basal-like breast cancer defined by five biomarkers has superior prognostic value than triple-negative phenotype*. Clinical cancer research: an official journal of the American Association for Cancer Research, 2008. **14**(5): p. 1368-1376.
28. Shah, S.P., et al., *The clonal and mutational evolution spectrum of primary triple negative breast cancers*. Nature, 2012. **486**(7403).
29. Taylor-Papadimitriou, J., et al., *Keratin expression in human mammary epithelial cells cultured from normal and malignant tissue: relation to in vivo phenotypes and influence of medium*. J Cell Sci, 1989. **94** ( Pt 3): p. 403-13.
30. Purkis, P.E., et al., *Antibody markers of basal cells in complex epithelia*. J Cell Sci, 1990. **97** ( Pt 1): p. 39-50.
31. Shackleton, M., et al., *Generation of a functional mammary gland from a single stem cell*. Nature, 2006. **439**(7072): p. 84-88.
32. Stingl, J., et al., *Characterization of bipotent mammary epithelial progenitor cells in normal adult human breast tissue*. Breast cancer research and treatment, 2001. **67**(2): p. 93-109.
33. Sleeman, K.E., et al., *CD24 staining of mouse mammary gland cells defines luminal epithelial, myoepithelial/basal and non-epithelial cells*. Breast Cancer Res, 2006. **8**(1): p. R7.
34. Keller, P.J., et al., *Defining the cellular precursors to human breast cancer*. Proc Natl Acad Sci U S A, 2012. **109**(8): p. 2772-7.
35. Rios, A.C., et al., *In situ identification of bipotent stem cells in the mammary gland*. Nature, 2014. **506**(7488): p. 322-327.
36. Visvader, J.E., *Keeping abreast of the mammary epithelial hierarchy and breast tumorigenesis*. Genes Dev, 2009. **23**(22): p. 2563-77.
37. Asselin-Labat, M.-L., et al., *Gata-3 is an essential regulator of mammary-gland morphogenesis and luminal-cell differentiation*. Nature Cell Biology, 2007. **9**(2): p. 201-209.

38. Clarke, R.B., et al., *P27KIP1 expression indicates that steroid receptor-positive cells are a non-proliferating, differentiated subpopulation of the normal human breast epithelium*. European Journal of Cancer, 2000. **36**, Supplement 4: p. 28-29.
39. Booth, B.W. and G.H. Smith, *Estrogen receptor-alpha and progesterone receptor are expressed in label-retaining mammary epithelial cells that divide asymmetrically and retain their template DNA strands*. Breast Cancer Res, 2006. **8**(4): p. R49.
40. Zhang, W., et al., *A NIK-IKK $\alpha$  Module Expands ErbB2-Induced Tumor-Initiating Cells by Stimulating Nuclear Export of p27/Kip1*. Cancer Cell, 2013. **23**(5): p. 647-659.
41. Lo, P.K., et al., *CD49f and CD61 identify Her2/neu-induced mammary tumor-initiating cells that are potentially derived from luminal progenitors and maintained by the integrin-TGF $\beta$  signaling*. Oncogene, 2012. **31**(21): p. 2614-2626.
42. Liu, J.C., et al., *Identification of Tumorsphere- and Tumor-Initiating Cells in HER2/Neu-Induced Mammary Tumors*. Cancer Research, 2007. **67**(18): p. 8671-8681.
43. Lim, E., et al., *Aberrant luminal progenitors as the candidate target population for basal tumor development in BRCA1 mutation carriers*. Nature Medicine, 2009. **15**(8): p. 907-913.
44. Molyneux, G., et al., *BRCA1 Basal-like Breast Cancers Originate from Luminal Epithelial Progenitors and Not from Basal Stem Cells*. Cell Stem Cell, 2010. **7**(3): p. 403-417.
45. Gorski, J.J., et al., *BRCA1 transcriptionally regulates genes associated with the basal-like phenotype in breast cancer*. Breast cancer research and treatment, 2010. **122**(3): p. 721-731.
46. Hosey, A.M., et al., *Molecular Basis for Estrogen Receptor  $\alpha$  Deficiency in BRCA1-Linked Breast Cancer*. Journal of the National Cancer Institute, 2007. **99**(22): p. 1683-1694.
47. Bonnet, D. and J.E. Dick, *Human acute myeloid leukemia is organized as a hierarchy that originates from a primitive hematopoietic cell*. Nature Medicine, 1997. **3**(7): p. 730-737.
48. Lapidot, T., et al., *A cell initiating human acute myeloid leukaemia after transplantation into SCID mice*. Nature, 1994. **367**(6464): p. 645-648.

49. Wang, J.C., et al., *High level engraftment of NOD/SCID mice by primitive normal and leukemic hematopoietic cells from patients with chronic myeloid leukemia in chronic phase*. Blood, 1998. **91**(7): p. 2406-2414.
50. Al-Hajj, M., et al., *Prospective identification of tumorigenic breast cancer cells*. Proceedings of the National Academy of Sciences, 2003. **100**(7): p. 3983-3988.
51. Singh, S.K., et al., *Identification of human brain tumour initiating cells*. Nature, 2004. **432**(7015): p. 396-401.
52. O'Brien, C.A., et al., *A human colon cancer cell capable of initiating tumour growth in immunodeficient mice*. Nature, 2006. **445**(7123): p. 106-110.
53. Ma, S., et al., *Identification and characterization of tumorigenic liver cancer stem/progenitor cells*. Gastroenterology, 2007. **132**(7): p. 2542-2556.
54. Li, C., et al., *Identification of Pancreatic Cancer Stem Cells*. Cancer Research, 2007. **67**(3): p. 1030-1037.
55. Prince, M.E., et al., *Identification of a subpopulation of cells with cancer stem cell properties in head and neck squamous cell carcinoma*. Proceedings of the National Academy of Sciences, 2007. **104**(3): p. 973-978.
56. Quintana, E., et al., *Efficient tumour formation by single human melanoma cells*. Nature, 2008. **456**(7222): p. 593-598.
57. Ginestier, C., et al., *ALDH1 Is a Marker of Normal and Malignant Human Mammary Stem Cells and a Predictor of Poor Clinical Outcome*. Cell Stem Cell, 2007. **1**(5): p. 555-567.
58. Kelly, P.N., et al., *Tumor Growth Need Not Be Driven by Rare Cancer Stem Cells*. Science, 2007. **317**(5836): p. 337-337.
59. Bao, S., et al., *Glioma stem cells promote radioresistance by preferential activation of the DNA damage response*. Nature, 2006. **444**(7120): p. 756-760.
60. Diehn, M., et al., *Association of Reactive Oxygen Species Levels and Radioresistance in Cancer Stem Cells*. Nature, 2009. **458**(7239): p. 780-783.
61. Lou, H. and M. Dean, *Targeted therapy for cancer stem cells: the patched pathway and ABC transporters*. Oncogene, 2007. **26**(9): p. 1357-1360.
62. Calabrese, C., et al., *A Perivascular Niche for Brain Tumor Stem Cells*. Cancer Cell, 2007. **11**(1): p. 69-82.

63. Hambardzumyan, D., et al., *PI3K pathway regulates survival of cancer stem cells residing in the perivascular niche following radiation in medulloblastoma in vivo*. Genes & Development, 2008. **22**(4): p. 436-448.
64. Sipkins, D.A., et al., *In vivo imaging of specialized bone marrow endothelial microdomains for tumour engraftment*. Nature, 2005. **435**(7044): p. 969-973.
65. Bhatia, R., et al., *Persistence of malignant hematopoietic progenitors in chronic myelogenous leukemia patients in complete cytogenetic remission following imatinib mesylate treatment*. Blood, 2003. **101**(12): p. 4701-4707.
66. Hamilton, A., et al., *BCR-ABL activity and its response to drugs can be determined in CD34+ CML stem cells by CrkL phosphorylation status using flow cytometry*. Leukemia, 2006. **20**(6): p. 1035-1039.
67. Balic, M., et al., *Most Early Disseminated Cancer Cells Detected in Bone Marrow of Breast Cancer Patients Have a Putative Breast Cancer Stem Cell Phenotype*. Clinical Cancer Research, 2006. **12**(19): p. 5615-5621.
68. Clevers, H., *The cancer stem cell: premises, promises and challenges*. Nature Medicine, 2011: p. 313-319.
69. Ebben, J.D., et al., *The Cancer Stem Cell Paradigm: A New Understanding of Tumor Development and Treatment*. Expert opinion on therapeutic targets, 2010. **14**(6): p. 621-632.
70. Reya, T., et al., *Stem cells, cancer, and cancer stem cells*. Nature, 2001. **414**(6859): p. 105-111.
71. Clevers, H., *Wnt/β-Catenin Signaling in Development and Disease*. Cell, 2006. **127**(3): p. 469-480.
72. Chu, E.Y., et al., *Canonical WNT signaling promotes mammary placode development and is essential for initiation of mammary gland morphogenesis*. Development (Cambridge, England), 2004. **131**(19): p. 4819-4829.
73. Hsu, W., R. Shakya, and F. Costantini, *Impaired mammary gland and lymphoid development caused by inducible expression of Axin in transgenic mice*. The Journal of cell biology, 2001. **155**(6): p. 1055-1064.
74. Weber-Hall, S.J., et al., *Developmental and hormonal regulation of Wnt gene expression in the mouse mammary gland*. Differentiation; research in biological diversity, 1994. **57**(3): p. 205-214.

75. Vaillant, F., et al., *The mammary progenitor marker CD61/beta3 integrin identifies cancer stem cells in mouse models of mammary tumorigenesis*. Cancer Res, 2008. **68**(19): p. 7711-7.
76. Lindvall, C., et al., *The Wnt signaling receptor Lrp5 is required for mammary ductal stem cell activity and Wnt1-induced tumorigenesis*. The Journal of biological chemistry, 2006. **281**(46): p. 35081-35087.
77. Li, Y., et al., *Evidence that transgenes encoding components of the Wnt signaling pathway preferentially induce mammary cancers from progenitor cells*. Proceedings of the National Academy of Sciences, 2003. **100**(26): p. 15853-15858.
78. Liu, B.Y., et al., *The transforming activity of Wnt effectors correlates with their ability to induce the accumulation of mammary progenitor cells*. Proceedings of the National Academy of Sciences, 2004. **101**(12): p. 4158-4163.
79. Teuli  re, J., et al., *Targeted activation of   -catenin signaling in basal mammary epithelial cells affects mammary development and leads to hyperplasia*. Development, 2005. **132**(2): p. 267-277.
80. Reya, T. and H. Clevers, *Wnt signalling in stem cells and cancer*. Nature, 2005. **434**(7035): p. 843-850.
81. Zhao, C., et al., *Loss of   -Catenin Impairs the Renewal of Normal and CML Stem Cells In Vivo*. Cancer Cell, 2007. **12**(6): p. 528-541.
82. Malanchi, I., et al., *Cutaneous cancer stem cell maintenance is dependent on   -catenin signalling*. Nature, 2008. **452**(7187): p. 650-653.
83. Eger, A., et al., *  -Catenin and TGF   signalling cooperate to maintain a mesenchymal phenotype after FosER-induced epithelial to mesenchymal transition*. Oncogene, 2004. **23**(15): p. 2672-2680.
84. Daniel, C.W., et al., *The in vivo life span of normal and preneoplastic mouse mammary glands: a serial transplantation study*. Proceedings of the National Academy of Sciences, 1968. **61**(1): p. 53-60.
85. Habas, R., I.B. Dawid, and X. He, *Coactivation of Rac and Rho by Wnt/Frizzled signaling is required for vertebrate gastrulation*. Genes & Development, 2003. **17**(2): p. 295-309.
86. Wansleeben, C. and F. Meijlink, *The planar cell polarity pathway in vertebrate development*. Developmental Dynamics, 2011. **240**(3): p. 616-626.

87. Anastas, J.N. and R.T. Moon, *WNT signalling pathways as therapeutic targets in cancer*. Nature Reviews Cancer, 2013. **13**(1): p. 11-26.
88. Kühl, M., et al., *Ca2+/Calmodulin-dependent Protein Kinase II Is Stimulated by Wnt and Frizzled Homologs and Promotes Ventral Cell Fates in Xenopus*. Journal of Biological Chemistry, 2000. **275**(17): p. 12701-12711.
89. Slusarski, D.C., et al., *Modulation of Embryonic Intracellular Ca2+Signaling byWnt-5A*. Developmental Biology, 1997. **182**(1): p. 114-120.
90. Westfall, T.A., et al., *Wnt-5/pipetail functions in vertebrate axis formation as a negative regulator of Wnt/β-catenin activity*. The Journal of Cell Biology, 2003. **162**(5): p. 889-898.
91. Yu, J., et al., *Altered Expression of Genes of the Bmp/Smad and Wnt/Calcium Signaling Pathways in the Cone-only Nrl-/- Mouse Retina, Revealed by Gene Profiling Using Custom cDNA Microarrays*. Journal of Biological Chemistry, 2004. **279**(40): p. 42211-42220.
92. Yuzugullu, H., et al., *Canonical Wnt signaling is antagonized by noncanonical Wnt5a in hepatocellular carcinoma cells*. Molecular Cancer, 2009. **8**(1).
93. Miyoshi, H., et al., *Wnt5a Potentiates TGF-β Signaling to Promote Colonic Crypt Regeneration After Tissue Injury*. Science, 2012. **338**(6103): p. 108-113.
94. Roarty, K. and R. Serra, *Wnt5a is required for proper mammary gland development and TGF-beta-mediated inhibition of ductal growth*. Development (Cambridge, England), 2007. **134**(21): p. 3929-3939.
95. Roarty, K., et al., *Loss of TGF-beta or Wnt5a results in an increase in Wnt/beta-catenin activity and redirects mammary tumour phenotype*. Breast cancer research: BCR, 2009. **11**(2).
96. Masiakowski, P. and R.D. Carroll, *A novel family of cell surface receptors with tyrosine kinase-like domain*. Journal of Biological Chemistry, 1992. **267**(36): p. 26181-26190.
97. Forrester, W.C., et al., *A C. elegans Ror receptor tyrosine kinase regulates cell motility and asymmetric cell division*. Nature, 1999. **400**(6747): p. 881-885.
98. Kaucká, M., et al., *Post-translational modifications regulate signalling by Ror1*. Acta Physiologica, 2011. **203**(3): p. 351-362.
99. Roszmusz, E., et al., *Localization of Disulfide Bonds in the Frizzled Module of Ror1 Receptor Tyrosine Kinase*. Journal of Biological Chemistry, 2001. **276**(21): p. 18485-18490.

100. Forrester, W.C., C. Kim, and G. Garriga, *The Caenorhabditis elegans Ror RTK CAM-1 Inhibits EGL-20/Wnt Signaling in Cell Migration*. Genetics, 2004. **168**(4): p. 1951-1962.
101. Mikels, A.J. and R. Nusse, *Purified Wnt5a Protein Activates or Inhibits  $\beta$ -Catenin-TCF Signaling Depending on Receptor Context*. PLoS Biol, 2006. **4**(4).
102. Fukuda, T., et al., *Antisera Induced by Infusions of Autologous Ad-CD154-Leukemia B Cells Identify ROR1 as an Oncofetal Antigen and Receptor for Wnt5a*. Proceedings of the National Academy of Sciences of the United States of America, 2008. **105**(8): p. 3047-3052.
103. Oishi, I., et al., *The receptor tyrosine kinase Ror2 is involved in non-canonical Wnt5a/JNK signalling pathway*. Genes to Cells, 2003. **8**(7): p. 645-654.
104. Paganoni, S., J. Bernstein, and A. Ferreira, *Ror1-Ror2 complexes modulate synapse formation in hippocampal neurons*. Neuroscience, 2010. **165**(4): p. 1261-1274.
105. Stephens, R.W., et al., *Heparin binding to the urokinase kringle domain*. Biochemistry, 1992. **31**(33): p. 7572-7579.
106. Mizuno, K., et al., *Hairpin loop and second kringle domain are essential sites for heparin binding and biological activity of hepatocyte growth factor*. Journal of Biological Chemistry, 1994. **269**(2): p. 1131-1136.
107. Mathews, I.I., et al., *Crystal Structures of the Recombinant Kringle 1 Domain of Human Plasminogen in Complexes with the Ligands  $\epsilon$ -Aminocaproic Acid and trans-4-(Aminomethyl)cyclohexane-1-carboxylic Acid†*. Biochemistry, 1996. **35**(8): p. 2567-2576.
108. Oishi, I., et al., *Spatio-temporally regulated expression of receptor tyrosine kinases, mRor1, mRor2, during mouse development: implications in development and function of the nervous system*. Genes to Cells, 1999. **4**(1): p. 41-56.
109. Yamaguchi, T., et al., *NKX2-1/TITF1/TTF-1-Induced ROR1 Is Required to Sustain EGFR Survival Signaling in Lung Adenocarcinoma*. Cancer Cell, 2012. **21**(3): p. 348-361.
110. Gentile, A., et al., *Ror1 Is a Pseudokinase That Is Crucial for Met-Driven Tumorigenesis*. Cancer Research, 2011. **71**(8): p. 3132-3141.
111. Hanks, S.K., A.M. Quinn, and T. Hunter, *The Protein Kinase Family: Conserved Features and Deduced Phylogeny of the Catalytic Domains*. Science, 1988. **241**(4861): p. 42-52.

112. Hikasa, H., et al., *The Xenopus receptor tyrosine kinase Xror2 modulates morphogenetic movements of the axial mesoderm and neuroectoderm via Wnt signaling*. Development, 2002. **129**(22): p. 5227-5239.
113. Wilson, C., D.C. Goberdhan, and H. Steller, *Dror, a potential neurotrophic receptor gene, encodes a Drosophila homolog of the vertebrate Ror family of Trk-related receptor tyrosine kinases*. Proceedings of the National Academy of Sciences, 1993. **90**(15): p. 7109-7113.
114. McKay, S.E., et al., *Aplysia Ror Forms Clusters on the Surface of Identified Neuroendocrine Cells*. Molecular and Cellular Neuroscience, 2001. **17**(5): p. 821-841.
115. Stricker, S., et al., *Cloning and expression pattern of chicken Ror2 and functional characterization of truncating mutations in Brachydactyly type B and Robinow syndrome*. Developmental Dynamics, 2006. **235**(12): p. 3456-3465.
116. Oishi, I., et al., *A Novel Drosophila Receptor Tyrosine Kinase Expressed Specifically in the Nervous System UNIQUE STRUCTURAL FEATURES AND IMPLICATION IN DEVELOPMENTAL SIGNALING*. Journal of Biological Chemistry, 1997. **272**(18): p. 11916-11923.
117. Matsuda, T., et al., *Expression of the receptor tyrosine kinase genes, Ror1 and Ror2, during mouse development*. Mechanisms of Development, 2001. **105**(1-2): p. 153-156.
118. Al-Shawi, R., et al., *Expression of the Ror1 and Ror2 receptor tyrosine kinase genes during mouse development*. Development genes and evolution, 2001. **211**(4): p. 161-171.
119. DeChiara, T.M., et al., *Ror2, encoding a receptor-like tyrosine kinase, is required for cartilage and growth plate development*. Nature Genetics, 2000. **24**(3): p. 271-274.
120. Oldridge, M., et al., *Dominant mutations in ROR2, encoding an orphan receptor tyrosine kinase, cause brachydactyly type B*. Nature Genetics, 2000. **24**(3): p. 275-278.
121. van Bokhoven, H., et al., *Mutation of the gene encoding the ROR2 tyrosine kinase causes autosomal recessive Robinow syndrome*. Nature Genetics, 2000. **25**(4): p. 423-426.
122. Afzal, A.R., et al., *Recessive Robinow syndrome, allelic to dominant brachydactyly type B, is caused by mutation of ROR2*. Nature Genetics, 2000. **25**(4): p. 419-422.

123. Takeuchi, S., et al., *Mouse Ror2 receptor tyrosine kinase is required for the heart development and limb formation*. Genes to Cells, 2000. **5**(1): p. 71-78.
124. Nomi, M., et al., *Loss of mRor1 Enhances the Heart and Skeletal Abnormalities in mRor2-Deficient Mice: Redundant and Pleiotropic Functions of mRor1 and mRor2 Receptor Tyrosine Kinases*. Molecular and Cellular Biology, 2001. **21**(24): p. 8329-8335.
125. Green, J.L., T. Inoue, and P.W. Sternberg, *The C. elegans ROR receptor tyrosine kinase, CAM-1, non-autonomously inhibits the Wnt pathway*. Development, 2007. **134**(22): p. 4053-4062.
126. Baskar, S., et al., *Unique Cell Surface Expression of Receptor Tyrosine Kinase ROR1 in Human B-Cell Chronic Lymphocytic Leukemia*. Clinical Cancer Research, 2008. **14**(2): p. 396-404.
127. Hudecek, M., et al., *The B-cell tumor-associated antigen ROR1 can be targeted with T cells modified to express a ROR1-specific chimeric antigen receptor*. Blood, 2010. **116**(22): p. 4532-4541.
128. Bicocca, Vincent T., et al., *Crosstalk between ROR1 and the Pre-B Cell Receptor Promotes Survival of t(1;19) Acute Lymphoblastic Leukemia*. Cancer Cell, 2012. **22**(5): p. 656-667.
129. Zhang, S., et al., *ROR1 Is Expressed in Human Breast Cancer and Associated with Enhanced Tumor-Cell Growth*. PLoS ONE, 2012. **7**(3).
130. Zhang, S., et al., *The Onco-Embryonic Antigen ROR1 Is Expressed by a Variety of Human Cancers*. The American Journal of Pathology, 2012. **181**(6): p. 1903-1910.
131. Daneshmanesh, A.H., et al., *Orphan receptor tyrosine kinases ROR1 and ROR2 in hematological malignancies*. Leukemia & Lymphoma, 2013. **54**(4): p. 843-850.
132. Barna, G., et al., *ROR1 expression is not a unique marker of CLL*. Hematological oncology, 2011. **29**(1): p. 17-21.
133. Frank, D.A., S. Mahajan, and J. Ritz, *B lymphocytes from patients with chronic lymphocytic leukemia contain signal transducer and activator of transcription (STAT) 1 and STAT3 constitutively phosphorylated on serine residues*. Journal of Clinical Investigation, 1997. **100**(12): p. 3140-3148.
134. Li, P., et al., *Stat3 Activates the Receptor Tyrosine Kinase Like Orphan Receptor-1 Gene in Chronic Lymphocytic Leukemia Cells*. PLoS ONE, 2010. **5**(7).
135. Daneshmanesh, A.H., et al., *Ror1, a cell surface receptor tyrosine kinase is expressed in chronic lymphocytic leukemia and may serve as a putative target for*

- therapy.* International journal of cancer. Journal international du cancer, 2008. **123**(5): p. 1190-1195.
136. MacKeigan, J.P., L.O. Murphy, and J. Blenis, *Sensitized RNAi screen of human kinases and phosphatases identifies new regulators of apoptosis and chemoresistance.* Nature Cell Biology, 2005. **7**(6): p. 591-600.
  137. Grumolato, L., et al., *Canonical and noncanonical Wnts use a common mechanism to activate completely unrelated coreceptors.* Genes Dev, 2010. **24**(22): p. 2517-30.
  138. Cui, B., et al., *Targeting ROR1 Inhibits Epithelial–Mesenchymal Transition and Metastasis.* Cancer Research, 2013. **73**(12): p. 3649-3660.
  139. Rabbani, H., et al., *Expression of ROR1 in patients with renal cancer--a potential diagnostic marker.* Iranian biomedical journal, 2010. **14**(3): p. 77-82.
  140. Hojjat-Farsangi, M., et al., *Inhibition of the receptor tyrosine kinase ROR1 by anti-ROR1 monoclonal antibodies and siRNA induced apoptosis of melanoma cells.* PLoS One, 2013. **8**(4): p. e61167.
  141. O'Connell, M.P., et al., *Hypoxia induces phenotypic plasticity and therapy resistance in melanoma via the tyrosine kinase receptors ROR1 and ROR2.* Cancer Discov, 2013. **3**(12): p. 1378-93.
  142. Yang, J., et al., *Therapeutic Potential and Challenges of Targeting Receptor Tyrosine Kinase ROR1 with Monoclonal Antibodies in B-Cell Malignancies.* PLoS ONE, 2011. **6**(6).
  143. Baskar, S., et al., *Targeting malignant B cells with an immunotoxin against ROR1.* mAbs, 2012. **4**(3): p. 349-361.
  144. Wicha, M.S., S. Liu, and G. Dontu, *Cancer Stem Cells: An Old Idea—A Paradigm Shift.* Cancer Research, 2006. **66**(4): p. 1883-1890.
  145. Visvader, J.E., *Cells of origin in cancer.* Nature, 2011. **469**(7330): p. 314-322.
  146. Subramanian, A., et al., *GSEA-P: a desktop application for Gene Set Enrichment Analysis.* Bioinformatics, 2007. **23**(23): p. 3251-3253.
  147. Cerami, E., et al., *The cBio Cancer Genomics Portal: An Open Platform for Exploring Multidimensional Cancer Genomics Data.* Cancer Discovery, 2012. **2**(5): p. 401-404.

148. Muller, W.J., et al., *Single-step induction of mammary adenocarcinoma in transgenic mice bearing the activated c-neu oncogene*. Cell, 1988. **54**(1): p. 105-15.
149. Yamaguchi, T.P., et al., *A Wnt5a pathway underlies outgrowth of multiple structures in the vertebrate embryo*. Development, 1999. **126**(6): p. 1211-23.
150. Henry, M.D., et al., *Parity-induced mammary epithelial cells facilitate tumorigenesis in MMTV-neu transgenic mice*. Oncogene, 2004. **23**(41): p. 6980-5.
151. Wagner, K.U., et al., *An adjunct mammary epithelial cell population in parous females: its role in functional adaptation and tissue renewal*. Development, 2002. **129**(6): p. 1377-86.
152. Boulanger, C.A., K.U. Wagner, and G.H. Smith, *Parity-induced mouse mammary epithelial cells are pluripotent, self-renewing and sensitive to TGF-beta1 expression*. Oncogene, 2005. **24**(4): p. 552-60.
153. Pukrop, T., et al., *Wnt 5a signaling is critical for macrophage-induced invasion of breast cancer cell lines*. Proc Natl Acad Sci U S A, 2006. **103**(14): p. 5454-9.
154. Kang, Y., et al., *Breast cancer bone metastasis mediated by the Smad tumor suppressor pathway*. Proceedings of the National Academy of Sciences of the United States of America, 2005. **102**(39): p. 13909-13914.
155. Kang, Y., et al., *A multigenic program mediating breast cancer metastasis to bone*. Cancer cell, 2003. **3**(6): p. 537-549.
156. Massagué, J., *TGFβ in Cancer*. Cell, 2008. **134**(2): p. 215-230.
157. Siegel, P.M., et al., *Transforming growth factor beta signaling impairs Neu-induced mammary tumorigenesis while promoting pulmonary metastasis*. Proceedings of the National Academy of Sciences of the United States of America, 2003. **100**(14): p. 8430-8435.
158. Tam, Wai L., et al., *Protein Kinase C α Is a Central Signaling Node and Therapeutic Target for Breast Cancer Stem Cells*. Cancer Cell, 2013. **24**(3): p. 347-364.
159. Brabertz, T., et al., *Variable beta-catenin expression in colorectal cancers indicates tumor progression driven by the tumor environment*. Proceedings of the National Academy of Sciences of the United States of America, 2001. **98**(18): p. 10356-10361.
160. Zavadil, J., et al., *Integration of TGF-beta/Smad and Jagged1/Notch signalling in epithelial-to-mesenchymal transition*. The EMBO journal, 2004. **23**(5): p. 1155-1165.

161. Peinado, H., M. Quintanilla, and A. Cano, *Transforming Growth Factor  $\beta$ -1 Induces Snail Transcription Factor in Epithelial Cell Lines MECHANISMS FOR EPITHELIAL MESENCHYMAL TRANSITIONS*. Journal of Biological Chemistry, 2003. **278**(23): p. 21113-21123.
162. Scheel, C., et al., *Paracrine and Autocrine Signals Induce and Maintain Mesenchymal and Stem Cell States in the Breast*. Cell, 2011. **145**(6): p. 926-940.
163. Shi, J., et al., *Disrupting the Interaction of BRD4 with Diacetylated Twist Suppresses Tumorigenesis in Basal-like Breast Cancer*. Cancer Cell, 2014. **25**(2): p. 210-225.
164. Mani, S.A., et al., *The Epithelial-Mesenchymal Transition Generates Cells with Properties of Stem Cells*. Cell, 2008. **133**(4): p. 704-715.
165. Morel, A.-P., et al., *Generation of Breast Cancer Stem Cells through Epithelial-Mesenchymal Transition*. PLoS ONE, 2008. **3**(8).
166. Pastan, I. and D. FitzGerald, *Pseudomonas exotoxin: chimeric toxins*. J Biol Chem, 1989. **264**(26): p. 15157-60.
167. Borcherding, N., et al., *ROR1, an embryonic protein with an emerging role in cancer biology*. Protein Cell, 2014.
168. Connolly, E.C., J. Freimuth, and R.J. Akhurst, *Complexities of TGF-beta targeted cancer therapy*. Int J Biol Sci, 2012. **8**(7): p. 964-78.
169. Ferraro, D.A., et al., *Inhibition of triple-negative breast cancer models by combinations of antibodies to EGFR*. Proc Natl Acad Sci U S A, 2013. **110**(5): p. 1815-20.
170. Carey, L.A., et al., *TBCRC 001: randomized phase II study of cetuximab in combination with carboplatin in stage IV triple-negative breast cancer*. J Clin Oncol, 2012. **30**(21): p. 2615-23.
171. Bouras, T., et al., *Notch signaling regulates mammary stem cell function and luminal cell-fate commitment*. Cell Stem Cell, 2008. **3**(4): p. 429-41.
172. Vogel, C.L., et al., *Efficacy and Safety of Trastuzumab as a Single Agent in First-Line Treatment of HER2-Overexpressing Metastatic Breast Cancer*. Journal of Clinical Oncology, 2002. **20**(3): p. 719-726.
173. Cobleigh, M.A., et al., *Multinational Study of the Efficacy and Safety of Humanized Anti-HER2 Monoclonal Antibody in Women Who Have HER2-Overexpressing Metastatic Breast Cancer That Has Progressed After*

*Chemotherapy for Metastatic Disease.* Journal of Clinical Oncology, 1999. **17**(9): p. 2639-2639.